OKLAHOMA TRANSPORTATION CENTER

ECONOMIC ENHANCEMENT THROUGH INFRASTRUCTURE STEWARDSHIP

INVESTIGATION OF THE INPUTS FOR THE MEPDG FOR RIGID PAVEMENTS

TYLER LEY, PH.D., P.E.
AMIR HAJIBABAEE
SHARDUL KADAM
ROBERT FRAZIER
MOHAMMED ABOUSTAIT
TRAVIS EBISCH
KYLE RIDING, PH.D.

OTCREOS10.1-24-F

DISCLAIMER

The contents of this report reflect the views of the authors, who are responsible for the facts and accuracy of the information presented herein. This document is disseminated under the sponsorship of the Department of Transportation University Transportation Centers Program, in the interest of information exchange. The U.S. Government assumes no liability for the contents or use thereof.

TECHNICAL REPORT DOCUMENTATION PAGE

1. Report No. OTCREOS10.1-24-F	2. Government Accession No.	3. Recipient's Catalog No.	
4. Title and Subtitle Investigation of the Inputs for the MEPDG for Rigid Pavements		**5. Report Date** March 2013	
		6. Performing Organization Code	
7. Author(s) Tyler Ley, Amir Hajibabaee, Shardul Kadam, Robert Frazier, Mohammed Aboustait, Travis Ebisch, and Kyle Riding, Ph.D.		**8. Performing Organization Report No.**	
9. Performing Organization Name and Address Oklahoma State University School of Civil and Environmental Engineering 207 Engineering South Stillwater, OK 74078		**10. Work Unit No. (TRAIS)**	
		11. Contract or Grant No. DTRT06-G-0016	
12. Sponsoring Organization Name and Address Oklahoma Transportation Center (Fiscal) 201 ATRC Stillwater, OK 74078 (Technical) 2601 Liberty Parkway, Suite 110 Midwest City, Oklahoma 73110		**13. Type of Report and Period Covered** Final February 2010 – February 2013	
		14. Sponsoring Agency Code	

16. Abstract

There are great advantages in the design of infrastructure if design procedures are used that are based on mechanisms and variables that determine the performance of the element in service. The American Association of State Highway and Transportation Officials (AASHTO) have recently published a new mechanistic and empirical pavement design guide (MEPDG) for flexible and rigid pavements which aims to accomplish this. This design guide is implemented through the use of computer software that provides an analysis of the performance of a given concrete pavement over time. The Oklahoma Department of Transportation (ODOT) is investigating the implementation of the MEPDG and has sponsored a research project at Oklahoma State University to help determine the recommended input parameters for concrete pavements in the state.

This reports completes a sensitivity analysis of the MEPDG based on Oklahoma pavements, provides a literature review of base material best practices, increases the Oklahoma weather data available for the MEPDG, investigates the impact of curing on curling from drying shrinkage and from temperature differentials in concrete pavements, provides regional input guidance for strength, coefficient of thermal expansion, and shrinkage for Oklahoma concrete mixtures.

17. Key Words Concrete, MEPDG, Curing, Coefficient of Thermal Expansion, Shrinkage		**18. Distribution Statement** No restrictions. This publication is available at www.oktc.org and from the NTIS.	
19. Security Classification (of this report) Unclassified.	**20. Security Classification (of this page)** Unclassified.	**21. No. of Pages** 201 + covers	**22. Price**

SI (METRIC) CONVERSION FACTORS

Approximate Conversions to SI Units

Symbol	When you know	Multiply by	To Find	Symbol
LENGTH				
in	inches	25.40	millimeters	mm
ft	feet	0.3048	meters	m
yd	yards	0.9144	meters	m
mi	miles	1.609	kilometers	km
AREA				
in²	square inches	645.2	square millimeters	mm
ft²	square feet	0.0929	square meters	m²
yd²	square yards	0.8361	square meters	m²
ac	acres	0.4047	hectares	ha
mi²	square miles	2.590	square kilometers	km²
VOLUME				
fl oz	fluid ounces	29.57	milliliters	mL
gal	gallons	3.785	liters	L
ft³	cubic feet	0.0283	cubic meters	m³
yd³	cubic yards	0.7645	cubic meters	m³
MASS				
oz	ounces	28.35	grams	g
lb	pounds	0.4536	kilograms	kg
T	short tons (2000 lb)	0.907	megagrams	Mg
TEMPERATURE (exact)				
°F	degrees Fahrenheit	(°F-32)/1.8	degrees Celsius	°C
FORCE and PRESSURE or STRESS				
lbf	poundforce	4.448	Newtons	N
lbf/in²	poundforce per square inch	6.895	kilopascals	kPa

Approximate Conversions from SI Units

Symbol	When you know	Multiply by	To Find	Symbol
LENGTH				
mm	millimeters	0.0394	inches	in
m	meters	3.281	feet	ft
m	meters	1.094	yards	yd
km	kilometers	0.6214	miles	mi
AREA				
mm²	square millimeters	0.00155	square inches	in²
m²	square meters	10.764	square feet	ft²
m²	square meters	1.196	square yards	yd²
ha	hectares	2.471	acres	ac
km²	square kilometers	0.3861	square miles	mi²
VOLUME				
mL	milliliters	0.0338	fluid ounces	fl oz
L	liters	0.2642	gallons	gal
m³	cubic meters	35.315	cubic feet	ft³
m³	cubic meters	1.308	cubic yards	yd³
MASS				
g	grams	0.0353	ounces	oz
kg	kilograms	2.205	pounds	lb
Mg	megagrams	1.1023	short tons (2000 lb)	T
TEMPERATURE (exact)				
°C	degrees Celsius	9/5+32	degrees Fahrenheit	°F
FORCE and PRESSURE or STRESS				
N	Newtons	0.2248	poundforce	lbf
kPa	kilopascals	0.1450	poundforce per square inch	lbf/in²

Acknowledgments

Investigation of the Inputs for the MEPDG for Rigid Pavements

Final Report: March, 2013

Tyler Ley, Ph.D., P.E.
Amir Hajibabaee
Shardul Kadam
Robert Frazier
Mohammed Aboustait
Travis Ebisch

Oklahoma State University

Civil and Environmental Engineering Department

207 Engineering South

Stillwater, OK 74078

Kyle Riding, Ph.D.

Kansas State University

Civil Engineering

2118 Fiedler Hall

Manhattan, Kansas 66506

TABLE OF CONTENTS

LIST OF FIGURES

LIST OF TABLES

1.0 INTRODUCTION

This document is the final report for Phase I of ODOT project 2208 and OkTC project "Development and Implementation of a Mechanistic and Empirical Pavement Design Guide (MEPDG) for Rigid Pavements". The focus of this project is to assist ODOT in implementing the MEPDG into their rigid pavement design practices. The following tasks will be covered in this document:

1. Review of the inputs to the MEPDG and determine the sensitivity on the final design values.
2. Investigate base material practices for concrete pavements through a literature review and survey of experiences from others.
3. Increase the quantity of weather sites in Oklahoma that provide environmental inputs for the MEPDG.
4. Examine different curing methods for rigid pavement construction and their impact on the early age curling and warping of continuous reinforced concrete pavements
5. Provide regional material input parameters that can be used in the MEPDG for the design of rigid pavements

Findings from all tasks are included in this report. A project with similar goals was funded by the Oklahoma Transportation Center (OkTC). This report combines the findings from both projects as their results are complimentary.

The OkTC funding was used to upgrade existing or add additional equipment for the project. It also provided support for graduate, undergraduate, and staff members to accelerate the completion of tasks and allow additional testing to be completed. Below is a summary of specific contributions to the project made possible by the OkTC funding:

- A weather station and instrumentation boxes were purchased that was used in Task D and will be used on Phase II of the project.
- A second frame for the coefficient of thermal expansion testing was purchased. This was essential for the project as it allowed repeatability to be compared between measurements. In addition, equipment was added that allowed the

frames to constantly measure the movement of the specimen in the test. This was an essential contribution to the project and allowed many useful findings.

- The relative humidity sensors used in Task D were purchased. These sensors were extremely helpful to understand the moisture gradients within the samples and to better understand the behavior of the samples under moisture loss.

- There were many challenges to overcome with the large concrete beams that were created in Task D. The funding from OkTC allowed much iteration of specimen sizes and setups to be completed. Useful data would not have been obtained without this funding.

- All of the large scale temperature gradient samples investigated for Task D were completed with the OkTC funding. These large samples provide improved measurements and recommendations for this work.

2.0 IMPACT OF DESIGN INPUTS ON THICKNESS DESIGN WITH MEPDG

2.1 INTRODUCTION

The goal of the MEPDG software is to replace the historic empirical pavement design methods. This software uses a new design methodology for concrete and asphalt pavements based on modern failure models in combination with empirical data from the performance of pavements in the field. One promise of the MEPDG software is that it will allow design engineers to make a comparison between different design options and determine their impact on the cost and long term performance of the pavement.

While portions of the MEPDG have been adopted by two states (Indiana and Missouri), several more are still investigating the method (Won 2009). The focus of this paper is to determine the sensitivity of the thickness design of rigid pavements with the MEPDG for twelve design and material variables between different realistic values.

The MEPDG software allows the user to investigate over 150 variables that are used to determine the performance of a pavement. While it can be useful to control this large number of variables, it can also be overwhelming to specify, measure, or control them. Because of this it would be useful for users to understand how these variables impact the required thickness design of rigid pavements. Other researchers have done work to examine the sensitivity of variables in rigid pavement design with the MEPDG (Zaghloul et. al 2006, Kannekanti 2006, Harvey 2006, Mallela et. al 2005). One challenge with these past investigations is that the MEPDG does not provide the user with the required pavement thickness to make a design satisfactory. Instead the analysis reports only if a design is satisfactory.

In this paper an iterative technique was used to find the required pavement thickness to make a pavement satisfactory. The impact of these different variables on the required design thickness is then quantified. Similar work was presented by ARRA for flexible pavements but little has been done for rigid pavements (ARRA 2004). In 2011 the new version of Darwin ME was available. This software still does not allow a direct calculation of the thickness design.

A summary of the variables and values investigated is shown in Table 2.1. These variables were chosen as they were reasonable ranges of materials observed in the state of Oklahoma.

Table 2.1 The variables and their ranges used in the sensitivity analysis for CRCP and JCP.

pavement opening	fall, spring, or summer
CTE	3.5-8 x 10^{-6} /$^\circ$F
cement type	type I or II
Curing	compound or wet
compressive stress	3000-6000 psi
cementitious material content	400-800 lbs/cy
asphalt layer thickness	0 - 6"
cement fly ash layer	0 - 8"
reinforcement ratio (CRCP)	0.5 – 1%
dowel diameter (in) (JPCP)	1-1.75"
unbound resilient modulus	3000 - 13000 psi
Climate	Stillwater, Clinton, Lawton, McAlester, Oklahoma City, Tulsa, Frederick

2.2 ANALYSIS METHODS

This sensitivity analysis was completed between March and August of 2009 with version 1.0 of the MEPDG software that was obtained from www.trb.org/mepdg/software. Along with this software, hourly climatic data files from version 0.910 were also downloaded. In September of 2009 version 1.1 of the software was released. Sixteen results were repeated with the new design software and there was no difference found. Furthermore, investigation of the changes made between version 1.0 and 1.1 did not mention any modifications to the methods used for concrete pavements. Unfortunately there is not enough guidance provided in the user manual to directly calculate the results of the MEPDG software. Therefore an iterative technique was used to investigate the impact of different variables on the needed concrete pavement thickness.

2.3 DETERMINING THE IMPACT OF A VARIABLE ON THE DESIGN THICKNESS

The first step in the analysis was to determine the Annual Average Daily Truck Traffic (AADTT) that made a model concrete pavement barely satisfy the specified design life. The variables for the model pavement were chosen based off typical design and construction practices of the Oklahoma Department of Transportation. This was done for both jointed plain concrete pavement (JPCP) and continuous reinforced concrete pavement (CRCP) of different thicknesses and joint spacing. An outline of the methodology used is shown in Figure 2.1.
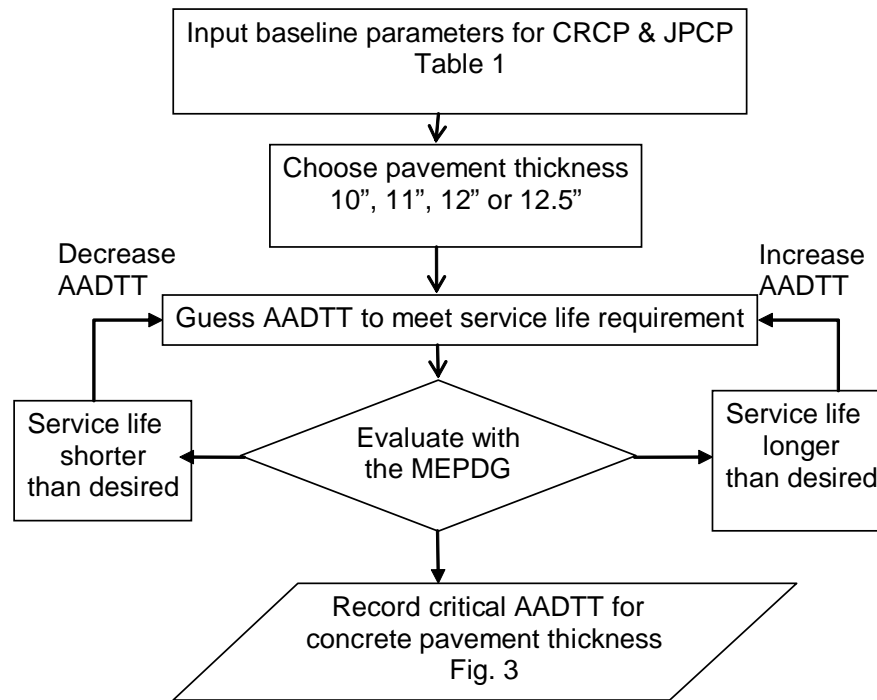
Figure 2.1 Flowchart showing the steps to find the critical AADTT for a typical pavement design.

For these pavements the edge support was assumed to be a tied PCC shoulder and PCC-base interface was kept as full friction contact. The material properties of the asphalt used in the base were chosen to meet typical standards (11% effective binder ratio, 8.5% air voids and 150 lb/ft^3) and not varied. The default parameters for the MEPDG were used unless noted in Table 2.2.

5

Table 2.2 The baseline values for a model pavement.

design life	20 years*
cement	600 lbs of type I
concrete flexural strength	690 psi*
curing	curing compound
shoulder	Tied
JCP dowel diameter	1.5"
CRCP reinf. ratio	0.70%
location	Stillwater
pavement opening	Fall
base layers	4" asphalt 8" chemically stabilized base
subgrade	8000 psi resilient modulus

The failure criteria used was the default values for the MEPDG. These are given in Table 2.3 a & b.

Table 2.3a Failure criteria used in the sensitivity analysis

CRCP failure criteria	limit	reliability
terminal IRI (in/mi)	172	90
CRCP Punchouts (per mi)	10	90
maximum CRCP crack width (in)	0.02	
minimum crack load transfer efficiency (LTE %)	75	

Table 2.3b Failure criteria used in the sensitivity analysis

JPCP failure criteria	limit	reliability
terminal IRI (in/mi)	172	90
transverse cracking (% slabs cracked)	15	90
mean joint faulting (in)	0.12	90

After the limiting AADTT was found an input variable was modified and the pavement was analyzed to see if the old thickness was still adequate. If it was not then the thickness was increased until the design was found to pass. If the pavement performance was improved then the thickness was decreased until the design barely passed. An outline of this methodology is shown in Figure 2.2. By using this iterative technique it was possible to find how a change in a single variable impacted the thickness design for a pavement.
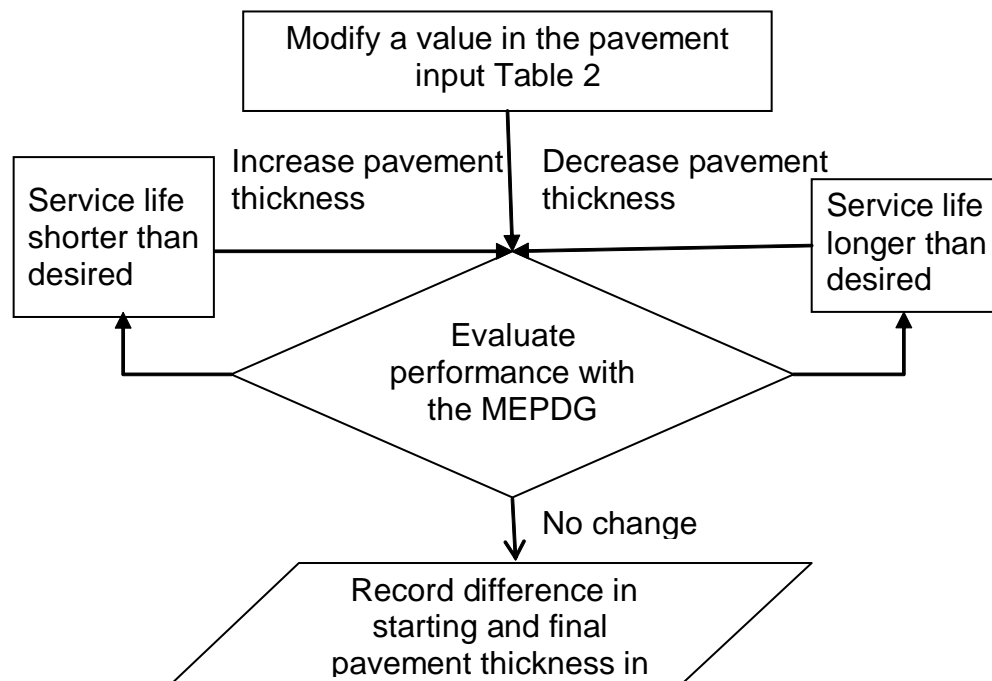
Figure 2.2 Flowchart showing the steps to find out the resulting change in the design thickness for a change of a given variable

2.4 RESULTS
The results for the maximum allowable AADTT for a model pavement and the default failure criteria used in the MEPDG are shown in Figure 2.3.
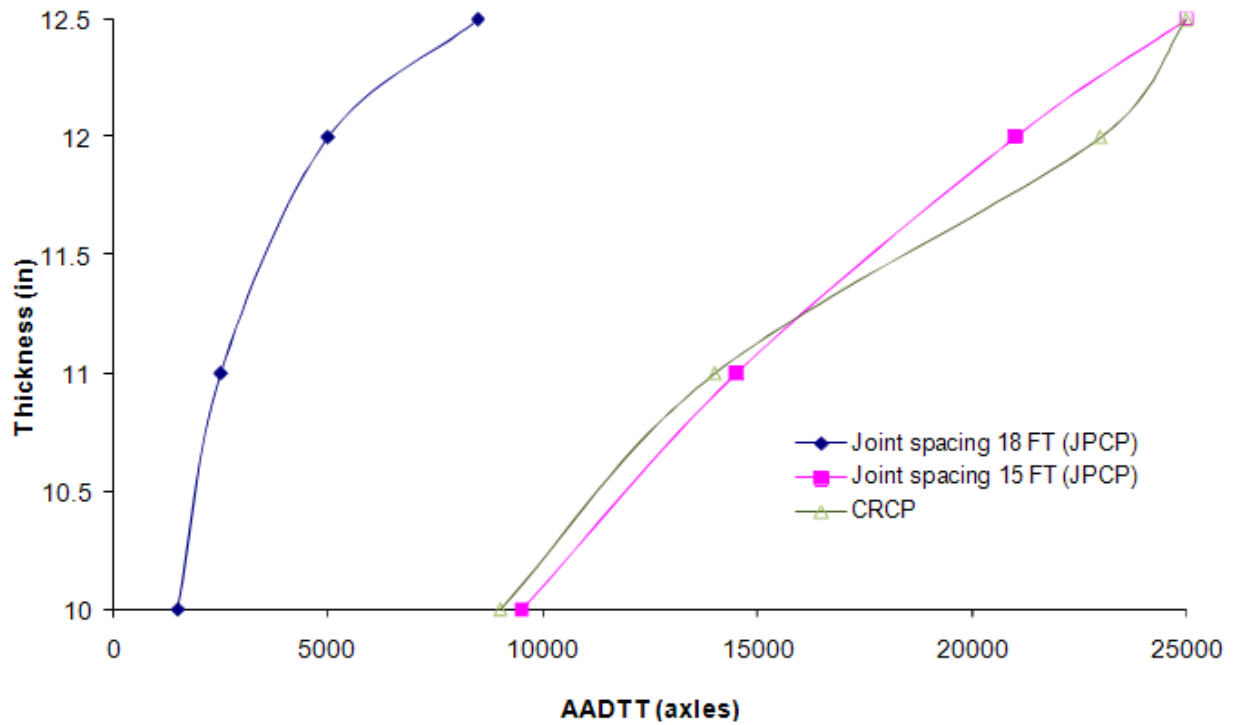
Figure 2.3 A plot of the required design thickness for JPCP and CRCP with different AADTTs.

The impact of specific variables is shown in Table 2.4 and 2.5 in terms of change in the required pavement thickness in the MEPDG to make the section adequate.

Table 2.4 Results from MEPDG sensitivity analysis for material parameters.

Parameters	CRCP				JPCP (spacing 18 FT)				JPCP (spacing 15 FT)			
	12.5"	12"	11"	10"	12.5"	12"	11"	10"	12.5"	12"	11"	10"
cement												
I*	0"L	0"P,L	0"P,L	0"P,L	0"T	0"T	0"T	0"T	0"J	0"J	0"J	0"T,J
II	-0.5"L	-0.5"P,L	- 0.5"P,L	0"L	0"T	0"T	0"T	0"T	0"J	0"J	-0.5"J	0"T,J
curing compound*	0"L	0"P,L	0"P,L	0"P,L	0"T	0"T	0"T	0"T	0"J	0"J	0"J	0"T,J
wet cure	-1" P,L	-0.5" L	-0.5"L	-0.5"P,L	0"T	0"T	0"T	0"T	0"J	0"J	-0.5"J	0"T,J
cement content (lbs/cy)												
500	-1"L	-0.5"L	-0.5"L	-0.5"P,L	0"T	0"T	0"T	0"T	0"J	0"J	-0.5"J	0"T,J
600*	0"L	0"C,L	0"P,L	0"P,L	0"T	0"T	0"T	0"T	0"J	0"J	0"J	0"J
700	>+3"C,L	>+3"P,C,L	>+3"P,C,L	>+3"P,C,L	+0.5"T	0"T	0"T	0"T	+1"J	+1"J	+0.5"J	+0.5"J
compressive strength (psi)												
3000	0"P,L	0"P,C,L	0"I,P,L	+0.5"P,L	+3.5"I,T	+3"I,T	+3"T	+3.5"T	+1.5"T	+1.5"T	+2"T	+1.5"I,T
4200	+0.5"L	+1"P,C,L	+0.5"P,C,L	+0.5"P,C,L	+1.5"I,T'	+1.5T	+1"T	+1.5"T	+0.5"J	0"J	0"T,J	+1"I,T
5000	0"C,P,L	+0.5"L	+0.5"C,L	+0.5"C,L	+0.5"T	+0.5"T	0"T	0"T	0"J	0"J	0"J	+0.5"T
6000	0"L	+0.5"L	0"P,L	+0.5"L	-0.5"T,J	-0.5"T	-1"T	-1"T	0"J	0"J	0"J	0"J
CTE (1x10-6/oF)												
4.5	-0.5"L	0"L	0"L	0"L	-3"T	-2"T	-2.5"T	-2"T	>+3.5"J	-1.5"J	-3"J	-1"I,T
5.5*	0"L	0"C,L	0"P,L	0"P,L	0"T	0"T	0"T	0"T	0"	0"J	0"J	0"J
6.5	+2"C,L	+1.5"C,L	+1.5"C,L	+1"C,L	+3.5"T	+2.5"I,T,J	+2"T	+2.5"T	+3"I,J,T	+1.5"I,T,J	+2"J	+2.5"I,T,J
resilient modulus (psi)												
3000	-0.5"L	0"L	0"L	0"L	0"J	-1.5T	-1.5T	-0.5T	+2J	+2J	+1"J	+1"J
5500	0"L	0"L	0"L	0"P,L	0"T	-0.5"T	-0.5"T	0"T	+0.5"J	+0.5"J	+0.5"J	+0.5"J
8000*	0"L	0"P,L	0"P,L	0"P,L	0"T	0"T	0"T	0"T	0"J	0"J	0"J	0"J
10500	0"L	+0.5"L	0" P,L	+0.5"L	+0.5"T	+0.5"T	0"T	0"T	0"J	0"J	-0.5"J	0"J
13000	0"L	+0.5"L	+0.5"L	+0.5"L	+1T	+0.5"T	+0.5"T	0"T	0"J	0"J	-0.5"J	+0.5"T

The required change in pavement thickness to insure comparable performance for the change in the variable. Positive values suggest an increase in thickness negative a decrease. The thickness change is measured in millimeters. *- values used to represent typical ODOT pavements, therefore they have no impact on the pavement thickness
Bold values correspond to a result that is unexpected and shaded values were investigated in version 1.1 and 1.0 of the MEPDG. The controlling failure mode is given by the letters.

L – load transfer efficiency   T – transverse cracking
P – punchouts   I – IRI
J – joint faulting   C- cracking

Table 2.5 Results from MEPDG sensitivity analysis for design parameters.

Parameters	12.5"		11"	10"	JPCP (spacing 18 FT)				JPCP (spacing 15 FT)			
					12.5"	12"	11"	10"	12.5"	12"	11"	10"
Pavement opening				CRCP								
Summer	-0.5" L	0" L	0" L	12"	+0.5" T	0"T	0"T	0"T	0"J	0"J	-0.5"J	0"I,T,J
Spring	-2"L	-2"P,L	-1.5"PL		+0.5"T	0"T	0"T	0"T	-0.5"J	-0.5"J	-1"J	0"I,T,J
Fall*	0" L	0" P,L	0" P,L	0" P,L	0"T	0"T	0"T	0"T	0"J	0"J	0"J	0"I,T,J
reinforcement steel (%)												
0.6	>+3.5"P,C,L	+2P,C,L	>+3.5"P,C,L	>+3.5"P,C,L	-	-	-	-	-	-	-	-
0.7	0" L	0" P,L	0" P,L	0" P,L	-	-	-	-	-	-	-	-
0.8	-1.5"L	-1"L	-0.5"L	-0.5"L	-	-	-	-	-	-	-	-
dowel diameter (in)												
1	-	-	-	-	>+3.5"I,J	+3.5"I,J	+3"I,J	+2.5"I,J	>+3.5"I,J	>+3.5"I,J	>+3.5"I,J	>+3.5"I,J
1.25	-	-	-	-	>+3.5"I,J	+3.5"I,J	+2.5J	0"T	>+3.5"I,J	>+3.5"I,J	>+3.5"I,J	>+3.5"I,J
1.5*	-	-	-	-	0"T	0"T	0"T	0"T	0"J	0"J	0"J	0"T,J
1.75	-	-	-	-	0"T	0"T	0"T	0"T	-0.5"J	-0.5"J	-1"J	0"J
Asphalt layer thickness (n)												
0	0"L	+0.5"L	+0.5"L	0"L	>-3.5"T	-2.5"T	>-3.5"T	>-3.5"T	-1"J	-2"J	-3"T	-1.5"T
2	0"L	0"L	0"P,L	0"P,L	+1"T	+0.5"T	+0.5"T	+0.5"T	+1"J	+0.5J	0"J	+1"T
4*	0"L	0"P,L	0"P,L	0"P,L	0"T	0"T	0"T	0"T	0"J	0"J	0"J	0"I,T,J
lime cement fly ash stabilized												
0	0"J	+0.5"P,L	0"P,L	+0.5"L	0"J	-0.5"T	-0.5"T	-0.5"T	+1.5J	+1"J	+0.5"J	+0.5"J
3	0"T	0"L	0"L	0"P,L	0"T	-0.5"T	-0.5"T	-0.5"T	+0.5"J	+0.5"J	-0.5"J	0"T
5	0"T	0"P,L	0"P,L	0"P,L	0"T	-0.5"T	-0.5"T	0"T	+1"J	+0.5"J	0"J	0"T,J
8*	0"T	0"P,L	0"P,L	0"P,L	0"T	0"T	0"T	0"T	0"J	0"J	0"J	0"T,J
Climate												
Clinton	>+3.5"C,L	>+3.5"C,L	+3"C,L	+1.5C,L	0"T	-0.5"T	0"T	-0.5"T	-0.5:J	-0.5"J	-1.5"T	0"T
Fredick	+0.5"L	+0.5"L	+0.5"L	+0.5"L	+0.5"L	+0.5"T	+0.5"T	+0.5"T	-0.5"J	-1"J	-1"T	+0.5"T
Lawton	0"L	+0.5"L	+0.5"L	+0.5"L	+1"T	0"T	0"T	0"T	-1"J	-1"J	-1"T	+0.5"T
Tulsa	-0.5"L	0"L	0"L	0"L	-0.5"T	0"T	-0.5"T	0"T	-0.5"J	0"J	0"J	0"T,J

| Stillwater* | 0"L | 0"L | 0"L | 0"L | 0"T | 0"T | 0"T | 0"T | 0"T | 0"T | 0"T | 0"T |
| McAlester | -0.5"L | 0"L | 0"L | 0"L | -0.5"T | 0"T | -0.5"T | 0"T | 0"J | -1"J | -1"T | 0"T |

The required change in pavement thickness to insure comparable performance for the change in the variable. Positive values suggest an increase in thickness negative a decrease.
The thickness change is measured in millimeters.
*- values used to represent typical ODOT pavements, therefore they have no impact on the pavement thickness
Bold values correspond to a result that is unexpected and shaded values were investigated in version 1.1 and 1.0 of the MEPDG.
The controlling failure mode is given by the letters.
L – load transfer efficiency   T – transverse cracking
P – punchouts   I – IRI
J – joint faulting   C- cracking

Table 2.4 contains summaries of the material parameters, and Table 2.5 shows the impact of the design parameters. For each case the pavement was varied in thickness in 0.5" increments. A plus (+) was used for a required increase in thickness and a minus (-) was used for a required decrease in thickness. In some cases there was no impact on the thickness and a "0" is reported. A letter is also reported next to each thickness change that designates the failure mode that governed for that analysis. All default values of the model pavement are indicated by an asterisk and values that were unexpected were shown in bold. A general summary of the sensitive parameters for an 11" thick pavement is shown in Table 2.6.

Table 2.6 A summary of the data for the 11" pavements

	CRCP	JPCP w/18' joint spacing
concrete strength	green stripes	red checker
cement strength	red checker	green stripes
CTE	red checker	red checker
% steel	red checker	-
dowel diameter	-	red checker
asphalt layer thickness	green stripes	red checker
stabilized layer thickness	green stripes	green stripes
resilient modulus	green stripes	yellow stripes
climate	red checker	green stripes

less than 1" thickness change	green stripes
more than 1" thickness change	yellow stripes
more than 2" thickness change	red checker

The following is a description of some of the failure criteria as defined in the MEPDG. The international roughness index (IRI) is a measurement of the smoothness of a

pavement. It is the ratio of the accumulated suspension motion to the distance traveled from a mathematical model. A punchout is a major distress in a CRCP. It consists of two transverse cracks that are intersected by a longitudinal crack. Under heavy loads the steel ruptures and the isolated slab changes elevation. Punchouts are measured by counting the numbers that exist per mile. For CRCP the crack width is assumed to play an important role in the ability of the slab to transfer load. The limiting mean crack width is taken as 0.02" at the depth of steel as per the default limits in the MEPDG. The load transfer efficiency (LTE) is the ability to transfer loads between the pavement slabs as well as between cracks. The default limiting value of LTE is 75%. For JPCP transverse cracking is a result of fatigue damage at the bottom face of the pavement and can lead to a rough ride. The transverse cracking is measured as a percentage of slabs and the default failure criteria are limited to 15% in MEPDG. Faulting is the difference in the elevation across a joint or crack. The MEPDG limits the mean joint faulting to 3mm. The following example is used to illustrate the use of Table 2.4 or 2.5. If the coefficient of thermal expansion (CTE) is changed from 5.5×10^{-6} to 6.5×10^{-6} /°F for a 12" CRCP pavement then the design thickness will have to be increased by 1.5" to 13.5" to make the pavement adequate for the same AADTT. The controlling failure mechanism will be cracking and inefficient load transfer. This suggests that the increase in CTE has caused the thickness of the pavement to be increased by 1.5" in order to be able to meet the same design criteria for the same AADTT.

2.5 DISCUSSION
Based on the results of the maximum AADTT for different model pavement types shown in Figure 2.3 one can see that there is a significant increase in the estimated maximum AADTT when a joint spacing of 15 ft. is used instead of 18 ft. for a JPCP. This is expected as a decrease in joint spacing should decrease the stresses on the slab and allow for a greater number of vehicles before failure. It is not clear if the magnitude of change of the joint spacing from 18 ft. to 15 ft. for a 12" thick JPCP would allow the AADTT to be increased from 5,000 to approximately 20,000 axles. This is an increase of 400% in AADTT for a 16% decrease in panel size. While the authors agree that the

14

behavior is within line with the classical solution, it is not clear if the magnitude of change is reasonable.

The results suggest that the performance of a CRCP and a JPCP with a 15 ft. joint spacing was almost identical between a thickness of 10" and 12.5". It is expected that as the panel size of a JPCP is decreased it will approach the performance of a CRCP. Again, based on classical solutions it is not clear at what size of panel the two systems should be equivalent. The analysis for the model pavement suggests that this JPCP joint spacing is 15 ft.

According to the results in Tables 2.4 and 2.5 the variables investigated had different levels of impact on the thickness design of the pavements. The discussions will be limited to the variables that were shown to have a significant impact on the thickness design requirements. Comments will be made about the agreement of the results with classical theory. Overall, many of the observations were in line with the expected behavior. The work gives the reader some idea on how the change in a given variable impacted the thickness requirement for the pavement. This information is powerful as these quantifications and comparisons were not possible in past design and evaluation methods. A few of the results were not as expected. It has been well documented that a few software bugs have existed in past versions of the MEPDG.

The cement type and curing method had little impact on the design thickness of the pavements. For both the JPCP and CRCP, as the compressive strength of the pavement was decreased the required pavement thickness increased and vice versa. This result was expected.

The type of curing had little impact on JPCP design thickness. However, the use of a wet cure instead of a spray-on curing compound allowed the CRCP design thickness to decrease by 0.5" consistently and up to 1" for a 12.5" thick pavement. According to the MEPDG design manual, the use of a wet cure minimizes the early temperature differentials between the top and bottom of the slab during set. This allows the pavement to have a consistent zero stress temperature. When the pavement experiences a different zero stress temperature between the top and bottom of the slab then it will have a permanent curl in the slab at a constant temperature. Having a

consistent temperature through the slab helps to minimize the differential movement from the top and bottom fibers of the slab.

When the cement content was increased in the mixture the amount of ultimate shrinkage was increased. This increase in cement content did not change the design strength as this is a separate parameter in the analysis. Shrinkage of concrete pavements can cause stresses because of friction between the pavement and the subgrade. These stresses are expected to be lower with JPCP because of the close joint spacing. This was reflected in the analysis as the thickness requirements for the JPCP with an 18 ft. joint spacing but required up to a 1" increase in thickness for a JPCP with a 15 ft. joint spacing. This result is not expected as a slab with a shorter distance between joints would be less impacted by shrinkage strains than the larger joint spacing because of the lower amount of contact with the subgrade and therefore lower stresses. The CRCP pavement was significantly impacted as an increase in cement content from 600 to 700 lbs/CY required a thickness increase of over 3". This increase is expected as the subgrade friction between a CRCP is the slab is continuous. The CTE is defined as the strain change per degree rise in temperature. When a pavement has a higher CTE it would be expected to curl more if there is a differential temperature between the top and bottom of a pavement. With this higher amount of curl then one would expect higher stresses from edge loadings. A high CTE may also increase the stresses in the pavement from the subgrade friction. Both of these can lead to slab cracking and increased stresses which further impact the performance of both CRCP and JPCP. The CTE was a variable that the MEPDG consistently showed as having a significant impact on the thickness design of both CRCP and JPCP. When a CTE value was increased from 5.5×10^{-6} to $6.5 \times 10^{-6}/\mathrm{^oF}$ all of the pavements showed a significant increase in the required design thickness. This thickness increase was typically more significant as the pavement thickness increased and showed a greater increase in JPCP than CRCP. As the CTE value was decreased from 5.5×10^{-6} to $4.5 \times 10^{-6}/\mathrm{^oF}$ the majority of the pavements were decreased in the recommended thickness. However the CRCP thickness design was not significantly impacted by the decrease in CTE. The required increase or decrease for each of the pavements does seem reasonable. It is also expected that these changes in CTE would have a greater impact

on JPCP than CRCP because of the curling at each of the joints. This can be especially seen with JPCP with a 15 ft. joint spacing as the required thickness changes are very high. With the MEPDG this is the first time that the CTE can be used as an input to the design of a concrete pavement.

The impact on the required pavement thickness was investigated for changes in the resilient modulus from 3000 to 13000 psi. The changes in the resilient modulus of the subgrade had a different impact for each type of pavement. These changes had little impact on the design thickness of CRCP. For the results of the JPCP with a 15 ft. joint spacing, the results were what would be expected. As the resilient modulus was decreased an increase in the resulting pavement thickness was required and the joint faulting failure mode controlled. However for these same changes with a 12" thick JPCP with an 18 ft. joint spacing the opposite results were found and the pavement thickness could be significantly decreased as the resilient modulus was decreased. In the extreme, these results suggest that if a material with a resilient modulus of 3000 psi is used instead of 8000 psi then the pavement thickness can be decreased by 1.5". It seems intuitive that as the panel size of a JPCP increased one would expect that it would be more reliant on the stiffness of the base for support. This means that as the stiffness of the subgrade is reduced the thickness should be larger. This idea is supported by the radius of relative stiffness concept was first discussed by Westergaard (1926a and 1926b) and later used by Bradbury (1938) and others for both loading and curling stresses. However the MEPDG seems to imply the opposite is occurring. The cause of this is not clear and should be investigated further.

The season that a pavement was constructed in did not have a large impact on the design thickness. Also the impacts of the local climate can be investigated on a pavement. For the cities investigated in Oklahoma there was no impact on the thickness. However, the climate for the city of Clinton did show a significant impact on the design thickness for CRCP. The weather for the cities is compared in Table 2.7 and the values are similar. This behavior was only observed for the CRCP as the JCPC were not significantly impacted by the environment in Clinton.

Table 2.7 Comparison of climatic parameters of Oklahoma cities

Climatic parameters	Clinton	Frederick	Lawton	McAlester	Tulsa	Stillwater
mean annual air temperature (ºF)	60.8	62.78	62.06	62.06	60.62	59.9
mean annual rainfall (in)	20.3	20.3	26.3	30.9	38.9	29.3
freezing index (ºF-days)	136.4	102.2	138.2	118.4	203	212
average annual number of freeze/thaw cycles	46	41	58	43	61	57

The reinforcing in CRCP is important to keep tight cracks over the design life of the pavement. The higher this value is one would assume that it would have a better performance. Changes in the reinforcement ratio from 0.7% to 0.6% and 0.8% were investigated. The increase in the reinforcement ratio showed some reductions in the design thickness for CRCP for larger sections. As expected a decrease in the reinforcement ratio showed an increase in the required pavement thickness; however the thickness increase were large. This small change in reinforcement ratio seems to require a significant increase in thickness. It seems that this may be a bug in the system.

Dowel diameter is one of the governing factors affecting the concrete bearing stresses and joint faulting in JPCP pavements. It is expected that an increase in the dowel diameter should reduce the distresses and possibly reduce the required design thickness. The results observed were expected for all of the results. It should be noted that when the dowel diameter was decreased from 1.5" to 1.25" then the pavement thickness could not compensate for this decrease in dowel size.

Base layers are important component of a pavement unit. Faulty or under designed base layers can affect crack spacing pattern, slab support, punchouts, and smoothness. One would suspect as this layer is reduced in thickness that the thickness of the concrete pavement would need to be increased to keep the performance the same. For the CRCP sections investigated the thickness of the asphalt base and fly ash stabilized layer does not seem to have an impact on the design thickness. For the JPCP sections as these layers were reduced the pavement thickness was increased. When the layer was removed from the system the analysis appears to become unstable. The replacement of the asphalt layer with a geotextile fabric is becoming popular in several states. The use of this layer may need more evaluation before being implemented in the MEPDG.

2.6 CONCLUSION

A sensitivity analysis was completed that quantitatively compare the impact of different variables on the design thickness reported in the MEPDG for CRCP and JPCP. The results from the analysis were found to largely match the expected values. The MEPDG is shown to be a great tool that allows a designer the ability to make quantitative comparisons between different variables. In the past these comparisons were very challenging to make with a design tool.

During this analysis several unexpected observations were made. In a few cases this performance was not able to be explained and is likely a bug in the software. Care should be taken by users of the MEPDG software to use engineering judgment and past experiences to verify results. No combination of variables was investigated beyond what is presented in this paper and so care should be taken in extrapolating the results in other ways then what is presented.

Results were investigated with version 1.0 and 1.1 of the software and there were no difference in the results obtained.

THIS PAGE IS INTENTIONALLY BLANK

3.0 INVESTIGATE BASE MATERIAL PRACTICES FOR CONCRETE PAVEMENTS THROUGH A LITERATURE REVIEW AND SURVEY OF EXPERIENCES FROM OTHERS

3.1 INTRODUCTION

The use of sub-grade drainage systems, in the form of permeable bases and/or the incorporation of edge drains, over the last few decades has been considered an option for improving the long term performance of concrete pavements. The effectiveness of these features as a means of draining water and consequently extending the life of a roadway is still unclear. A major problem with this subject is that past investigations have not been able to monitor the performance of these drainage systems from their installation throughout the lifetime of the pavement to monitor their performance. Also, most projects have focused on only the effectiveness of subsurface drainage systems without monitoring the structural effect of these systems over the life of the pavement surface.

For this task the research team has investigated the current literature over permeable bases and subsurface drainage for concrete pavements. Each document is summarized in a section. The summary was written to provide a pavement designer with as many useful findings as possible.

The most significant findings from this review were from "Pavement Subsurface Drainage Design Reference Manual" (FHWA-NHI-08-030). This document states the designs of the subgrade, drainable base, separator layer, and water removal system should be completed as a system. Guidance is provided to help the designer best to choose these systems for different cases and materials. This allows the designer flexibility to adjust their subgrade design based on other materials.

Next the findings from several research projects are summarized. These include National Cooperative Highway Research Program's (NCHRP) Project 1-34, "Performance of Pavement Subsurface Drainage" and studies from several other DOTs.

3.2 PAVEMENT SUBSURFACE DRAINAGE DESIGN REFERENCE MANUAL (FHWA-NHI-08-030)

3.2.1 Introduction

The objective of this report is to summarize the current design and construction methods recommended by the FHWA regarding subsurface drainage systems that incorporate permeable bases. Although permeable bases are concentrated on in this report, the construction of an effective drainage system depends on the success of all components within the system. For this reason, specifications and discussion for bases, sub-bases, sub-grade, and water removal components are provided as well. Each of these components have multiple design options and thus after a summary of each component, comprehensive drainage system options will be provided.

The basis for this report is the Pavement Subsurface Drainage Design Reference Manual (FHWA-NHI-08-030) which was a supplemental document for a short course given by FHWA and NHI. The document represents the culmination of experiences from Departments of Transportation across the nation as well as research project findings, thus the specifications and methods described are founded in the success and failures of drainage systems across the country. For this reason, this manual was used as a reference for all statements made herein.

3.2.3 Permeable bases

Creating a base layer that is permeable enough to quickly drain excess water from the pavement while maintaining the structural integrity to support construction traffic before paving and the load of the pavement after has proven to be a precarious balance. Many of the specifications to follow are to ensure that this balance is maintained.

3.2.3.1 Material specifications

Beginning with aggregate qualities, FHWA specifies a number of characteristics including class, texture, soundness, sand fraction and wear that must be met to ensure the strength and stability of the base. These specifications along with the testing procedures needed to verify them are provided in Table 3.2. These specifications are to apply for both unstabilized and stabilized permeable bases. The gradation of the aggregate, available for use in the permeable base, is a key factor in determining if an unstabilized permeable base is sufficient for a design. Typically a more open-graded

aggregate is needed to ensure an adequate permeability, but if the gradation is too open then the base will lack stability, thus the need for stabilization through asphalt or cement treatment. Many states typically use AASHTO No. 57 and 67 aggregate because the gradations reflect stability and a high permeability although No. 57 has a low coefficient of uniformity which implies low stability and strength. For this reason, No. 57 aggregate is a good choice for a stabilized permeable base.

Some useful tables have been included from the FHWA report. Table 3.3 summarizes gradations commonly used for unstabilized bases. Tables 3.4 and 3.5 summarize gradations used for asphalt treated and cement treated permeable bases respectively. It should also be noted that if the road being constructed is to handle a heavy traffic load, a stabilized permeable base is recommended due to the added strength and stability

Table 3.2 Recommended physical property requirements for aggregates used in permeable bases (FHWA-NHI-08-030)

Specification	Requirement	Test Method
Aggregate classification	Aggregates for the permeable base should at least meet the requirements for class B aggregate in accordance with AASHTO specifications.	AASHTO M 283-83, Coarse Aggregate for Highway and Airport Construction
Aggregate wear	Maximum L.A. abrasion wear should be 40 to 45 percent.	AASHTO T 96-87, Resistance to Abrasion of Small-Size Coarse Aggregates by Use of the Los Angles Machine
Aggregate texture	Use only crushed aggregate material with at least two mechanically fractured faces as determined by the material retained on the 4.75-mm (#4) sieve.	ASTM D 5821-95, Determining Percentage of Fractured Faces in Coarse Aggregates
Aggregate soundness	For pavements subjected to freeze-thaw permeable base aggregates soundness loss should not exceed 12 percent as determined by the sodium sulfate soundness test, or 18 percent, as determined by the magnesium sulfate test.	AASHTO T 104 (ASTM C 88), Soundness of Aggregate by the Use of Sodium Sulfate or Magnesium Sulfate
Fraction of natural sand	Not more than a maximum of 15 percent natural sand by weight is recommended in aggregate mixtures for permeable bases.	ASTM C 125-88, Standard Terminology Relating to Concrete and Concrete Aggregates

Table 3.3 Unstabilized aggregate permeable base gradations. (FHWA 1994)

Percent Passing Sieve Size												
Gradation	50 mm (2in)	37.5 mm (1-1/2 in)	25.4 mm (1in)	19.0 mm (3/4 in)	12.5 mm (1/2 in)	9.52 mm (3/8 in)	4.75 mm (#4)	2.36 mm (#8)	1.18 mm (#16)	0.425 mm (#40)	0.30 mm (#50)	0.075 mm (#200)
AASHTO # 57		100	95-100		25-60		0-10	0-5				
AASHTO # 67			100	90-100		20-55	0-10	0-5				
Iowa			100					10-35			0-15	0-6
Minnesota			100	65-100		35-70	20-45			2-10		0-3
New Jersey		100	95-100		60-80		40-55	5-25	0-12		0-5	
Pennsylvania	100			52-100		33-65	8-40		0-12			0-5

Table 3.4 Asphalt-stabilized permeable base (NAPA 1991)

Percent Passing Sieve Size						
State	25 mm (1 in)	19 mm (3/4 in)	9.5 mm (3/8 in)	4.75 mm(#4)	2.36 mm(#8)	0.075 mm (#200)
California	100	90-100	20-45	0-10		0-2
Florida	100	90-100	20-45	0-10	0-5	0-2
Illinois	90-100	84-100	40-60	0-12		
Kansas	100	90-100	20-45	0-10	0-5	0-2
Ohio	95-100			25-60	0-10	
Texas	100	95-100	20-45	0-15	0-5	2-4
Wisconsin	95-100	80-95	25-50	35-60	20-45	3-10
Wyoming	90-100	20-50		20-50	10-30	0-4

Table 3.5 Cement-stabilized permeable base (FHWA 1994)

Percent Passing Sieve Size							
State	37.5 mm (1-1/2 in)	25.4 mm (1 in)	19 mm (3/4 in)	12.5 mm (1/2 in)	9.5 mm (3/8 in)	4.75 mm (#4)	2.36 mm (#8)
California	100	88-100	X±15*		X±15*	0-16	0-6
Virginia		100		25-60		0-10	0-5
Wisconsin		100	90-100		20-55	0-10	0-5

 * The value X should be proposed by the contractor.

If it is determined that a stabilized permeable base is required, it is necessary to ensure that the asphalt or cement treatments used will create a stable and workable mixture without hindering the base's ability to drain water quickly. The intention is to coat aggregates and allow contact points between them to "cement". Recommendations suggest the treatments meet certain specifications including content, workability, permeability and grade. These recommendations are displayed in Tables 3.6 and 3.8, while Table 3.7 lists the asphalt treatments used in various states. Generally, asphalt or cement content in a mixture is a function of the gradation of the aggregate used because more open-graded aggregates have less surface area and thus need less

treatment to coat them. Most agencies use 1.5 to 2.5 percent asphalt content by weight. For cement treated bases, an application rate of 8 lb/ft^3 to 10.5 lb/ft^3 is recommended.

Table 3.6 Recommended asphalt cement stabilizer properties (FHWA-NHI-08-030)

Specification	Requirement	Test Method
Asphalt cement content	Asphalt content must ensure that aggregates are well coated. Minimum recommended asphalt content is 2 percent by weight. Final asphalt content should be determined according to mix gradation and film thickness on coarse aggregates.	ASTM D 2489. Test Method for Degree of Particle Coating of Bituminous-Aggregate Mixtures
Ahphalt cement grade	Recommended grade is AC-30 or stiffer.	ASTM D 946. Penetration-Graded Asphalt Cement for Use in Pavement Construction ASTM D 3381. Viscosity-Graded Asphalt Cement for Use in Pavement Construction
Anti-stripping	See figure 6.3.	Lottman Test (Lottman 1979) Modified Lottman Test (Tunnicliff and Root 1984) ASTM D 1075-81. Test Method for Effect of Water on Compressive Strength of Compacted Bituminous Mixtures
Anti-stripping agents	Aggregates exhibiting hydrophilic characteristics can be counteracted with 0.5 to 1 percent lime.	NCHRP Report No. 274 (Tunnicliff et al. 1984)
Permeability	Minimum mix permeability is 300 m day (1000 ft day).	AASHTO T 3637. Permeability of Bituminous Mixtures

Table 3.7 Asphalt stabilized permeable base mix material specifications (NAPA 1991)

State	Anti-Strip Test	% Asphalt	Asphalt Grade	Permeability Test
California	Yes	3	Ar-8000/AC-40	No
Florida	No	2.5	AC-30	No
Georgia	Yes	3-2.5	AC-30	Constant Head
Illinois	No	2-3	AC-20	No
Indiana	No	3-4.5	AC-20	AASHTO T-215
Kansas	No	2	AC-10	Constant Head
Kentucky	No	1.5-2.5	AC-20	No
Maryland	Yes	2.5-3.5	AC-20	AASHTO T-167
Ohio	-	2	AC-20	No
Pennsylvania	No	1.5-3.5	AC-20	No
Tennessee	Yes	2.5-7	AC-20/AC-30	No
Texas	-	2-4	AC-10/AC-20	No
Virginia	Yes	2.5-3.5	AC-30	Constant Head
Washington	Yes	1.5-2.5	AR-4000	No
Wisconsin	No	1.5-2.5	60/70-200/300 pen	Falling Head
Wyoming	Yes	-	AC-20	Yes

Table 3.8 Recommended Portland cement stabilizer properties (FHWA-NHI-08-030)

Specification	Requirement	Test Method
Portland cement content	Portland cement content selected must ensure that aggregates are well coated. An application rate of 130 to 170 kg/m^3 (8.1 to 10.6 lb/ft^3) is recommended.	ASTM C 1078. Determining Cement Content of Freshly Mixed Concrete
Water-cement ratio	Recommended water-cement ratio to ensure strength and workability is 0.3 to 0.5.	ACI *Manual of Concrete Practice.* Part 1. American Concrete Institute. ASTM C 1079. Determining Water Content of Freshly Mixed Concrete
Workability	Mix slump should range from 25 to 75 mm (1 to 3 inches).	ASTM C 143. Test Method for Slump of Portland Cement Concrete
Cleanliness	Use only clean aggregates.	ASTM C 33. Concrete Aggregates
Permeability	Minimum mix permeability it 300 m day (1000 ft/day).	

3.2.3.2 Construction specifications

As equally important as the material specifications for a drainable base are certain minimum requirements for the construction of the layer. Again these specifications were formulated to ensure that the drainable base is permeable enough to allow a coefficient of permeability of at least 1000 ft/day but stable enough to support the designed traffic flow for the roadway. Generally speaking, if the permeable base is able to withstand construction traffic without showing signs of pumping or rutting, it should be stable enough to support the design traffic for the roadway.

FHWA recommends that the drainable base should be at least 4 inches thick to overcome any construction variances and provide an adequate hydraulic conduit to transmit water to an edge drain.

There are also concerns when compacting the permeable base during construction, including crushing of the aggregate, intermixing of sub layers, and general overcompaction. With this in mind, suggestions have been made based on successful compaction techniques used by other DOT's. For untreated permeable bases, most agencies specify one to three passes of a 5 to 10 metric ton steel roller. The maximum lift thickness should not exceed 6 inches. Vibratory rollers should be used with extreme caution with all base types because of intermixing concerns. It was found that in order to prevent intermixing, a geotextile separator layer should be used underneath the permeable base to prevent pumping and mixing. For permeable asphalt treated bases, the most common problem reported occurred when the base material was rolled at elevated temperatures. Although compaction procedures are the same as those listed above, in most cases compaction was deferred until the next day or treated with water beforehand. Cement treated permeable bases present problems with workability during the paving process. Typically a paver should follow a spreading machine, but in the event that the workability of the mixture causes issues with the paver, a subgrade paver should be used in its place. In order to prevent further problems a mix should be designed with a minimum water to cement ratio of 0.45 and the minimum cement content which still meets other strength requirements. For compaction, the Wisconsin and Illinois DOT's have had success with attaching vibratory pans to the subgrade planer.

3.2.2 Subsurface drainage systems

The main objective of any subsurface drainage system is to remove excess water from the pavement structure, then deflect the water to an appropriate location. The need for such a system is evident in the list of distresses due to excessive or prolonged moisture. Table 3.1 summarizes the distresses found in PCC pavements due to moisture. The prevention of distresses and thus the extension of a pavement's service life is the goal of every drainage design, but there are many ways that a systems function or an individual components function may be compromised. The specifications

given herein reflect current measures to prevent the failure of each component but it is critical to understand the mechanisms that the design specifications are trying to prevent. The structure of this report is such that these mechanisms are explained so that design engineers may understand why components have certain limitations and when to turn to another viable drainage design. Although there are multiple means by which excess water may enter the pavement, drainage systems are only intended and designed to handle surface infiltration, the flow of water through the top of the pavement. The implications of this statement will be discussed further in the design section of the report. A standard profile for a roadway with a subsurface drainage design system includes a pavement layer, a drainable base, a separator layer and/or longitudinal drainage, and the subgrade. Figure 3.1 below displays a typical profile for a PCC pavement with a basic drainage system.

Table 3.1 Moisture related distresses (adapted from Carpenter et. Al 1979)

Type	Distress Manifestation	Moisture Problem	Climatic Problem	Material Problem	Load Associated?	Structural Defect Begins in		
						PCC	Subbase	Subgrade
Surface Defects	Spalling	Possible	Freeze-thaw Cycles	Mortar	No	Yes	No	No
	Scaling	Yes	Freeze-thaw Cycles	Chemical Influence	No	Yes Finishing	No	No
	D-Cracking	Yes	Freeze-thaw Cycles	Aggregate Expansion	No	Yes	No	No
	Crazing	No	No	Rich Mortar	No	Yes Weak Surface	No	No
Surface Deformation	Blow-up	No	Temperature	Thermal Properties	No	Yes	No	No
	Pumping & Erosion	Yes	Moisture	Inadequate Strength	Yes	No	Yes	Yes
	Faulting	Yes	Moisture-Suction	Erosion-Settlement	Yes	No	Yes	Yes
	Curling/ Warping	Yes	Moisture & Temperature	Moisture & Temperature Differentials	No	Yes	No	No
Cracking	Corner	Yes	Moisture	Cracking follows Erosion	Yes	No	Yes	Yes
	Diagonal Transverse Longitudinal	Yes	Moisture	Follows Erosion	Yes	No	Yes	Yes
	Punchout (CRCP)	Yes	Moisture	Deformation Follows Cracking	Yes	No	Yes	Yes
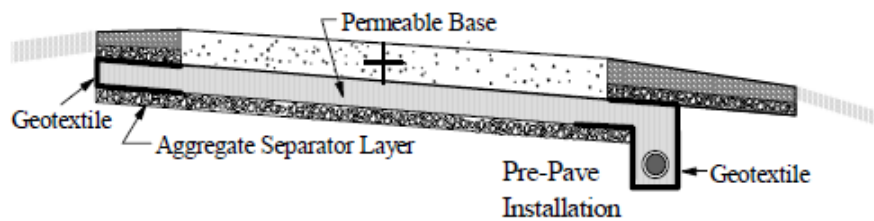
Figure 3.1 Typical cross-section of subsurface drainage system (FHWA 1994)

Each component serves a distinct purpose in the overall function of removing water from the structure. The role of the permeable base is to allow excess water in the pavement structure to quickly drain. It achieves this role by balancing a high permeability, which allows for quick draining, and a reasonable stability for supporting the pavement structure and construction traffic. This balance of stability and permeability define the two different approaches to constructing permeable bases. Unstabilized permeable bases use a dense-graded aggregate to achieve stability through aggregate interlock but lack a high permeability due to their gradation. Stabilized permeable bases, which are generally more open-graded, are treated with asphalt or cement to add stability to an otherwise unstable gradation. The open gradation offers a high permeability. The role of the separator layer or subbase is to direct water that passes through the permeable base away from the substructure as well as prevent the intermixing of layers. A very dense-graded aggregate layer with a low permeability and/or a geotextile layer are typically used to accomplish this. Removing water via the separator layer is accomplished by either daylighting the layer or using longitudinal drains which have multiple options for drain schemes. The subgrade is to serve as a solid foundation for the structure above, as are all layers that constitute the pavement structure and substructure. Figure 3.2 below visualizes the entire process described above.
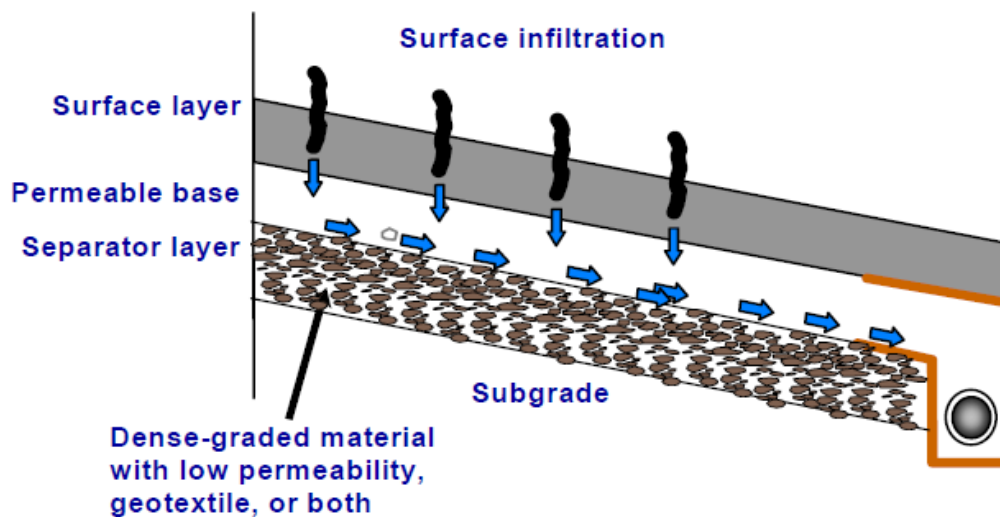
Figure 3.2 Concept of drainage provided by separator layer (FHWA-NHI-08-030)

Over the years, a number of factors have been discovered that can limit the effectiveness of a subsurface drainage system. Each system component is susceptible to loss of performance given certain conditions. FHWA has reflected these conditions in their recommendations for the design and construction of each component. Following is a summary of recommendations for each component type along with an explanation behind the recommendation.

3.2.4 Separator layer

The separator layer is the layer of soil, rock or fabric below the permeable base meant to deflect water which passes through the permeable base away from the subgrade. It also serves as a stable platform for construction of the permeable base and pavement layers as well as a means for preventing fines in the subgrade from intermixing with the permeable base. In order to satisfy these requirements, the separator layer must be stable enough to support construction traffic and have a low enough permeability to prevent the flow of water or the pumping of fines.

The three basic types of separator layers are untreated aggregate, treated aggregate and a combination of a geotextile with an aggregate layer. The reference manual

provides the designer with a table (T7.1) to help in selecting the most appropriate type of separator layer. The key criteria for selection are rainfall, design traffic and subgrade properties.

3.2.4.1 Material specifications

After a separator layer type has been selected, the design process begins with determining proper material properties. In the case of an untreated aggregate separator layer, the reference manual provides a typical gradation suitable for the design purposes mentioned earlier. This gradation is shown in Table 3.9 below. However, the given gradation must be adjusted to account for the gradation of the permeable base above and the subgrade below. This is to ensure that intermixing at the interfaces is limited. Equations 7.1 through 7.4 in the reference manual detail the nature of these changes to the separator layer.

Table 3.9 Aggregate separator layer gradation (FHWA-1994a)

Sieve Size, mm	U.S. Customary Sieve Size	Percent Passing
37.5	1-1/2 in	100
19	3/4 in	95-100
4.75	#4	50-80
0.425	#40	20-35
0.075	#200	5-12

Aggregate gradation for a treated separator layer should be similar to that of an untreated layer. This is because the deflection of water and the prevention of intermixing of layers are the primary purposes for the separator layer. An asphalt or cement treatment should be used to increase stability but this should not be a tradeoff for permeability. Asphalt and cement contents should be determined similarly to typical treated sub-bases. The previous data for treatment contents and properties with permeable bases may be used as a guideline.

The use of a geotextile layer alone should only be used in cases where an aggregate layer is not possible. This could be possible where height requirements are a concern such as under bridges. Otherwise, a geotextile layer should be used in conjunction with a subbase. In these circumstances the geotextile layer only serves as protection from

the intermixing of layers. The role of water deflection is then deferred to the subbase or subgrade layer. This means that the permeability should be high enough to allow passage of water without impediment. A typical failure results from the clogging of the geotextile, resulting in backup of water within the permeable base. In order to prevent this, calculations must be done to determine the apparent opening size of the pores in the fabric as well as the gradient ratio. These values are based on the properties of the layers above and below the geotextile. More information on the procedures for design of the geotextile can be found in section 7 of the reference manual, in particular Figure 7.7 which displays a flow chart for design criteria. Also page 7-19 in the reference manual provides detailed design guidelines.

3.2.4.2 Construction specifications

In addition to material specifications, there are also certain construction procedures that must be followed. Among these for an aggregate separator layer are a minimum thickness of 4 inches and a density of 95 percent of the modified Proctor maximum density. The aggregate layer should also show no signs of distress prior to the placement of the permeable base. Treated bases should be constructed in accordance with typical asphalt or cement treated base procedures.

3.2.5 Drainage

After the water has been deflected to the sides of the substructure by the separator layer, a system must be in place to continue water flow away from the substructure. This can be accomplished by either daylighting the permeable base or by using a system of longitudinal edge drains. Typically daylighting is sufficient for normal design flows, but in areas of high annual rainfall, edge drains may need to be considered. Also, the geometry of the roadway may require the use of edge drains to ensure water does not puddle inside of the substructure.

The function of the drainage system is certainly critical to the success of a permeable base in protecting the roadway from moisture related distresses. In fact, most of the issues reported from state DOT's originate with failure of the drainage system, either from lack of proper maintenance or poor construction techniques. The reference manual provides a detailed account of these collective experiences and bases its guidelines on this knowledge.

There are many types of edge drains including pipes, prefabricated geocomposites called fin drains, and aggregate trench drains. It is recommended that only pipe edge drains be used. This is because both fin drains and aggregate trenches are unable to be maintained and flushed. As stated earlier, maintenance is the key to drainages systems working properly over time so only pipe edge drains will be discussed. Figure 3.3 displays a typical profile of a pipe edge drain embedded in an aggregate trench.
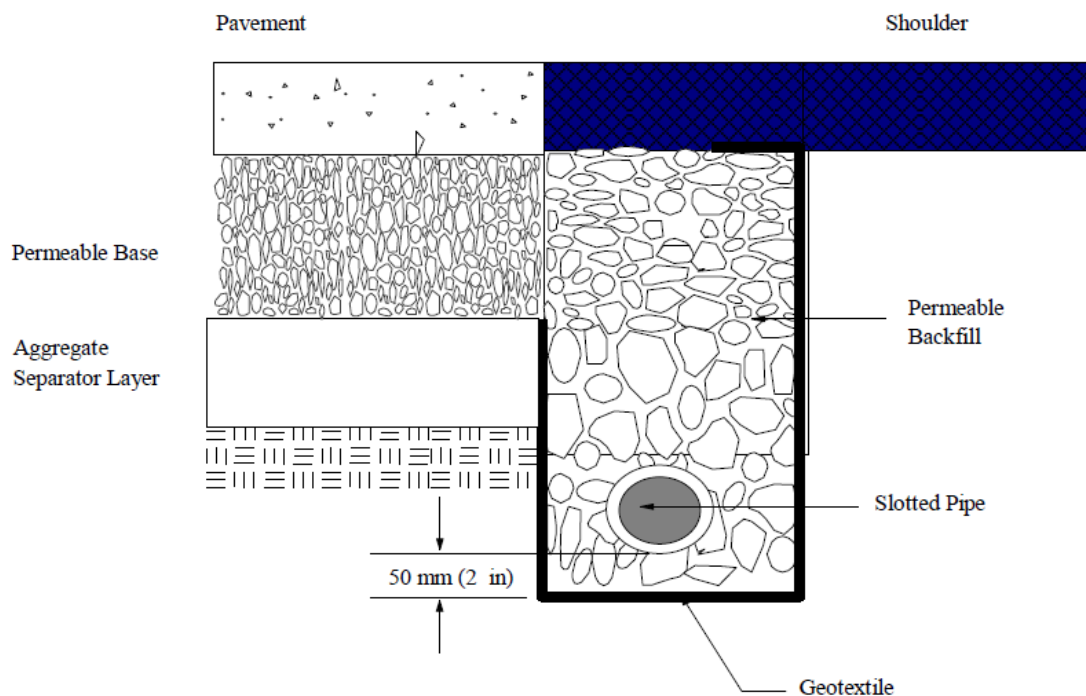
Figure 3.3 Permeable base section with longitudinal edge drains. (FHWA-NHI-08-030)

It is recommended that the design of drainage components is based on the Time to Drain method. More information on this approach and its governing equations can be found in Section 8 of the reference manual.

3.2.5.1 Material specifications

A typical design of an edge drain system will include longitudinal pipes, outlet pipes, an aggregate trench and typically some degree of geotextile wrapping around the trench. As with other components, the design starts with material specifications. The reference manual suggests that all longitudinal pipes be made of flexible, corrugated polyethylene (AASHTO M252) or PVC (AASHTO M278). It is noted that if an asphalt treatment is to

be used that excessive temperatures may cause problems in the edge drains. In this case, PVC electric conduit like EPC 40 or 80 is suggested. Outlet pipes are exposed to higher stresses from construction traffic and for this reason are recommended to have solid walls as opposed to the corrugated walls of longitudinal pipes. The backfill used around the longitudinal drains in the aggregate trench must be at least as permeable as the base material and is typically the same gradation as the base material. Also D_{85} of the backfill should be 1.2 times larger than the openings in of the corrugated pipe to prevent clogging of the longitudinal drains.

3.2.5.2 Construction specifications

The minimum diameter for the longitudinal pipes should be 4 inches. This is not for flow reasons as this rarely controls sizing of the pipe, but to ensure maintenance techniques are effective. The drainage trench should be deep enough so that the top of each pipe may be at least 2 inches below the bottom of the permeable base as well as 2 inches of bedding below the pipe. For the minimum 4 inch diameter pipe, this puts the trench depth at 8 inches. During construction, a minimum of 6 inches of cover is required to protect the pipes during compaction. Figure 3.4 below provides information on specifics regarding outlet pipes and ditches. Figure 3.5 provides details for headwall construction. There are numerous other specifications given in Section 8 of the reference manual concerning construction of drainage systems involving longitudinal pipes. Please refer to this section for more information regarding specifics of geotextile placement, trench depths, and construction overview.
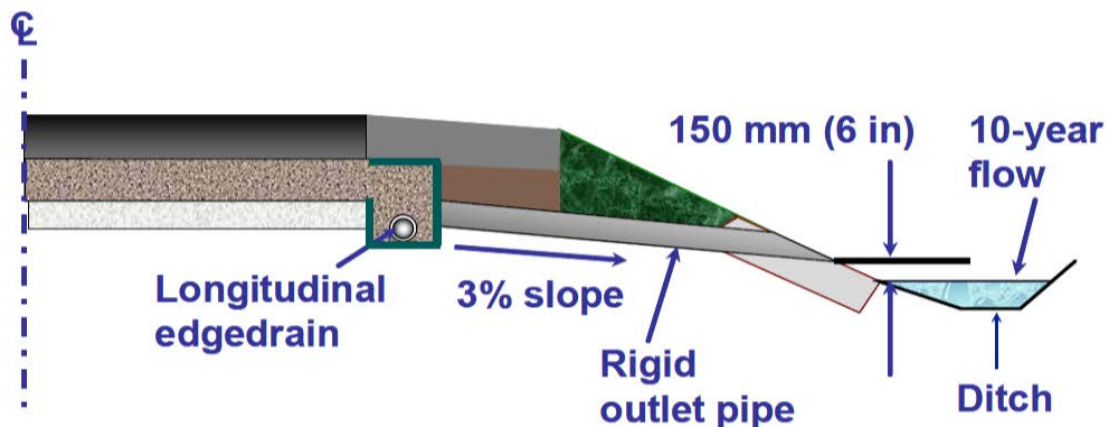
Figure 3.4 Recommended design for edge drain outlet (FHWA-NHI-08-030)

Top View Detail of Slotted Headwall

50 mm (2 in)
20 mm (0.8 in)
45 Deg.

Rodent Screen Detail

150 mm (6 in)
150 mm (6 in)
Openings: 5 to 10 mm (0.2 to 0.4 in) Square

Side View

75 mm (3 in)
75 mm (3 in)
125 mm (5 in)
100 mm (3 in)
75 mm (3 in)
900 mm (35 in)

Front View

200 mm (8 in)
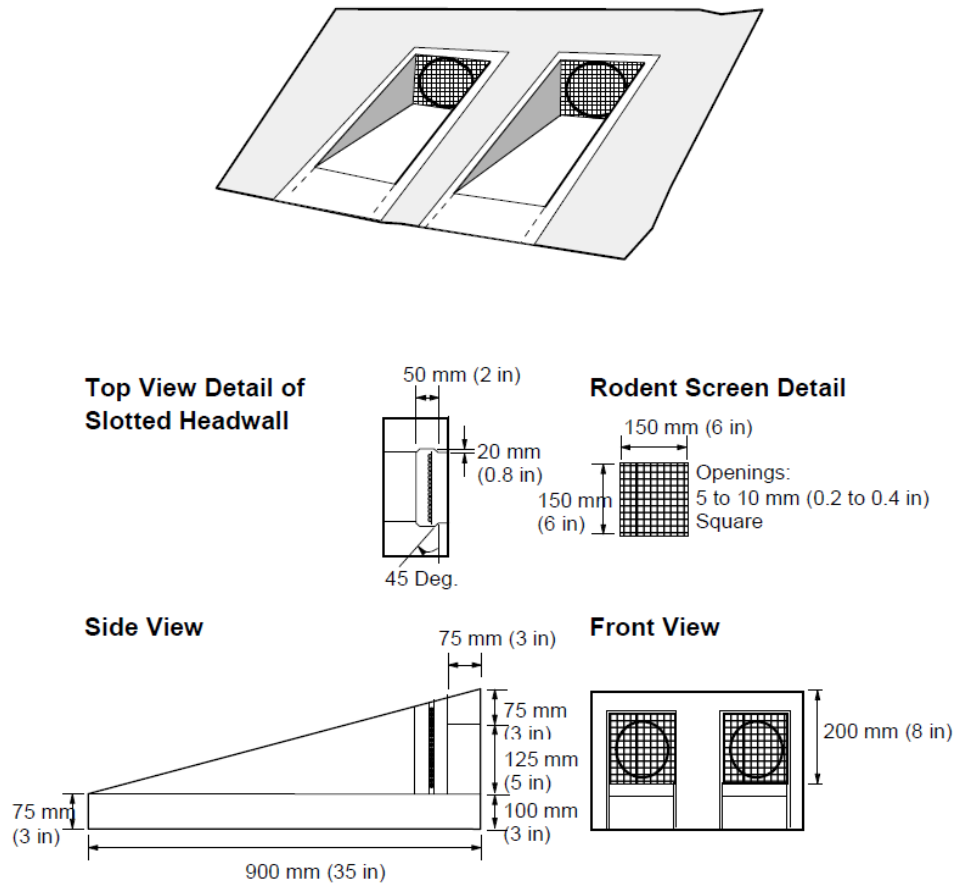
Figure 3.5 Recommended headwall design for dual outlet system (FHWA-NHI-08-030)

3.2.6 Summary guidelines

Overall the choices made on what option to use for a drainable base, separator layer, and water removal system are often governed by a single characteristic of the site conditions – often subgrade quality. This is because the recommendations made above for each individual option often tie together into comprehensive design schemes. For instance, a weak subgrade may require that a treated separator layer is used. A treated permeable base is then necessary to accommodate the separator layer. Daylighting the permeable base to remove water is now an acceptable option for the dominant portion of the roadway. This example demonstrates how the choices made for one component leads to choices for other components due to compatibility recommendations made above.

With this in mind, if a particular component option is desired, such as an untreated permeable base of a certain gradation, designers may follow compatibility requirements to design the remaining components. This example may require a geotextile separator layer to prevent intermixing of layers, longitudinal edge drains, and a stabilized subgrade if the subgrade has insufficient strength.

3.3 "AN EVALUATION OF IDOT'S CURRENT UNDERDRAIN SYSTEMS"; ILLINOIS DEPARTMENT OF TRANSPORTATION, 1995

Illinois as a state has been using underdrain systems since the 1970's. In 1995 IDOT evaluated the effectiveness of pipe and mat underdrains. Both have been heavily used in the state and it was unclear if one performed better than the other. The experiment consisted of unearthing a section of shoulder at 52 locations which had underdrain systems. The removed sections were then examined for damage and later tested in a lab for flow rates. The results of which provide valuable recommendations for agencies considering either. The recommendations include:

- Discontinuing the use of polypropylene products because they tend to collect fines and lose functionality
- Discontinuing the use of two manufacturers drainage mats as they are prone to structural damage and loss of functionality; drainage mats are typically plastic with circular openings that are placed below the pavement surface and act as a highly permeable layer
- Revised maintenance procedures to ensure screens are in place at all drain outlets and that mowing occurs as close to the outlets as possible

3.4 "EVALUATION AND ANALYSIS OF HIGHWAY PAVEMENT DRAINAGE"; KENTUCKY TRANSPORTATION CENTER, 2003

The Kentucky Transportations Center conducted an analysis of drainage system performance by utilizing finite element models to investigate various pavement designs incorporating subsurface drainage components. The models assumed a steady state saturated flow. In these models the drainage system components and pavement materials and conditions were varied. The project was interested in not only determining the effectiveness of drainage systems but what factors affect the inflow of water into the pavement layers. The results of this modeling led to the following conclusions:

- Pavement geometry affects surface drainage but not subsurface drainage
- Cracks in the pavement increase the inflow of water into subsurface layers and thus the need for subsurface drainage features
- For widening projects, longitudinal drains should be placed at the interface of new and old layers to shorten the drainage path
- A surface drainage layer with low permeability should have underlying layers with increasing permeability to ease the movement of subsurface water while still maintaining structural integrity

3.5 "COMPARISON OF PAVEMENT DRAINAGE SYSTEMS"; MNROAD, 1995

This project detailed the effectiveness of drainage in four test sections. These sections were designed with varying subsurface drainage features including one control section without subsurface drainage designs. The remaining three sections utilized longitudinal drains and/or permeable asphalt treated layers. Reflectometers were placed in the constructed layers of the sections so that saturation and flow could be measured at the time of construction and after rain events. The conclusions for this experiment include:

- Although all sections demonstrated the ability to drain subsurface water, sections with a permeable asphalt treated layer drained the most volume of water, typically within two hours
- About 40% of all rainfall penetrates the pavement surface
- Sealing longitudinal and transverse joints provided protection from inflow for roughly two weeks before typical inflow resumed
- The project recommended that measurements continue to be made and that structural performance of the surface pavement be monitored.

3.6 NCHRP PROJECT 1-34

In this section a summary of the methodology, results, and recommendations of all four phases is provided. Project 1-34, phase A was the first attempt for the NCHRP at characterizing the performance of subsurface drainage systems. This project was completed in 1998. Once complete, the NCHRP financed phase B to critically review the original project as well as establish a blue print for long-term evaluation. This plan

was enacted upon in phase C of the project through the Special Pavement Study-2 (SPS-2). Phase C ran from 1998 until 2002. The final installment, phase D, continued analyses of the SPS-2 sections in addition to focusing on testing the long term functionality of the drainage systems. This phase included data through 2005.

3.6.1 Project 1-34 A and B

NCHRP Project 1-34A and B provided an initial look at the performance of subgrade drainage systems in use at that time. The bulk of observations made were from databases provided by the Federal Highway Administration (FHWA) and from visual distress surveys performed on rigid pavements found throughout the country. Data collected through these methods was then used to create mechanistic-empirical models. Visual surveys were completed for each section in which a verbal description was provided on the condition of the roadway. Rutting, fatigue cracking, and the condition of the drain outlets were the predominant comments for the surveys. Additionally, information was collected on the age, repair history, and traffic volume seen at each location. Table 3.10 provides a summary of the test sections surveyed. States represented in this phase include: Kansas, Minnesota, North Carolina, Pennsylvania, Wisconsin, Illinois, Oklahoma and Ontario. For JPCP sections, three of the nine locations investigated had drained and undrained sections at the same location; for JRCP and CRCP sections each had one location with both a drained and undrained sections.

Table 3.10 Summary of pavement sections investigated in NCHRP 1-34A and B.

Pavement Type	JPCP	JRCP	CRCP
Sections with permeable base	11	4	10
Sections with edge drains	19	5	12
Number of Locations	9	3	4

The findings for this project were reported by identifying the pavement type and then summarizing visual distress surveys. Ideally, direct comparisons between undrained sections and drained sections were made and the performance could be evaluated. However this was rarely possible. Most observations revealed that small, if any;

statistical differences existed between drained and undrained sections if the undrained sections "were properly designed". Of the observations where statistical evidence existed, conclusions made by the research team include:

- The number of deteriorated cracks in JRCP was lower for permeable bases
- Cement-treated permeable bases (CTB) should not be used in conjunction with CRCP due to excessive bonding
- Concrete sections with permeable bases averaged less than half the amount of deteriorated joints than that of sections with dense-graded bases
- Permeable bases are easily penetrated by fines
- Edge drain outlets must be well maintained to function properly due to vegetation overgrowth and other means of clogging such as rodent nests

Upon completion of this phase, the research team noted that any conclusions presented were with the limited amount of data available and should be investigated with a larger sample group along with more numerical methods as opposed to subjective visual reports. It was with this knowledge that Project 1-34B was able to create a plan that would eliminate many of the shortcomings of Project 1-34A. Among their suggestions for future research were longer analysis of sections, direct comparisons between drained and undrained sections at the same location to eliminate doubt about climactic and geological variables, and more advanced analytical techniques (coring, deflection data, roughness measurements, video inspection of edge drains).

3.6.2 Project 1-34 C

With the recommendations of Project 1-34B and the inclusion of SPS-2 sections, Project 1-34C undertook a long-term evaluation of rigid pavements with subsurface drainage features. The SPS-2 experiment was designed to assess the influence of concrete width and thickness, flexural strength, base type, sub drainage, climate and traffic level.

Some specifics of the investigation are given below:

- Fourteen locations were investigated to represent varied climactic variables (rain and temperature)
- Each location has 12 sections of varying width, flexural strength and thickness – 4 drained and 8 undrained

- Every drained section (asphalt treated permeable base) has two control sections – 1 dense graded aggregate and 1 lean concrete base

The focus of this project was on the structural performance of the trial sections, thus parameters reflecting the structural integrity were measured throughout the project. Parameters of interest include transverse and longitudinal cracking, faulting, rutting and the International Roughness Index (IRI). IRI calculations were made by averaging the IRI value of each wheel path at the time of construction and periodically throughout the phase. The conclusions for this project were framed around the statistical differences in these parameters by comparing numerical values of undrained sections versus drained sections.

The team found that for transverse and longitudinal cracking as well as faulting, the control sections tended to deteriorate first, although in most cases the differences were statistically insignificant. In the case of IRI, they determined that the quality of drainage was not a factor.

Recommendations from the 1-34C team include:
- Adding deflection data to the list of structural integrity parameters used above (cracking, faulting, rutting and IRI)
- Testing the capabilities of the drainage systems in place by measuring flow rates
- Determining the effect of filter fabrics on flow rates
- Adding the data from the SPS-2 to the most recently completed database

The team found that the largest shortcoming of their findings was differentiating what effects were due to base type and which were due to drainage capabilities.

3.6.3 Project 1-34 D

With the recommendations of Project 1-34C, the methodology of Project 1-34D would continue to collect structural data such as cracking, faulting, rutting and IRI values in addition to the collection of deflection data, the measurement of flow rates through the drainage systems and the use of video equipment to survey the condition of drainage pipes below the ground surface. Flow rates through the sections were tested by coring and removing a hole in the pavement surface, then running water through the hole. The outlets were then monitored to measure flow through them. The sections analyzed in

this project include not only the SPS-2 sites but also related data from the Minnesota Road Research Project and the Wisconsin Department of Transportation. This allowed for analysis to be done for the sections of 10 years or more.

Highlights from the findings of this project are found below:

- Edge drains may never function fully or at all due to the nature of some subgrade soils. Water may be more conducive to flowing downwards through the soil as opposed to laterally through the edge drains
- Deflection data suggests that deformation in a section is related to the stiffness of the base material rather than the quality of drainage.
- Load transfer values for undrained sections are no worse than drained, permeable base sections
- IRI values, initial and final, are predominantly due to base stiffness
- In terms of faulting, sections with undrained lean concrete bases or permeable asphalt-treated base are slightly better than sections with dense graded aggregate bases
- In terms of cracking, lean concrete bases (LCB) performed the worst, followed by dense aggregate bases and then permeable asphalt treated bases; more than 60% of the LCB sections had some cracking while only 30% of the aggregate-base and PATB sections had only nominal cracking
- Edge drain pipes were sometimes crushed during construction
- Outlets that received little maintenance would become overgrown with foliage and lose functionality

Overall, the research team concluded that performance of the test sections was related more with the stiffness of the base material rather than the drainage capabilities of the base. This however should not deter agencies from considering subgrade drainages systems. Project 1-34D makes these final recommendations to agencies:

- Consider climate and soil taxonomy as to identify sites that are at risk for excessive moisture and poor natural drainage
- Review visual distress surveys from local roads for signs of poor drainage (pumping, potholes, etc.)

Due to the conclusion that stiffness of the base layers contribute more to structural performance than drainage, it is recommended that designers consider a stiffer base layer, although a base layer that is too stiff such as LCB showed increased cracking in a significant number of sections investigated.

3.7 CONCLUSIONS

The majority of the reports reviewed suggested that roadways with subgrade drainage systems tend to perform closely with that of their undrained counterparts in terms of structural integrity. Furthermore, with subgrade drainage systems, proper construction procedures and periodic maintenance of drainage outlets must be taken into consideration to ensure the effectiveness of these systems. Areas with high annual precipitation or soils with low permeability appear to be good candidates for these drainage features.

4.0 INCREASING THE QUANTITY OF WEATHER SITES WITH CLIMATIC DATA IN OKLAHOMA

4.1 INTRODUCTION

Reliable climatic inputs are critical to produce high quality results with the AASHTO MEPDG. The temperature and moisture gradients in the pavement and subsurface and consequently the pavement stresses are directly dependent on the weather inputs. In the current version of the MEPDG, the user may select several weather stations that can be interpolated based on the project location to produce a virtual weather station (ARA 2004). At least 2 years of data is required for a station to be used in the MEPDG, however more data is recommended. Having more weather stations over a longer period of time will greatly improve the reliability of the designs made using the MEPDG. This project involved the updating or creation of 39 weather files in Oklahoma, along with 14 in neighboring states. This is an increase from only 15 weather files previously available for Oklahoma. A map and data file compatible with Google Earth of depths to groundwater in Oklahoma have been made for guidance in selecting the average annual depth of water table for input in the MEPDG.

4.2 WEATHER FILES CREATION AND VALIDATION

The weather data used for the MEPDG climate file upgrading and creation was supplied by the National Climatic Data Center (NCDC), which is part of the National Oceanic and Atmospheric Administration of the U.S. Department of Commerce. The Global Integrated Hourly Surface dataset is available via free online access for unrestricted use inside the U.S. This data can be accessed using the NCDC Climatic Data Online system at http://cdo.ncdc.noaa.gov/. After obtaining this data it was imported into a spreadsheet for filtering and editing. The data was first filtered to ensure that only one data point per hour was included, as some weather stations collected data at more frequent intervals. Next, the hourly relative humidity was calculated from the dry and wet bulb temperatures contained in the weather files. The sky cover was converted to a numeric value according to the following scale: clear skies were assigned to be 100, scattered clouds were assigned to be 67, broken sky cover was assigned to be 33, and overcast was assigned to be 0. Missing weather values, which are inevitable for any

weather station because of maintenance, malfunction, or extreme weather, were corrected in to supply the software with a continuous set of data. Missing values of less than 3 hours in a row were filled in from the average of the weather data from the hours immediately before and after the missing data points. This method was chosen for continuity of data, and barring an unusually short and extreme event is believed to be the most probable values for the missing data. When less than two days in a row of data was missing, the missing data was calculated as the average of the value from the same hour on the days before and after the missing data points. When more than two days of data in a row was missing, the missing data was calculated from the average of the weather values from the same date and time from the data from other available years of that weather station. When these longer periods of data were missing, it was considered necessary to use the average of the values from the remaining year's data so as to not bias the weather data towards any particular year's data. It was also considered unlikely that the data from surrounding days would be representative for these missing days.

Fifteen weather files that were created by ARA, Inc. and included as part of the original data available with the MEPDG were updated to include available data from 2006 to the present. Weather files were created from weather station data available from 24 additional cities in Oklahoma. The weather files are comma separated text files with the extension .hcd. Each line of data contains one hour of weather information for the city of interest in the following format:

"YYYYMMDDHH,Temperature,WindSpeed,%Clouds,Precipitation,RelativeHumidity".

The file number needs to match that found in the station.dat file used by the MEPDG, and is the Weather-Bureau-Army-Navy (WBAN) ID number assigned to the weather station. The station.dat file contains the file number, the city name, the weather station description, the Latitude and Longitude, the elevation, the first date found in the climatic data file, and if the data file is clean "C" or has a missing month "M1". It is the station.dat file that is used during the weather station selection process in the MEPDG, so it is important that the information in the station.dat file match that found in the climatic data file. The existing data files were updated by simply appending the new weather information in the correct format to the end of the existing files. Fourteen

additional weather files were created from weather stations available in neighboring states that are close to the Oklahoma border. These climatic data files will be useful when using the MEPDG to create a virtual weather station by interpolation. Table 4.1 shows the cities now available, the dates previously available in the climatic data files, and the date ranges now available.

Table 4.1 Dates contained in previous and new climatic data files

Weather Station Location	Weather Station Description	Previous File		New File	
		Date Started	Dated Ended	Date Started	Date Ended
ADA, OK	ADA MUNICIPAL AIRPORT	-	-	4/1/2004	3/31/2009
ARDMORE, OK	ARDMORE DOWNTOWN AIRPORT	-	-	6/1/2005	4/30/2009
BARTLESVILLE, OK	BARTLESVILLE FP FIELD	-	-	6/1/2003	5/31/2009
CHANDLER, OK	CHANDLER MUNICIPAL AIRPORT	-	-	7/13/2004	4/30/2008
CHICKASHA, OK	CHICKASHA MUNICIPAL AIRPORT	-	-	12/29/2004	3/31/2009
CLAREMORE, OK	CLAREMORE REGIONAL AIRPORT	-	-	8/1/2004	3/31/2009
CLINTON, OK	CLINTON-SHERMAN AIRPORT	11/1/1996	2/28/2006	11/1/1996	3/31/2009
CUSHING, OK	CUSHING MUNICIPAL AIRPORT	-	-	7/1/2005	3/31/2009
DUNCAN, OK	HALLIBURTON FIELD AIRPORT	-	-	7/14/2004	3/31/2009
DURANT, OK	DURANT EAKER FIELD	-	-	5/1/2004	3/31/2009

Weather Station Location	Weather Station Description	Previous File		New File	
		Date Started	Dated Ended	Date Started	Date Ended
	AIRPORT				
EL RENO, OK	EL RENO MUNICIPAL AIRPORT	-	-	9/1/2005	3/31/2009
ENID WOODRING, OK	ENID WOODRING MUNICIPAL AIRPORT	-	-	4/1/2005	4/30/2009
ENID VANCE, OK	ENID VANCE AFB	-	-	11/2/2006	4/30/2009
FREDERICK, OK	FREDERICK MUNICIPAL AIRPT	2/1/1998	2/28/2006	2/1/1998	3/31/2009
GAGE, OK	GAGE AIRPORT	11/1/1996	2/28/2006	11/1/1996	3/31/2009
GROVE, OK	GROVE MUNICIPAL AIRPORT	-	-	8/1/2004	3/31/2009
GUTHRIE, OK	GUTHRIE MUNICIPAL AIRPORT	4/1/1998	2/28/2006	4/1/1998	3/31/2009
GUYMON, OK	GUYMON MUNICIPAL AIRPORT	12/1/1998	2/28/2006	12/1/1998	3/31/2007
HOBART, OK	HOBART MUNICIPAL	8/1/1996	2/28/2006	8/1/1996	3/31/2009

Weather Station Location	Weather Station Description	Previous File		New File	
		Date Started	Dated Ended	Date Started	Date Ended
	AIRPORT				
IDABEL, OK	IDABEL RGNL AIRPORT	-	-	8/1/2005	3/31/2009
LAWTON, OK	LAWTON-FORT SILL RGNL ARPT	10/1/1996	2/28/2006	10/1/1996	3/31/2009
MC ALESTER, OK	MC ALESTER REGIONAL ARPT	8/1/1996	2/28/2006	8/1/1996	3/31/2009
MUSKOGEE, OK	DAVIS FIELD AIRPORT	8/1/1996	2/28/2006	8/1/1996	3/31/2009
NORMAN, OK	NORMAN WESTHEIMER AIRPORT	-	-	2/1/2005	3/31/2009
OKLAHOMA CITY, OK	WILEY POST AIRPORT	8/1/1996	2/28/2006	8/1/1996	3/31/2009
OKLAHOMA CITY, OK	WILL ROGERS WORLD AIRPORT	7/1/1996	2/28/2006	7/1/1996	7/31/2008
OKMULGEE, OK	OKMULGEE MUNICPAL AIRPORT	-	-	5/26/2004	3/31/2009
PAULS VALLEY	PAULS VALLEY MUNICIPAL AIRPORT	-	-	11/1/2004	3/31/2009

Weather Station Location	Weather Station Description	Previous File		New File	
		Date Started	Dated Ended	Date Started	Date Ended
PONCA CITY, OK	PONCA CITY REGIONAL ARPT	36831	38776	11/1/2000	3/31/2009
POTEAU, OK	POTEAU ROBERT KERR AIRPORT	-	-	6/1/2004	3/31/2009
SALLISAW, OK	SALLISAW MUNICIPAL AIRPORT	-	-	6/1/2004	3/31/2009
SEMINOLE, OK	SEMINOLE MUNICIPAL AIRPORT	-	-	2/1/2006	4/30/2009
SHAWNEE, OK	SHAWNEE NAS	-	-	6/1/2004	3/31/2009
STILLWATER, OK	STILLWATER REGIONAL ARPT	12/1/1996	2/28/2006	12/1/1996	3/31/2009
TAHLEQUAH, OK	TAHLEQUAH MUNICIPAL AIRPORT	-	-	6/1/2004	3/31/2009
TULSA, OK	TULSA INTERNATIONAL ARPT	7/1/1996	2/28/2006	7/1/1996	9/30/2008
TULSA, OK	RICHARD LLOYD JONES JR APT	8/1/1998	2/28/2006	1/1/1998	3/31/2009
WATONGA, OK	WATONGA AIRPORT	-	-	12/1/2004	1/31/2009

Weather Station Location	Weather Station Description	Previous File		New File	
		Date Started	Dated Ended	Date Started	Date Ended
WEST WOODWARD, OK	WEST WOODWARD AIRPORT	-	-	6/1/2004	3/31/2009
Coffeyville, KS	Coffeyville Municipal Airport	7/1/1996	2/28/2006	7/1/1996	7/31/2009
Elkhart, KS	Elkhart, KS	-	-	11/1/2003	7/31/2009
Liberal, KS	Liberal Municipal Airport	-	-	5/1/2004	7/31/2009
Parsons, KS	Tri-City Airport	7/1/1996	2/28/2006	7/1/1996	7/31/2009
Winfield, KS	Strotner Field Airport	7/1/1996	2/28/2006	7/1/1996	7/31/2009
Canadian-Hemphill, TX	Canadian, TX	-	-	8/1/2003	7/31/2009
Clarksville, TX	Clarksville Red River Airport	-	-	6/1/2004	5/31/2009
Gainsville, TX	Gainesville, TX	-	-	6/1/2004	5/31/2009
Mt. Pleasant, TX	Mount Pleasant Airport	7/1/1996	2/28/2006	7/1/1996	5/31/2009
Perryton, TX	Perrytown Ochiltree Airport	-	-	6/1/2004	5/31/2009
Randolph, TX	Randolph Air Force Base	-	-	1/1/2004	5/31/2009
Sherman, TX	Grayson Co Airport	-	-	6/1/2004	5/31/2009
Vernon, TX	Vernon Wilbarger Co Airport	-	-	6/1/2004	5/31/2009
Wichita Falls, TX	Shephard AFB	7/1/1996	2/28/2006	7/1/1996	5/31/2009

The MEPDG currently does not consider any data in the climatic files after February of 2006, which is the most relevant data and also the majority of the new data included from this project. After conversations with Mike Darter, one of the lead researchers on the development of the MEPDG, it was determined that the best course of action for the weather files would be to backdate the years of the weather data created in this project from anywhere between one and three years. Any data from February 29 was then moved to the nearest leap year to prevent any program errors. This would allow for the maximum amount of weather data to be used in the MEPDG calculations, and would not affect the values calculated since the years of the climatic data are not used in the calculations. A copy of the original weather files before backdating is also included with this report for archival purposes and for when this problem with the MEPDG is corrected. Figure 4.1 shows a map of the location of the MEPDG climate files upgraded or created as part of this project.
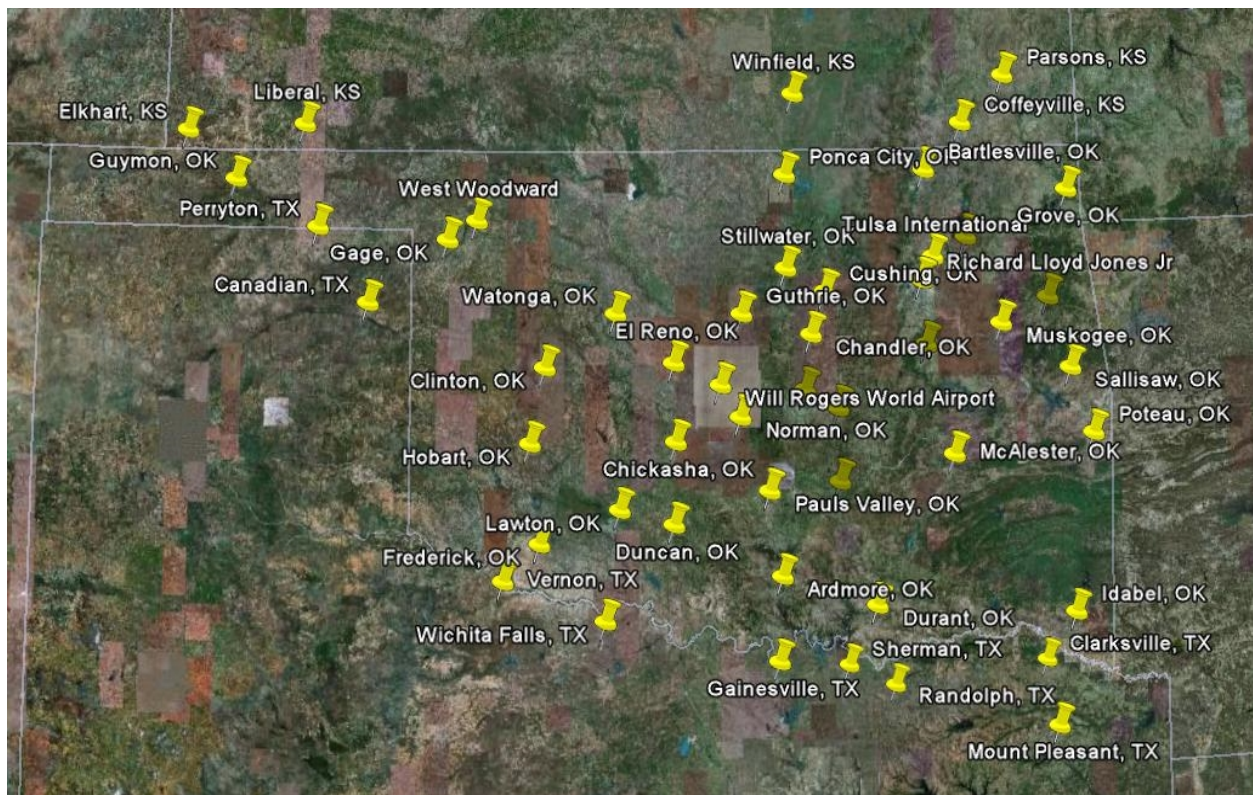
Figure 4.1 Location of weather stations used to update and create new MEPDG climate files.

A program has been created to install the MEPDG climate files in the proper folders on the user's computer. The file installer begins by double clicking on the setup.exe file, and is installed by following the on-screen directions. The program when launched will ask for the root folder containing the MEPDG and all of its subfolders and files, which is usually "C:\DG2002". Once the folder is selected and the user clicks the OK button, the program will automatically install the new climate files and station master list file to the correct locations for use by the MEPDG. To install the climate files manually, simply copy the climate files and paste them in the "HCD" subfolder of the MEPDG program folder. Then, the station.dat file must be copied to the "HCD" subfolder and the "Defaults" subfolder.

4.3 CONCLUSION

Climatic data files have been updated and created for use in designing rigid and flexible pavements in the state of Oklahoma. Average yearly depth to groundwater values have also been compiled for a wide range of geographical locations in Oklahoma. This is expected to result in better pavement designs which should translate into an overall reduced life-cycle cost.

5.0 IMPACT OF CURING TO REDUCE CURLING IN CONCRETE

Currently, the MEPDG requires that the user input the curing methodology to be used in a pavement's construction. From investigations on this project it appears that this is a major parameter in the design of continuous reinforced concrete pavement (CRCP). The wet mat cure has been indicated by the MEPDG to be the most effective curing technique; however, it is also the least economical to be implemented in the field. Classically, the primary reason that curing is required in concrete is to promote hydration, which in turn decreases the permeability and increases the strength of the surface concrete. One challenging aspect of this task is that there is not a standard method for investigating the effectiveness of different curing techniques.

Curing can have a number of interesting impacts on the curling of a concrete pavement. These include differential shrinkage of the concrete at the surface compared to the concrete at depth. Also, differential temperatures during set of the concrete can lead to an increase in curl to a concrete pavement that may increase stresses and lead to premature cracking. Much new information was learned from this work that has allowed wet curing to be directly compared to the use of curing compounds. This data provides new insights into the curling and warping of concrete pavement and the long term performance.

5.1 THE IMPACT OF WET AND SEALED CURING TECHNIQUES ON CURLING FROM DRYING SHRINKAGE

5.1.1 Introduction

The purpose of curing is to maintain adequate moisture content and temperature in concrete for a period of time immediately after placing and finishing in order to develop the desired properties. Proper curing can increase durability, strength, water-tightness, abrasion resistance, volume stability, and resistance to freezing and thawing and deicers; therefore, the exposed slab surfaces are significantly sensitive to curing. The improvement in concrete properties is rapid at early ages but continues more slowly thereafter for an indefinite period (Kosmatka, Kerkhoff, Panarese 2003).

Wet curing methods maintain the presence of mixing water and saturation in the concrete during early ages. Wet curing methods include ponding, fogging, and saturated wet coverings. These methods afford some cooling through evaporation, which can be beneficial in hot weather. Fabric coverings saturated with water, such as burlap, cotton mats, rugs and etc. are commonly used for wet curing.

The early age period in the life of concrete is approximately the first seven days after final set. Concrete properties change rapidly at early ages. Change in properties continues more slowly thereafter. Rapid and large moisture loss from the surface of a slab can reduce the degree of hydration. Also, harmful consequences like plastic shrinkage cracking, and decreases in strength, durability, and abrasion resistance can occur without precautionary curing. Some amount of curling is expected on every pavement project (ACI 302.1R). For the large moisture loss at the top layers, the difference in moisture content results in more drying shrinkage at the top than the bottom causing the slab to curl upward at the edges as shown in Figure 5.1 (Ytterberg 1987, Parts I, II, III). If the concrete is restrained, either internally or externally, restraint may cause the concrete to crack due to drying shrinkage.
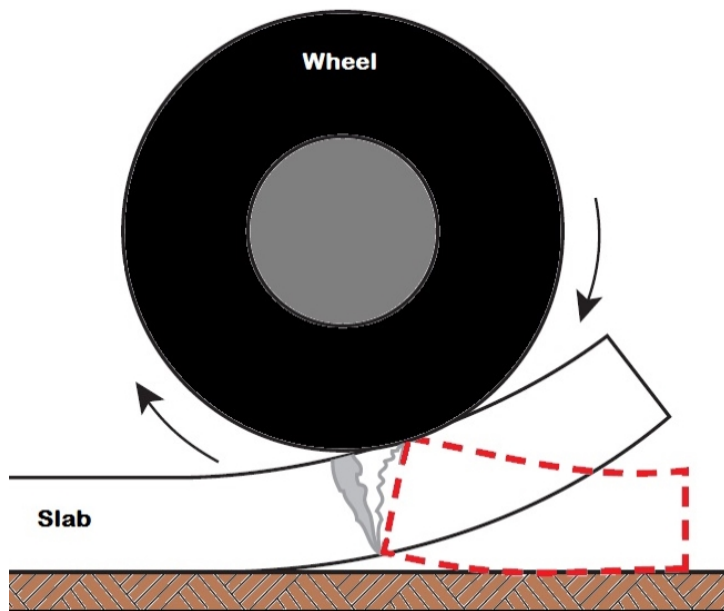
Figure 5.1 Warped slab cracks under the heavy wheel loading (Kosmatka et al 2003)

The amount and type of curing can affect the rate and ultimate amount of drying shrinkage. Wet curing methods, such as fogging or wet burlap, hold off shrinkage until curing is terminated, after which it has been reported that concrete dries and shrinks at a normal rate (Kosmatka et al 2003). The slab starts drying and shrinking immediately after the termination of the curing if the concrete has been kept continuously moist since casting and finishing. The moisture distribution in a hardened slab is assumed to be uniform before drying begins (Hanson 1968) and it starts changing as concrete loses moisture (Hedenblad 1997). Depending on the length of the drying period, drying conditions, and the initial water content, the RH at equilibrium varies (Hedenblad 1997). To avoid or lessen this moisture gradient, the top and the bottom of the slabs should be uniformly kept moist or dry. For points deeper within the concrete the drying time will increase to reach to a certain RH (Monfore 1963), and curing for longer than one day will significantly add to the drying time (Hedenblad 1997).

The drying shrinkage of the cement paste is six to eight times greater than amount observed in concrete (Bisschop 2002). The paste shrinks about 1.7 times more than mortar (Holt 2002). The shrinkage can be decreased by reducing the paste content, adding aggregate content (Tazawa et al. 1995). The impact of fly ash was found to either have no impact or increase the shrinkage of a mixture (Setter and Roy 1978; Justnes et al, 1998). Air content less than 8% was found to not influence shrinkage (Davis and Troxell 1954). So the shrinkage of the concrete (S_C) is highly affected by the shrinkage of the cement paste (S_P) and aggregate volumetric fraction (g) because the aggregate restrains the shrinkage of the cement paste in the concrete (Pickett 1956):

Equation 5.1

$$s_c = s_P \left(1 - g\right)^n$$

The capillary forces during drying are generally the reason for shrinkage (Lane, Scott, and Weyers 1997). The drying shrinkage in cement paste is caused by a negative pressure called capillary tension (P_{cap}) inside the liquid phase after formation of menisci (curved liquid-vapor interfaces); so shrinkage of paste (S_P) can be defined as a function of capillary tension (P_{cap}), degree of saturation of cement paste (S), bulk modulus of paste (K), and modulus of solid skeleton inside cement paste (K_s) (Mackenzie 1950; Bentz et al.1998):

Equation 5.2

$$s_p = \frac{s}{3} P_{cap} \left(\frac{1}{k} - \frac{1}{k_s} \right)$$

Due to the generation of the hydration products in the cement matrix, autogenous shrinkage occurs; this component may be more important for concrete mixtures with w/c less than 0.40 (Tazawa 1999). The autogenous shrinkage will increase by reducing the w/cm and increasing the cement fineness since the capillary tension mechanism will cause higher tension in the pore water of the finer structure (Bentz et al. 2001a, Jensen and Hansen 1996). Also, due to the smaller volume of the hydration products than that of the reactants, there is an approximately 8% to 9% reduction in volume after hydration reactions called chemical shrinkage (Jensen and Hansen 2001). Due to lack of water, concrete sealed against moisture loss with w/c < 0.5 cannot progress to its complete potential hydration (Powers, 1948). Concrete with w/c < 0.4 can dry itself from inside (Powers 1948; Mills 1966; Cather 1994; Meeks and Carino 1999). Due to low permeability at those low w/c ratios, the curing water does not infiltrate away from the surface (Cather 1994; Meeks and Carino 1999). This layer of the concrete is highly affected by the curing water (Cather, 1992), which continues to a depth of approximately 1/4" to 3/4" depending on the concrete characteristics (Carrier 1983; Spears 1983). The lower permeability of the concrete causes the slower moisture movement between the cured surface and the interior (Pihlajavaara 1964, 1965). The formation of the menisci occurs in external drying as well; the specimen suffers from both external drying at the exposed surface and internal drying (self-desiccation) in an unsealed specimen. The radius of these menisci is reduced as moisture evaporates, and the internal RH of the cement paste decreases until the internal RH reaches the ambient RH, or equilibrium (Radlinska et al. 2008). The formation of the menisci and generation of the capillary tension (P_{cap}) can be related, according to the Laplace equation, if γ is surface tension of pore fluid, θ is the liquid-solid contact angle, and r is the radius of the curvature of the meniscus (Adamson and Gast 1997):

Equation 5.3

$$p_{cap} = -\frac{2 y \cos(0)}{r}$$

The solid surfaces or pore walls will be pulled together by this negative pressure, causing the volume change or shrinkage. The capillary tension is also related to the RH of the cement paste by the Kelvin equation (Adamson and Gast 1997):

Equation 5.4

$$p_{cap} = \frac{RT \ln (RH)}{V_m}$$

Where R is the universal gas constant, T is the temperature and RH is the internal relative humidity, and V_m is the molar volume of pore solution.

Others have suggested that the drying shrinkage may be increased by curing longer than 4 to 8 days and less than 35 to 50 days (Perenchio 1997). The shorter curing time will result in a faster drying rate (Hedenblad 1997; Jackson and Kellerman 1939). Wet curing for 28 days was found to increase the time needed to reach a certain RH by approximately 1 month (Hedenblad 1997). Slabs should not be cured by adding water like wet burlap and should be protected from any external water if drying time is critical (ACI 302.2R-06).

It has been shown that the drying shrinkage and curling may get worse when a vapor barrier is used immediately under the concrete. This causes the slab to lose little or no water from the bottom, while the top dries and shrinks at a faster rate (Anderson and Roper 1977, Nicholson 1981, Turenne 1978). Installing an impervious membrane like vapor/moisture barrier below the slab makes maintaining the moisture at the top of the slab highly essential to minimize curling. Therefore, ACI 302.1R suggests placing a 4 in. drainable, compressed fill on top of the vapor barriers to minimize this moisture gradient and to consequently decrease the curling. Also, for avoiding or minimizing this problem after curing, the wet burlap should be replaced with a plastic sheet until the concrete surface has become dry under the sheets (ACI 308R-01). Using a sheeting material to cure for 3 days is recommended for floor slabs (Suprenant and Malisch 1999c). Installing a floor covering causes the moisture movement from the bottom to the top of the slab; this movement will reduce the curling initially due to the expansion at the top as the moisture content there increases and the shrinkage at the bottom as the moisture content there decreases (Tarr et al. 2006).

While it is common to recommend that concrete receive a prolonged wet cure, some previous literature suggests that this may promote drying shrinkage. In a concrete pavement one concern is differential drying shrinkage that would occur over the cross section. This would cause curling and possibly cause damage to the pavement because of loss of support. Currently in the literature there is almost no work that has been done to investigate the impact of sustained wet curing on curling. This research will use paste and concrete specimens to further explore these concepts.

5.1.2 Experimental investigations

5.1.2.1 Paste beams

5.1.2.1.1 Materials
The Portland cement used in these tests was a type I/II, according to ASTM C 150, and its oxide analysis per ASTM C 114 and the phases' concentrations are shown in the following Table 5.1. The paste mixutures in this experiment had a water to cement ratio (w/c) of 0.34, 0.42, and 0.5.

Table 5.1a Oxide analysis of the cement used for paste beams and the phase concentrations

Chemical Test Results			
SiO_2	20.23	Fe_2O_3	3.23
Al_2O_3	4.77	CaO	64.15
MgO	1.90	SO_3	2.52

Table 5.1b Oxide analysis of the cement used for paste beams and the phase concentrations

Phase concentrations			
C_3S	70.69	C_3A	7.18
C_2S	4.68	C_4AF	9.83

5.1.2.1.2 Sample preparation and methods
The paste mixtures were prepared according to ASTM C 305. Three paste beams with dimensions of 39.4" x 2.4" x 0.5" were prepared in plastic molds from each mixture.

After casting all specimens were cured with wet burlap for 24 hours.   To restrict the moisture loss to a single surface the sides and bottom face of the beam were sealed with melted wax after demolding. Testing was also done with aluminum tape to compare the results. Little difference was found in the specimens and so the wax was used for all subsequent testing. The finished surface of the beam was exposed to different curing techniques for different durations. An overview of these specimens is shown in Figure 5.2. Thinner concrete members were chosen as they shrink faster than the thick members due to the faster drying rate; the shrinkage rate is generally assumed to be related to the ratio of the specimen's volume to its surface area (Hansen and Mattock 1966). The shape of the specimen determines the distance for water movement to the dry surface and the internal strains caused by the non-uniform shrinkage; the developed stresses and shrinkage strains due to the moisture gradients during drying is highly related to the specimen size (McDonald and Roper 1993; Pickett 1946; Browne 1967).
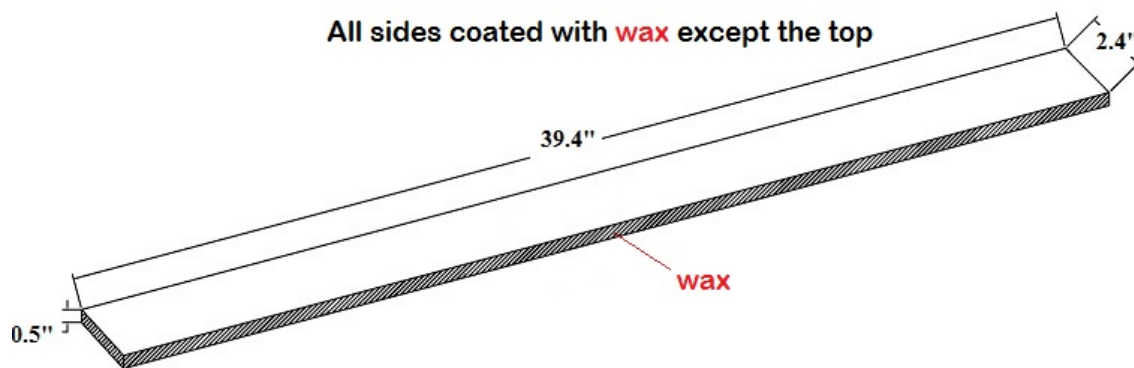
Figure 5.2 A waxed paste beam on all sides except the finished surface

The specimens were demolded, weighed, sealed with wax, and reweighed. Finally these specimens were stored in an environmental chamber at 73°F and 40% relative humidity. This caused a moisture gradient to form in the beam over time due to the water loss from only one side.

In this experiment since the top of the surface was not sealed with wax and water was allowed to evaporate. This differential loss of moisture caused a shrinkage gradient in the specimen. This gradient caused differential strain to occur and results in the curling of the specimen. This test is advantageous, as the moisture loss is quick and the

resulting gradients can be quite large. This leads to a significant deformation of the specimens that is easy to measure. To ensure that the curling measurements were only the result of this differential in strain caused by the drying, the beams were stored on their sides. This test is similar to previous work done by Burke (2004) to investigate the effectiveness of shrinkage reducing admixtures.

5.1.2.1.3 Test Procedure and measurement

To measure the curling, two ends of the specimen are attached to a flat aluminum plate with the uncoated surface facing the plate, as shown in Figure 5.3. The distance between the aluminum plate and the specimen is measured at regular locations along the length with a caliper that reads to 0.0005". The curling of the beam is symmetric and the maximum is at the middle of the beam. The weight of the sample is also measured at different times with a scale accurate to 0.1 grams. This measurement was used to get information about the moisture content of the specimen.
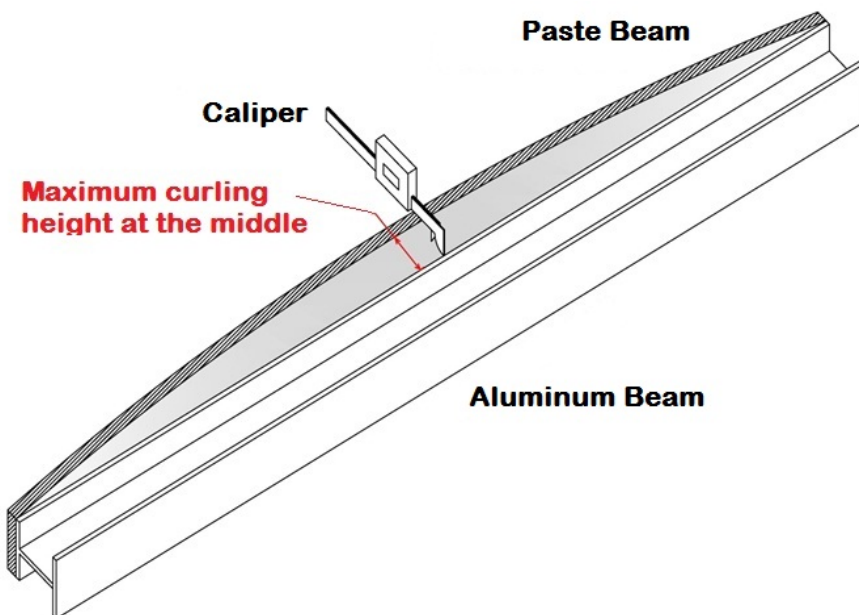
Figure 5.3 Measuring the curling height using a caliper

The focus of this work was to compare the performances of different durations of wet and sealed curing. All samples were wet cured at 73˚F for 1 day before demolding. This was necessary to ensure the specimens gained enough strength. Some samples were also kept in wet burlap for 1, 3, 7, and 14 days of additional curing after demolding

and waxing. The curing was then removed, and the specimens were subjected to the 40% relative humidity and 73 ˚F drying environment. In addition to wet curing, several specimens were cured in a sealed plastic bag for 1 and 3 days. This curing was similar to the wet burlap cure, but no external moisture was added to the specimens during the sealed curing process. Other samples received no curing after demolding.

5.1.2.2 Concrete beams

5.1.2.2.1 Materials

The cement used in this test is type I, according to ASTM C 150, and its chemical analysis is per ASTM C 114 shown in the following Table 5.2 beside the phases' concentrations.

Table 5.2 Chemical analysis of the cement used in this project for concrete beams

Chemical Test Results			
SiO_2	21.13	Fe_2O_3	2.55
Al_2O_3	4.71	CaO	62.06
MgO	2.37	SO_3	3.18
Phase concentrations			
C_3S	52.14	C_3A	7.69
C_2S	20.22	C_4AF	7.96

Samples were made with dolomitic limestone aggregate and natural river sand. An ASTM C 618 class C fly ash was also used. Wood rosin AEA was used for the first and second beams with no curing and 3 days wet curing techniques, but not for any others. During the testing it was found that it was too difficult to produce consistent air content between mixtures, and so the AEA was no longer used. The concrete beams were sealed in a similar manner to the paste beams. A moisture barrier was used as a form liner. This material had a plastic waterproof membrane on one side and fibers on the other. The fibers were oriented so that they bonded to the wet concrete and provided a tight fit of the water proof layer on the outside of the beam. The interface between the beam and the water membrane was sealed with hot glue to insure a good bond was

**5.1.2.2.2 Mixture proportions and Procedures**

In this experiment we used water to cement ratio equal to 0.41 for concrete beams. All of the aggregate, both coarse and fine, were charged into the mixer along with approximately two-thirds of the mixing water. The combination was mixed for three minutes. Next any clumped fine aggregate was removed from the walls of the mixer. Then the cement was loaded into the mixer, followed by the remaining mixing water. The mixer was turned on for an additional three minutes. Once this mixing period was complete, the mixture was left to "rest" for the following two minutes while the buildup of material along the walls was removed. Next the mixer was started and the admixtures were added and the mixer was allowed to run for the remainder of the three minutes. The slump (ASTM C 143), unit weight (ASTM C 138) and the air content (ASTM C 231) were measured. The typical mix proportion used in this test is presented in Table 5.3 for on a cubic yard basis.

Table 5.3 Mix proportion used in this experiment per Cubic Yard

Cement (lb)	451.2
Fly Ash (lb)	112.8
Course aggregate (lb)	1842.1
Fine aggregate (lb)	1276.1
Water (lb)	207.1

5.1.2.2.3 Sample preparations, casting and curing

In this experiment the size of the concrete specimen investigated was 7.5′×6″×8″. All sides of the beam were sealed with a synthetic moisture barrier except the top surface for each specimen. An overview of this specimen is shown in Figure 5.4. This specimen is similar to work done by Hansen et al. (2007) and Springenschmid et al (2001), with some modifications.
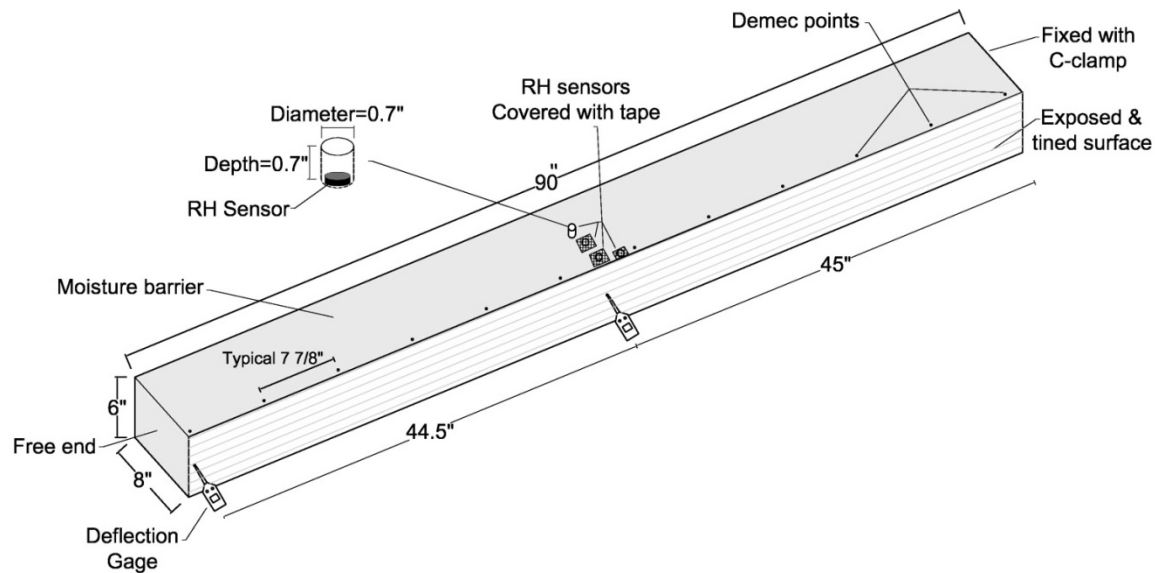
Figure 5.4 Concrete beam dimension and details

After placing and vibrating the concrete in 3 different layers the top surface was screeded with a piece of wood; burlap was dragged over it , and finally it was tined with a steel comb, creating tines with transverse grooves 1/16″ wide, 1/4″ deep, and with center to center spacing of 1″. The sample was carefully demolded 5 hours after casting. Then it was sealed at the seams with wax. Specimens were prepared with no curing and 1 and 3 days of wet cure with wet burlap and a plastic tarp. The beams were flipped on their side and placed on wooden dowels after the curing was completed. This was done to minimize the influence of gravity on the results. After placing the beam on its side, it was fixed at the end with a C-clamp, steel plates, and rubber bearing pads in an environmental chamber at 73° F temperature and 40% relative humidity.

5.1.2.2.4 Test procedure and measurement

The relative humidity was measured at 0.5″, 1″, 3″, and 5″ from the finished surface by using the DS1923 Hygrochron Temperature/Humidity Logger iButtons. The sensors were placed in 0.7″ deep holes with 0.7″ diameter that were cast into the side of the concrete beam as shown in Figure 5.5. During demolding the forms used to make these holes were removed and the holes were sealed with waterproof tape. Five days after the beam was stored on its side relative humidity gages were inserted into the beam.

These sensors were programmed to take relative humidity measurements every hour. This wait period was used so that the gages did not fail due to the high amount of moisture in the beam. The holes were again sealed with water poof tape after the gages were added. This tape was removed briefly when data was obtained from the sensors.

Figure 5.5 Plan view of the test setup showing the holes covered by tape, deflection gauge secured to the beam, and demec points glued on the surface of the concrete

The curling height of the beam was measured at two different locations: 45″ and 89.5″ from the end that is clamped. The accuracy of this gage was 0.0005". Also the surface strain of the beam was measured at 10 different locations, as shown in Figure 5.4 and Figure 5.5. Surface mounted stainless steel gage points were glued to the surface of the concrete beam. This was achieved by burning through the membrane in a localized area and then gluing one of these gage points. A mechanical strain gage was used to measure the movement of machined cones in points over time. The accuracy of this gage was 4 microstrain. These measurements were taken to check the curling measurements of the beam.

5.1.2.2.5 Calibration of RH sensors

The iButton sensors were calibrated according to ASTM E 104 "Standard Practice for Maintaining Constant Relative Humidity by Means of Aqueous Solutions" with four different salt saturated solutions. The relative humidity calibration range was between 57.6% and 97.3%. This was chosen in order to cover the ranges of humidity expected in the testing. A specific calibration was generated for each iButton.

5.1.3 Results

5.1.3.1 Paste beams

A typical result for a paste beam is shown in Figure 5.6. This figure shows the typical curves gained by measuring the deflection of the beam at different locations over time for a sample that was not cured after demolding with a 0.5 w/c. The maximum curling is at the middle of the specimen.
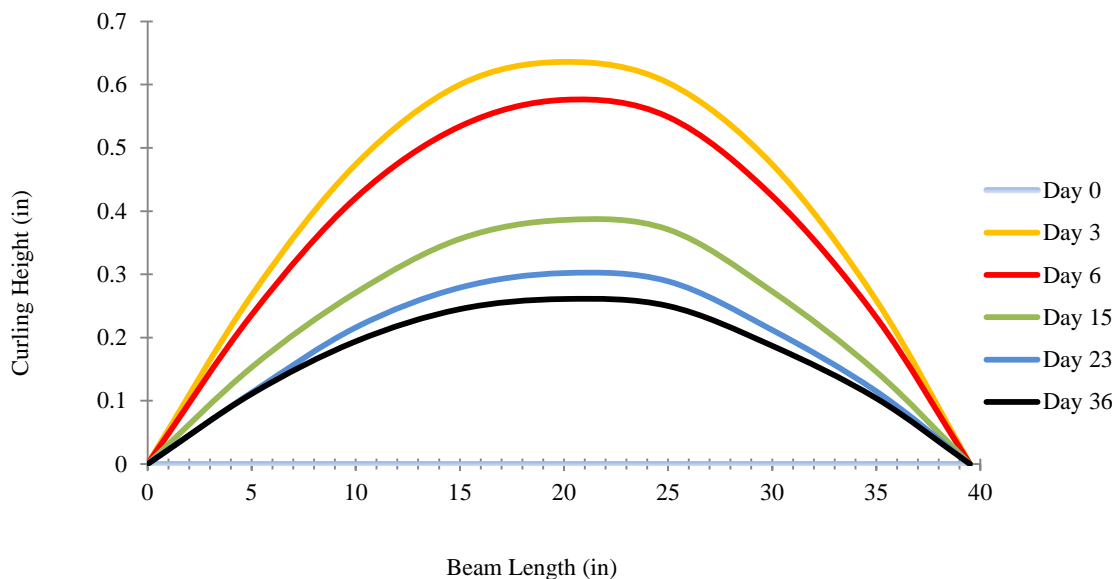
Figure 5.6 Curling height of a no-cured paste beam mixed with w/c=0.5

The following Figure 5.7 shows the change of the beam's weight after being exposed to the drying environment.
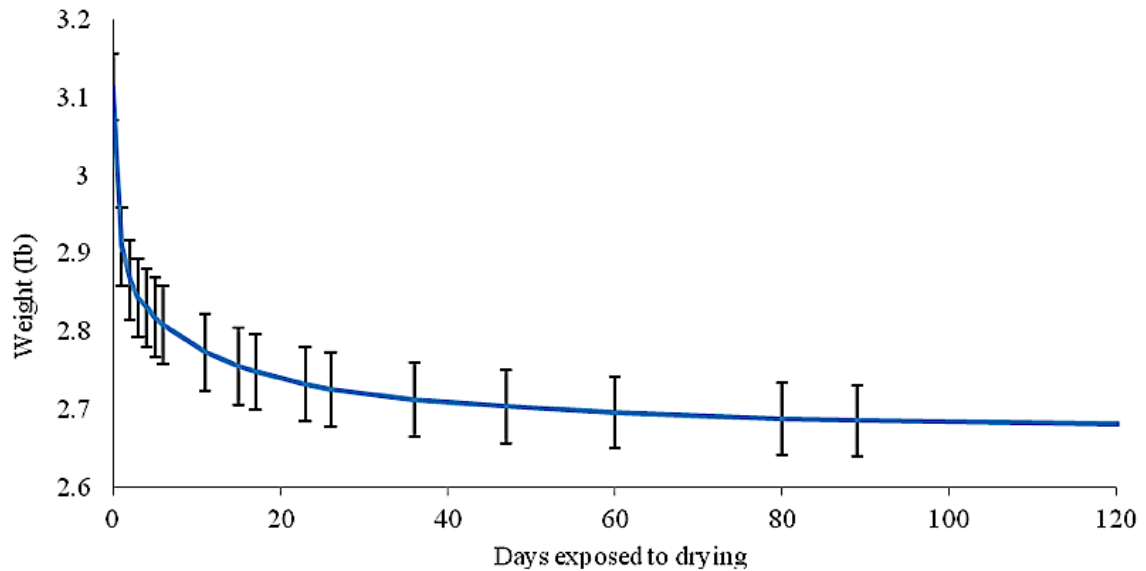
Figure 5.7 No-cured paste beam's weight vs. age

The moisture loss and the maximum curling height of samples of w/c=0.42 cured with wet burlap for additional 1, 3, 7, and 14 days and the measurements for a no-cured specimen over the time periods are shown in Figure 5.8 and Figure 5.9 respectively. The red markers show the point of maximum curling. Note that the time to this point increases with more curing. This was consistent for all of the specimens.
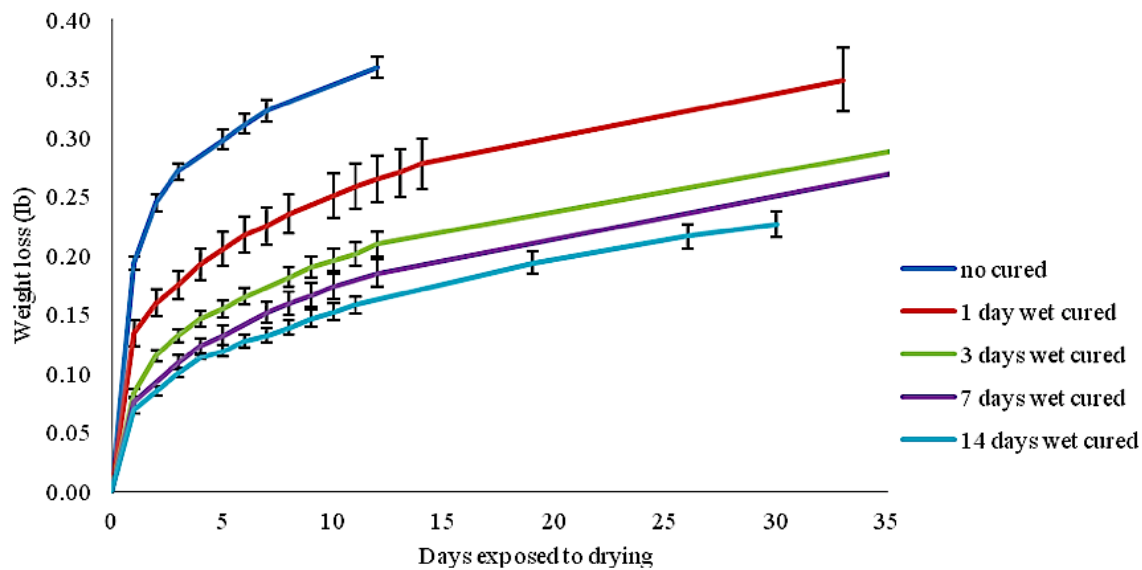
Figure 5.8 Weight loss vs. the age of the paste specimen
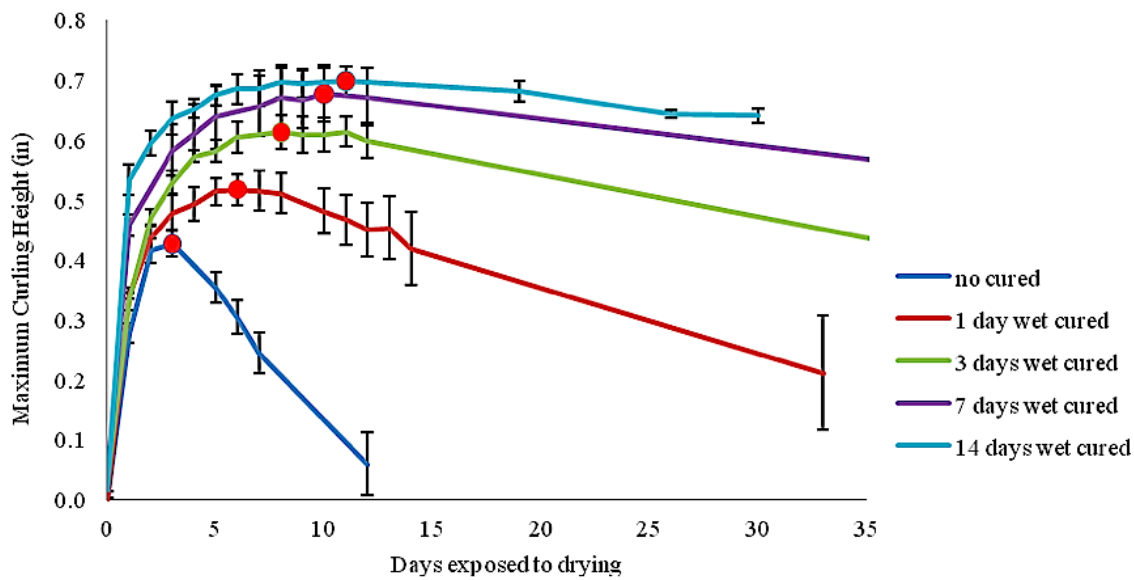
Figure 5.9 Paste beam's maximum curling height vs. time

The moisture loss and the maximum curling height of samples with the same w/c=0.42 sealed with a plastic bag for 1 and 3 days and the measurements for a no cured specimen at the same ages are shown in Figure 5.10 and Figure 5.11 compared to specimens of 1 and 3 days of additional wet curing.
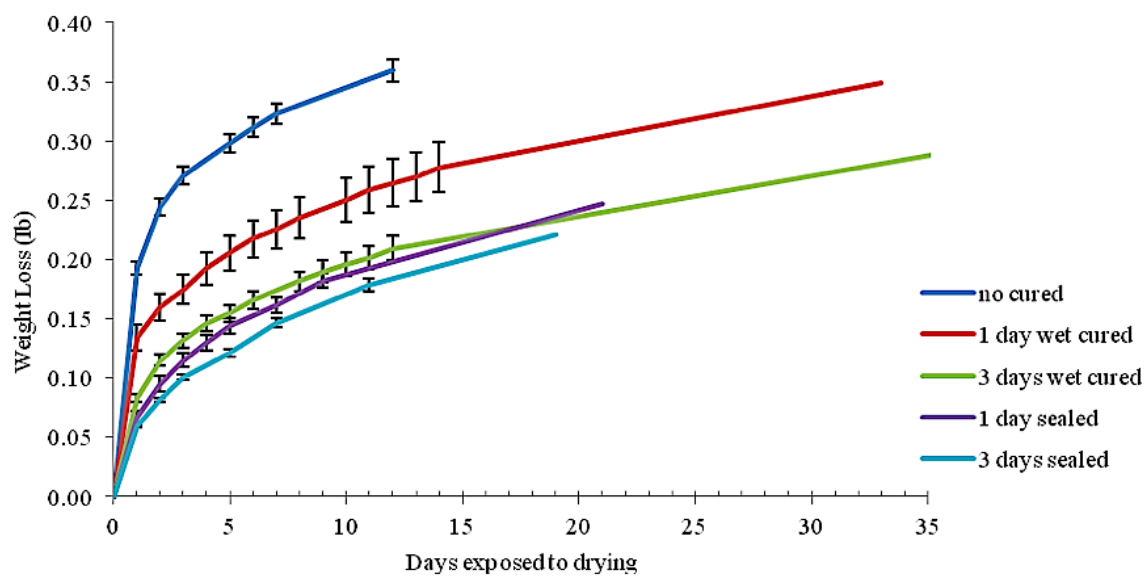
Figure 5. 10 Weight loss vs. age of the paste specimen
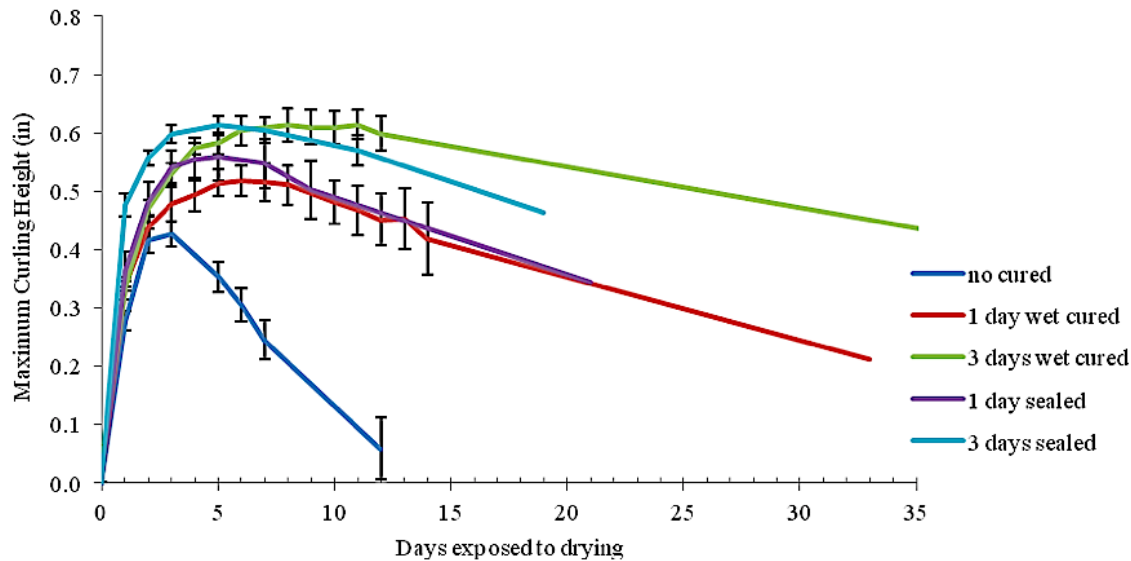
Figure 5.11 Paste beam's maximum curling height vs. days exposed to drying

Figure 5.12 summarizes the response of the samples with different w/c and curing

period.
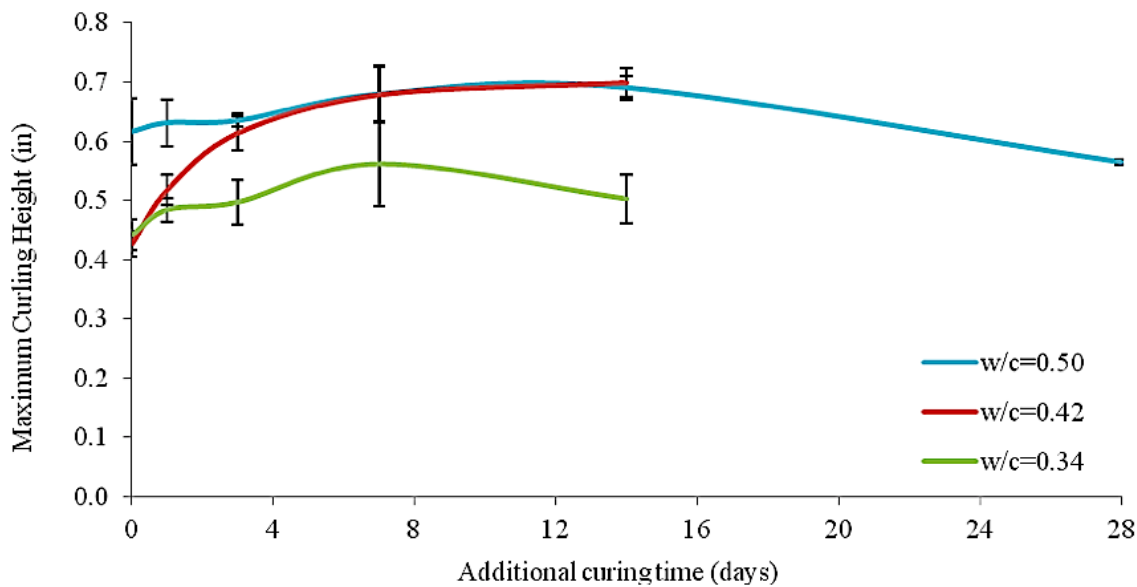
Figure 5.12 Comparison between the maximum deflections of paste beams with different w/c ratios

Figure 5.13 presents the weight loss of the specimens at maximum deflection versus

curing time.
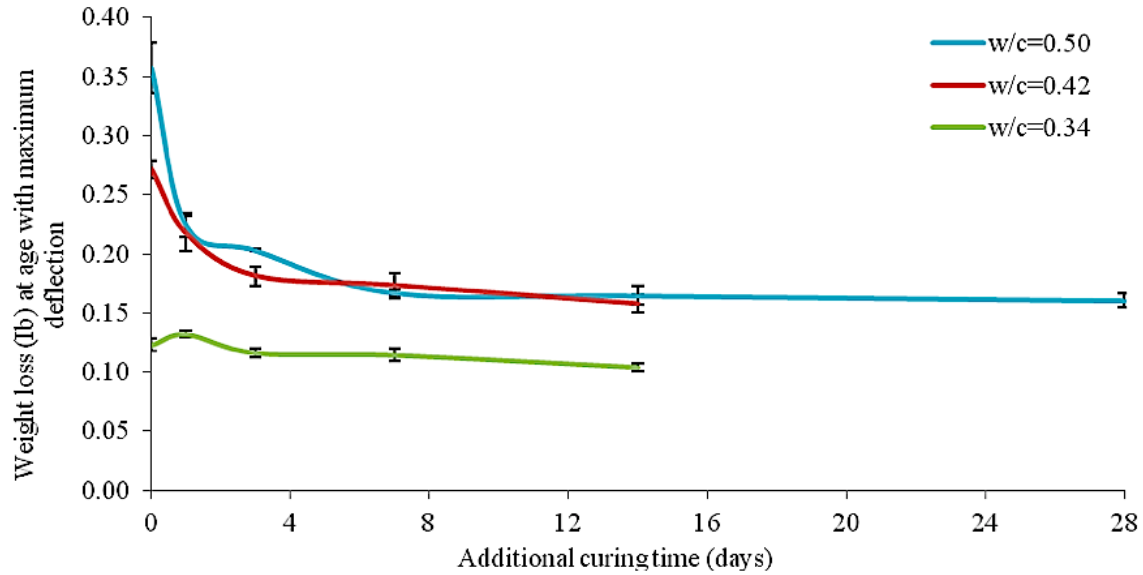
Figure 5.13 Weight losses of paste beams with different w/c ratios at age with maximum curling height

Figure 5.14 presents the weight loss after 11 days versus the additional curing time.
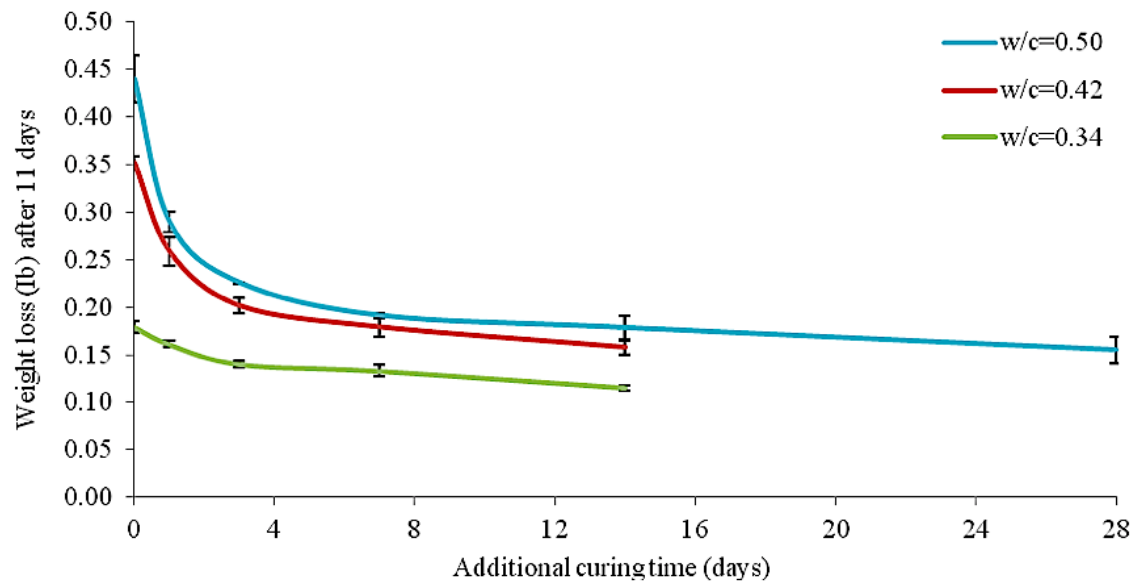
Figure 5.14: Weight losses of paste beams with different w/c ratios after 11 days

5.1.3.2 Concrete Beams

The average surface strain over the length of the beam and the tip deflection during the drying period are shown in Figures 5.15 and 5.16 for the specimens investigated. The methods used in this experiment are no-curing, 1-day wet curing, and 3-day wet curing.
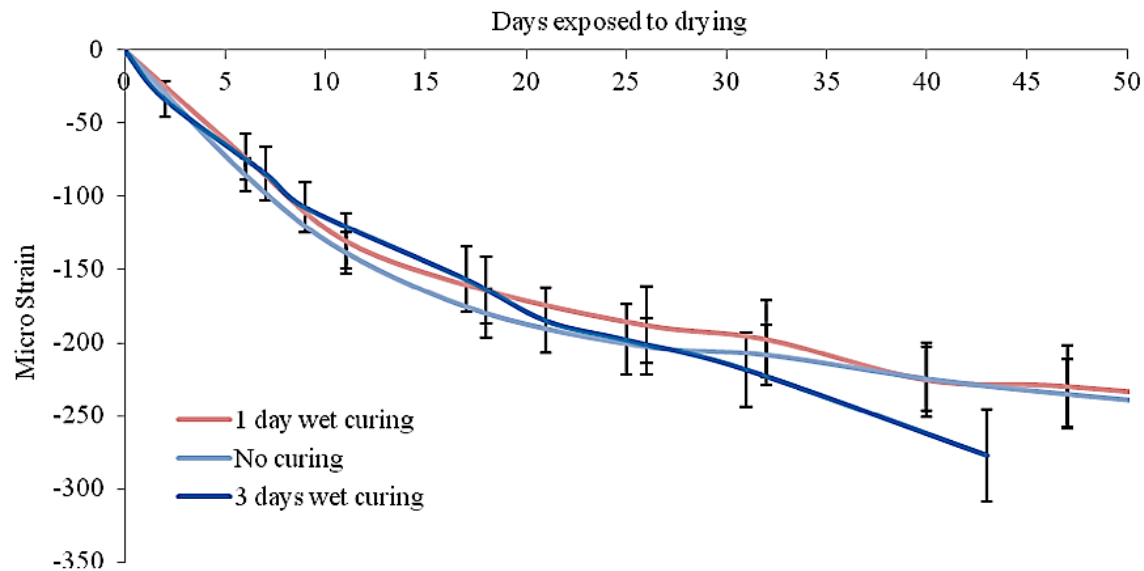
Figure 5.15 Average surface strain vs. concrete beam's length with age
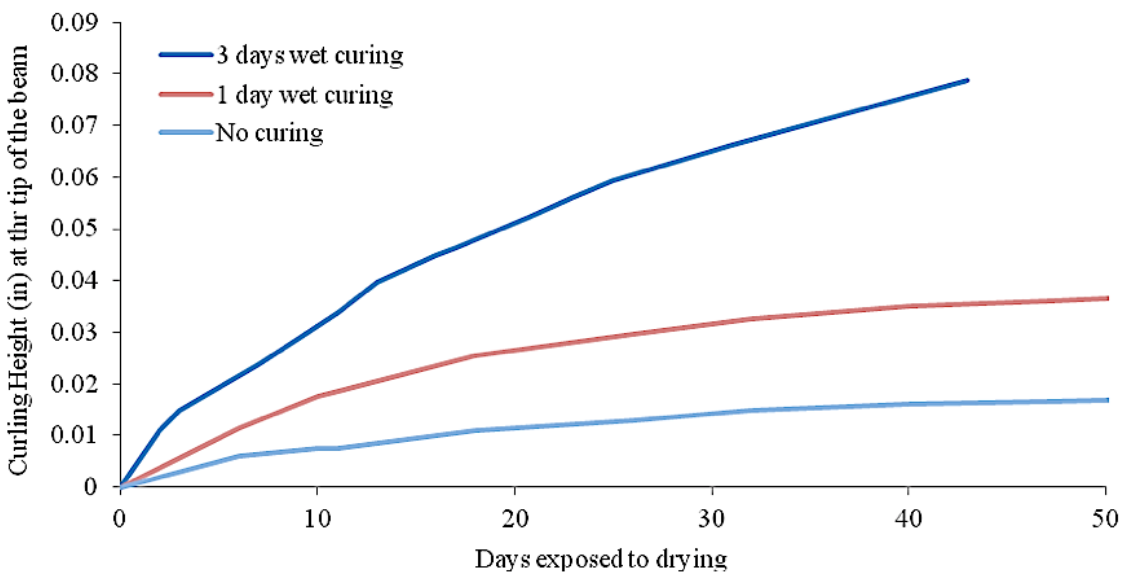
Figure 5.16 The tip deflection for the specimens investigated

A typical plot of the relative humidity versus the days of drying is shown for a beam that was not cured is shown in Figure 5.17 for different depths.
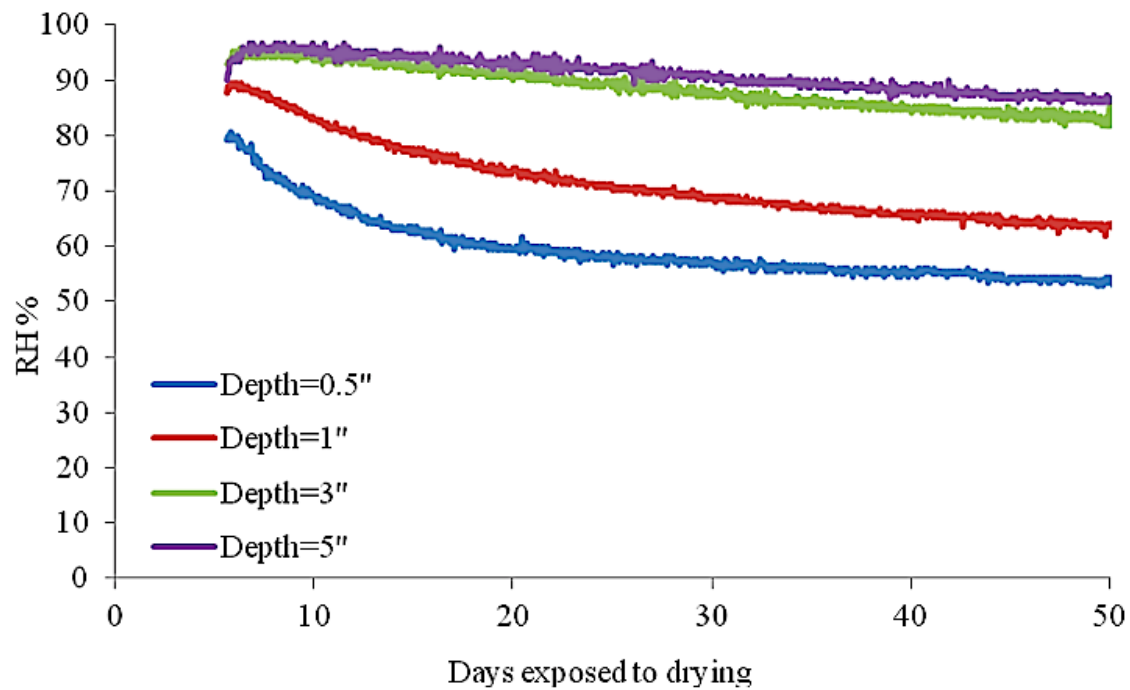
Figure 5.17 The relative humidity of the no-curing technique in different depths vs. age for concrete beams

The relative humidity profiles for no-curing at 6, 15, 25 and 50 days after exposure are all shown in Figure 5.18.
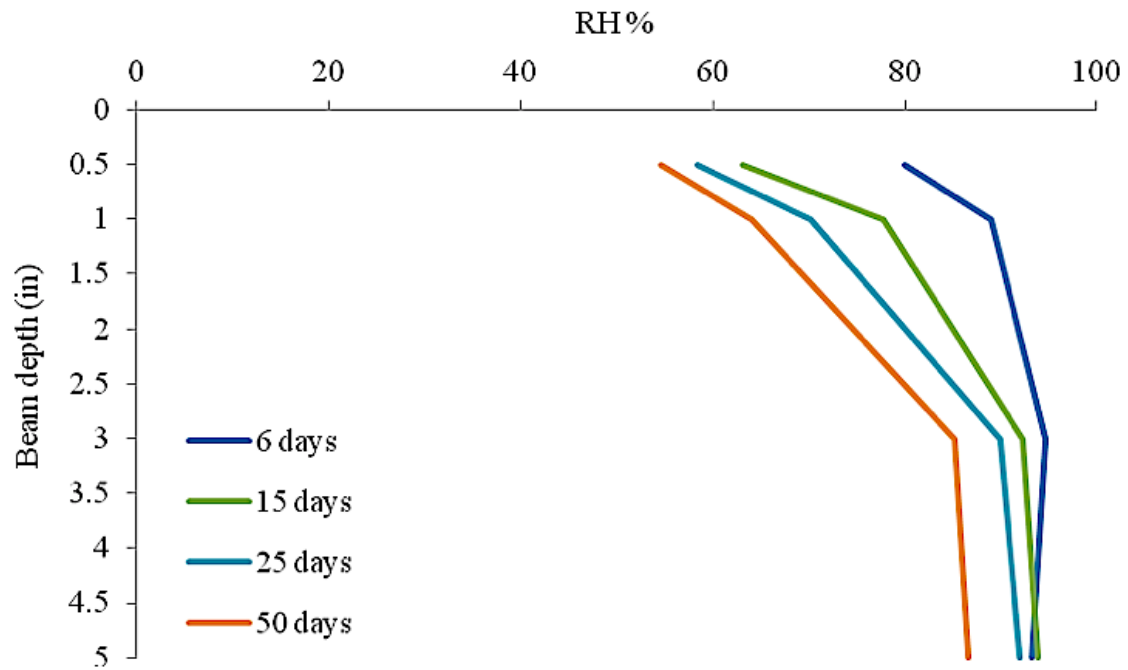
Figure 5.18 The RH profiles for no-curing at 6, 15, 25 and 50 days after exposure for concrete beams

The relative humidity profiles for 1 day wet curing at 6, 15, 25, and 50 days are shown in Figure 5.19.
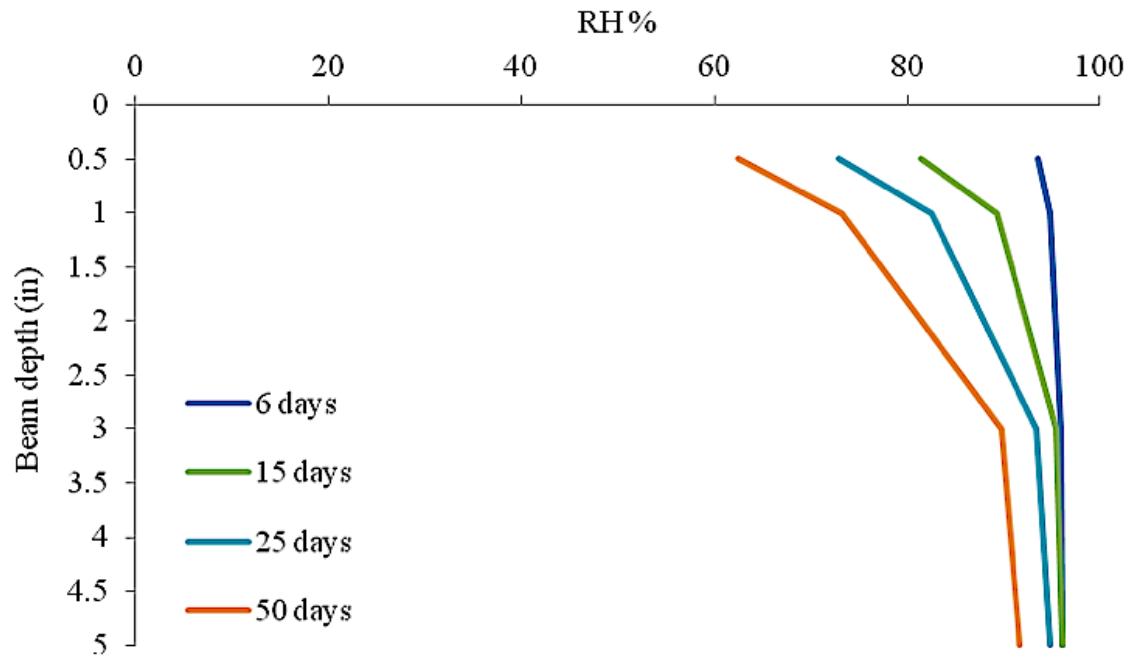
Figure 5. 19 The RH profiles for 1-day wet curing at 6, 15, 25 and 50-days after exposure for concrete beams

The relative humidity profiles for 3 days wet curing at 8, 15, 25, and 50 days after exposure are all shown in Figure 5.20.
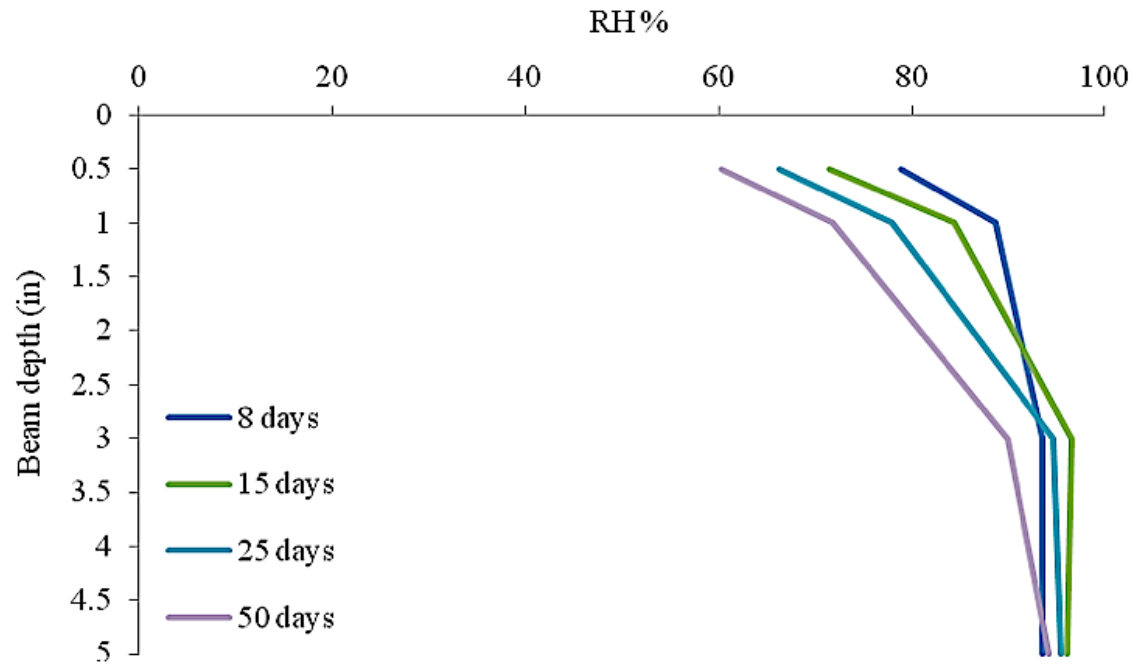
Figure 5.20 The RH profiles for 3-days wet curing at 8, 15, 25 and 50-days after exposure for concrete beams

The following Figure 5.21 shows the comparison between the RH profiles of the considered techniques after 50 days.
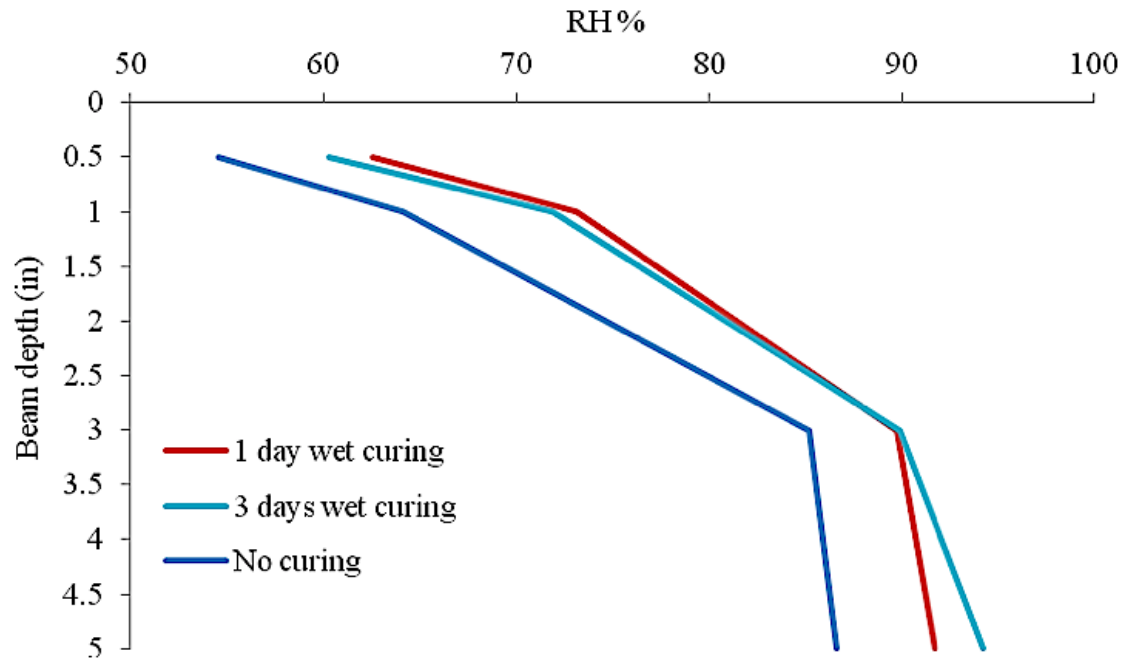
Figure 5.21 The RH profiles after 50-days for different methods for concrete beams

Figure 5.22 shows the integrated area under the RH profiles over the age for the wet curing and no curing methods. This graph is an indication of the total moisture loss for the sample.
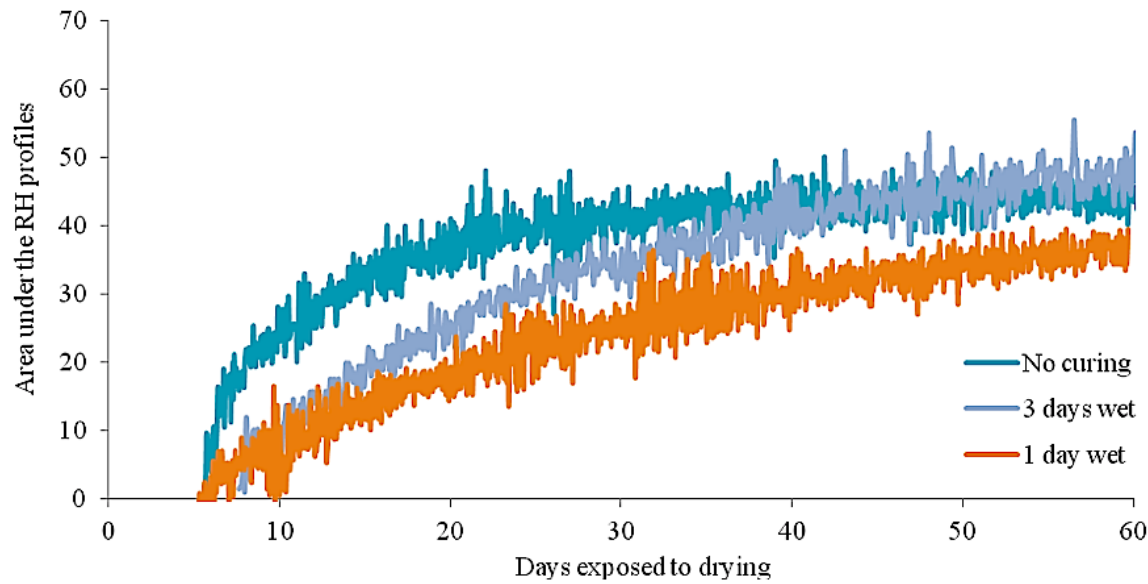
Figure 5.22 Integrated area under the RH profiles (Depth x RH) over the age for concrete beams

5.1.4 Discussion

5.1.4.1 Paste Beams

With this technique the maximum deflection was always found to be at the middle of the beam. This is to be expected since the beam was not restrained and is assumed to lose water uniformly over its surface. This means that there should be a consistent moisture gradient throughout the entire specimen. As is observed in Figure 16, the paste beam starts to deflect downwards. This is because the moisture gradient in the beam decreases with increased drying. This water loss would be expected until the internal RH of the beam reaches equilibrium with the surroundings.

Figure 5.8 shows that the specimens that did not receive curing lost moisture faster than the specimens that had received some amount of wet curing. This result suggests that there is a decreased porosity in the specimens that received the extended curing. In

Figure 5.9 it can be seen that the wet curing lead to a greater degree of maximum deflection on drying. It can also be seen that this point of maximum curling occurred after a later number of drying days with prolonged curing times. Again this data suggests that the prolonged wet curing refined the pore structure of the paste.

It is likely that when the moisture is lost in the small capillaries that this will cause a greater amount of shrinkage in the cement paste. This statement is supported by Equation 5.3. As the radius of the pore decreases the pressure produced should increase by an inverse relationship.

Others have noticed similar observations. Hedenblad (1997) suggested that with prolonged wet curing that the top surface will have fine capillary pores due to the longer hydration process. Moreover, additional curing may increase the water content of the thin paste bars, which will increase the drying time. Findings are in conflict to work by Suprenant (2002) who claims that curing primarily impacts when concrete will start to curl and not the magnitude of curling. Others have also suggested that extended curing only delays curling; it does not reduce curling (ACI 360R-2006).

The results in Figure 5.10 show that when the beam is cured by sealing it in a plastic sheet that the beam lost moisture more slowly than wet curing. Figure 5.11 shows that the maximum deflection was very similar between the wet curing and the sealed specimens for the same duration of curing. Again, it was witnessed that the longer the material was cured, the more curling occurred.

Specimens that are cured by not supplying extra water but sealing them seem to have a similar performance as the wet curing techniques. They seem to promote hydration and the production of small pore size distribution. One difference between the specimens is that the sealed cure seems to lose less moisture than the wet cured samples. This suggests that additional water is added to the wet cured samples during the curing process. However, this additional water does not seem to largely impact the amount of curling that occurs. This observation is in line with the current mechanisms for drying shrinkage that suggest water loss at the walls of a capillary are the primary cause of drying shrinkage and not losses in the bulk. By adding more bulk water to the paste then this does not impact the water at the capillary walls.

Figure 5.12 shows that the additional wet curing seems to increase the maximum curling of the paste for curing up until 14 days and then ultimately decrease the curling for longer curing. This can be seen that the curling for mixtures with a 0.50 w/c start to decrease after 28 days of wet curing and after 14 days for 0.34 w/c. A specimen was not investigated for a 0.42 w/c but this would be expected to be between these values. The reason for this behavior is not clear. Other researchers have reported similar observations in concrete. Work by Perenchio relating the period of moist curing and drying shrinkage for concrete with various w/c, showed that periods of curing greater than 4 to 8 days and less than 35 to 50 days may increase the drying shrinkage (ACI 209.1R-2005).

Considering the specimens with no additional curing in Figure 5.12, the maximum deflection of the sample with 0.42 w/c has a similar performance to 0.34 w/c for a low amount of curing and then increases to be very similar to a 0.50 w/c after 7 days of curing.

Past researchers have shown that as the w/c increases so does the drying shrinkage (U.S. Bureau of Reclamation 1975; Schmitt and Darwin 1999; Darwin et al. 2004). In general, samples of higher w/c ratios have more construction water and, due to less fine pores at the surface, they start drying earlier, which will increase the drying rate (Hedenblad 1997). It is not clear why the 0.42 w/c specimen showed similar performance to the 0.50 w/c after 7 days of curing.

Figure 5.13 and 5.14 summarize the weight loss of the specimens for different w/c ratios at the maximum curling deflections (before curling down) and at 11 days. Both graphs show less moisture loss with an extended curing period. The reason, as explained earlier for Figure 5.12, is due to the finer pores at the surface of the sample after the wet curing which delay the external drying and reduce the drying rate (Hedenblad 1997).

5.1.4.2 Concrete Beams

The surface strain and tip deflection results after about 40 days in Figures 5.15 and 5.16 show that there does not seem to be much difference in performance with no curing and 1 day. However increased curling was observed for 3 days of wet curing. After about 20 days, the curling deflection of the 3 day wet cure specimen is higher than that of the

1 day wet curing method, and it demonstrates the maximum deflection amongst all techniques after 40 days. This is similar to the data found with the paste beams. Others, Lyse (1935), Carlson (1938), Keene (1961), and California Department of Transportation (1963), have reported that the duration of moist curing of concrete does not have much effect on ability of a structure to resist drying shrinkage. More work may be needed to look at curing periods longer than 3 days in the concrete testing. It may be possible that the improvements in tensile strength created by wet curing are offset by the increases in drying shrinkage.

Because the shrinkage of the concrete is caused by the shrinkage of the paste as shown in Equation 5.1 (Pickett 1956); therefore it is expected that similar results would be observed in concrete and paste. In both systems it appears that samples that have finer capillary pores from curing would have a higher capillary tension as expressed in Equation 5.2 and 5.3 (Mackenzie 1950; Adamson and Gast 1997; Bentz et al.1998). Figure 5.17 shows that the relative humidity of the top surface at 0.5" from the exposed side changes faster than the measurements at the bottom of the beam. This is expected as the surface of the beam is exposed to a much greater degree of drying. Figures 5.18, 5.19, and 5.20 show the RH profiles for no curing, 1-day, and 3-day wet curing. They present that the no curing has a faster decrease in relative humidity over the depth after exposure, while the 1-day and 3-day wet curing methods have slower moisture loss over time. Figure 5.21 compares the RH profiles of the abovementioned methods after 50 days; the no-curing methods has less humidity at and near the top surface while the RH values near the bottom layers are very close together for no-curing and wet curing methods.

Figure 5.22 shows the integrated area under the RH profiles for the aforementioned methods. The graph for no-curing technique is above those for the wet curing techniques at the early ages, but they meet each other at later ages.

These graphs for no curing technique validate the reason for having the faster weight losses due to the higher porosity concrete. The graphs for wet curing techniques keep increasing, showing their continuous water losses, their slower drying rates, and their delay in reaching the maximum curling deflections which could be expected in later ages, as seen in Figure 5.15.

5.1.5 Conclusions

In this chapter wet curing methods were compared to sealed and no-curing methods; it was found that wet curing on the exposed surface of a sealed beam decreases the rate of weight loss from drying but increases ultimate curling deflection. This data suggests that extended wet curing would be expected to cause an increase in the amount of curling that occurs in a slab on grade. Similar observations have been observed for drying shrinkage in concrete beams but never applied to increases in curling. Due to the wet curing process, the surface of the beam has a finer pore-structure (Hedenblad 1997) and consequently a higher negative pressure or capillary tension upon drying (Mackenzie 1950; Adamson and Gast 1997; Bentz et al.1998). This increase in capillary tension has been suggested to be the primary mechanism for drying shrinkage (Lane, Scott, and Weyers 1997).

In all of the tests presented a one dimensional drying front was used through use of impermeable boundaries. Nicholson (1981) showed that serious shrinkage curling due to an increase in moisture gradient can occur when concrete slabs are cast on an impervious base. Because curling and drying shrinkage are both a function of potentially free water in the concrete at the time of concrete set, curing methods that retain water in the concrete will delay shrinkage and curling of enclosed slabs-on-ground. If the drying front occurs from the top and bottom of the concrete then the curling would be reduced because of the decrease in the gradient.

5.1 IMPACT ON CURING COMPOUNDS TO REDUCE CURLING IN CONCRETE FROM DRYING SHRINKAGE

5.2.1 Introduction

This chapter reviews the effectiveness of curing compounds to resist curling from differential drying by comparing one of the common curing techniques to wet curing methods.

Liquid membrane-forming compounds consist of waxes, resins, chlorinated rubber, and other materials that reduce evaporation of moisture from concrete. They are the most widely used method for curing not only freshly placed concrete, but also for extending the curing of concrete after the removal of forms or after early wet curing (Kosmatka et al 2003).

According to ACI 308R-01 curing compounds have several advantages:

1. They do not need to be kept wet to ensure that they do not absorb moisture from the concrete;
2. They are easier to handle than burlap, sand, straw or hay; and
3. They can often be applied earlier than water-curing methods (immediately after finishing without the need to wait for final setting of the concrete).

Liquid membrane-forming compounds for curing concrete meet the requirements of ASTM C 309 include:

- Type 1, clear;
- Type 1D, clear with fugitive dye;
- Type 2, white pigmented;
- Class A, unrestricted compositions or wax-based products; and
- Class B, resin-based compositions

Loss of some moisture from the surface of concrete cured with these compounds is allowable; depending on the application and ambient conditions in the field, these compounds have a variable potential for water retention (Mather 1987, 1990; Shariat and Pant 1984; Senbetta 1988). The amount and type of curing can affect the rate and ultimate amount of drying shrinkage. Curing compounds, sealers, and coatings can trap free moisture in the concrete for long periods of time, resulting in delayed shrinkage (Kosmatka et al 2003).

The curing compounds should be agitated or stirred before use and applied uniformly at the recommended rate. Since a textured surface has a larger surface area then a flat surface then more coverage would be expected. Some have reported that a tined surface has at least twice the area of a floated surface and verification of coverage rate is more difficult for deeply textured surfaces. It has been recommended that curing compounds should be applied in two applications to ensure uniform and more complete coverage (Shariat and Pant 1984). They can be applied by hand or power sprayer with proper nozzles in the pressure range of 25 to 100 psi. Also, they should be applied immediately after the surface water disappears or after the final finishing of the concrete. A delay in application could cause the concrete surface to dry and the compound might absorb into the concrete, which would deter the formation of the desired membrane (ACI 308R-01). On the other hand, applying the curing compound on freshly cast concrete might result in map cracking; the disappearance of surface water will be stopped temporarily, but bleeding might continue. The bleed water will reduce the capability of the compound to maintain the moisture content of the concrete. White-pigmented compounds help guarantee uniform coverage and are considered to reflect light. A typical application of a curing compound is shown in Figure 5.23.

Figure 5.23 The power-driven spray to perform a uniform application on a tinned surface (Ye et al, TxDOT 2009)

The application rate of the curing compound should be determined based on surface texture and application device in order to obtain uniform coverage. The five factors listed below affect the curing compound application (Minnesota DOT 2001; Texas DOT 2009; Iowa DOT 2002):

- nozzle type: spray pattern, droplet size, pump pressure, spray angle, flow rate
- nozzle spacing and boom height:
- nozzle orientation
- cart speed
- wind speed

It was concluded that non-uniform coverage could be caused by damage or clogging of the nozzle or orifice. Complete coverage of the surface must be attained because even small pinholes in the membrane will increase the evaporation of moisture from the concrete. Curing compounds should be uniform and easy to maintain in a thoroughly mixed solution (Kosmatka et al 2003).

It is the goal of this research project to examine the performance of different curing compounds on the ability to reduce curling in concrete and paste specimens from differential drying. The results from different types of curing compounds, application rates, and single and double coatings are investigated.

5.2.2 Experimental investigations

5.2.2.1 Paste Beams

5.2.2.1.1 Materials

The Portland cement used in these tests was a type I/II according to ASTM C 150, and its oxide analysis per ASTM C 114 and the phases' concentrations are shown in the following Table 5.4. The paste mixtures in this experiment had a water to cement ratio (w/cm) of 0.42.

Table 5.4 Oxide analysis of the cement used for paste beams and the phase concentrations

Chemical Test Results			
SiO_2	20.23	Fe_2O_3	3.23
Al_2O_3	4.77	CaO	64.15
MgO	1.90	SO_3	2.52
Phase concentrations			
C_3S	70.69	C_3A	7.18
C_2S	4.68	C_4AF	9.83

Three different curing compounds were used in this project; these products were chosen as they were from different chemical families and were used by three different states. The standardized specifications are summarized in Table 5.5 according to the MSDS for the product. The first curing compound (C1) is high solids, white-pigmented, and Poly-alphamethylstyrene-resin-based and it dries in approximately one hour. The second curing compound (C2) is a water-based, white-pigmented curing compound series; it has resin-based dispersions with selected white pigments and typically dries in 1-2 hours. The third one (C3) is of a water-based, white-pigmented concrete curing

compound series, with a wax-based dispersions and selected white pigments and typically dries in two hours.

Table 5.5 Curing compound specifications

Curing compounds	Type (Per ASTM C 309)	Drying time	Basis
C1	Type 2, Class B	1 hour	Poly-Alphamethylstyrene
C2	Type 2, Class B	1-2 hours	Water-Based, Resin-Based
C3	Type 2, Class A	2 hours	Water-Based, Wax-Based

5.2.2.1.2 Sample preparation and methods

The paste mixtures were prepared according to ASTM C305. Three paste beams with dimensions of 39.4" x 2.4" x 0.5" were prepared in plastic molds from each mixture. For this testing, all specimens were stored in an environmental chamber at 73° F and 40% relative humidity. All specimens were cured using wet burlap for 5 hours before being covered in curing compound. Before and after the application of the curing compound, the samples were weighed and finally stored in the chamber room until 24 hours after mixing. Next the samples were demolded, weighed, sealed with wax on all sides but the finished surface, reweighed and stored on their sides in the chamber room. Figure 5.24 shows the specimens covered with different curing compounds inside the chamber room. This test was adopted from previous work done by Burke (2004) to investigate the effectiveness of shrinkage reducing admixtures.

Figure 5.24 The specimens covered with curing compounds and stored in the chamber room

5.2.2.1.3 Test procedure and measurement

For this testing the three different types of curing compounds were applied 5 hours after casting. This time period was chosen as it was the time required for the bleed water to disappear from the surface of the specimen. Each curing compound was applied in three different volumes. A coverage that was about equal to the manufacturer's recommended dosage was used, as well as ones that were about 50% lower (low dosage) and 50% higher (high dosage), were used to evaluate the performance of different curing compounds and coverage. The curing compound was applied in a single layer with a Chapin 5797 flat nozzle for all products with a pump pressure of 40 psi, as suggested by the manufacturer. To modify the application of the compounds, three different nozzle distances were used with the same cart velocity as suggested by Minnesota DOT (Vandenbossche 2001). For this purpose, a cart was constructed that runs on tracks and holds the nozzle at a controlled height. The cart was moved along the sample at a constant velocity. This constant velocity was obtained by using a metronome and marks with a known distance on the track. The cart was moved so that it crossed a mark at the exact same time the metronome sounded. Because the metronome supplied a beat at a constant interval, and the cart operator was able to move between the marked locations at a constant rate then this allowed the cart to move at an almost constant velocity. This velocity could be easily changed by changing the rate of the metronome. For all testing the

velocity was kept constant and the coverage rate was adjusted by changing the height of the spray nozzle.

The coverage rate on samples cured by the curing compound was determined by the following Equation 5.5 (Vandenbossche 2001):

Equation 5. 5

$$v = \frac{Coeff. * F}{C * w}$$

Where:

v = Cart speed, kilometers per hour (miles per hour)

Coeff. = 6 when using SI units (0.13636 with Imperial)

F = Flow rate, liters per minute per nozzle (gallons per minute per nozzle)

C = Desired coverage, liters per square meter (gallons per square foot)

w = Nozzle spacing, cm (inches)

The following picture in Figure 5.25 shows the schematic view of the spray coverage calculated by Equation 5.5. This equation is commonly suggested by the curing compound manufacturers to determine the correct coverage rate.
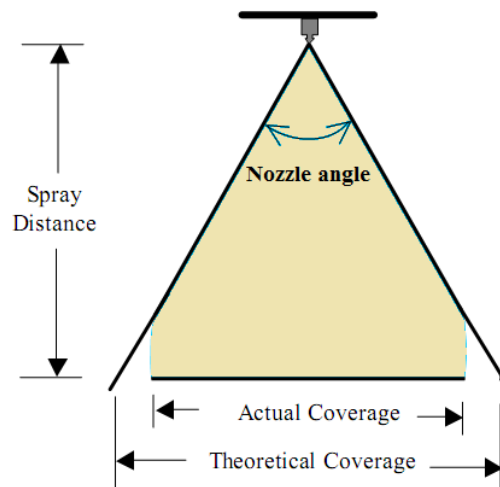
Figure 5.25 Schematic view of the spray coverage

The flow rate, cart speed, desired coverage, and spray distance used in this study to spray the curing compounds were computed by the equation. The velocity applied for all dosages was 1.33 ft./sec and the coverage time was 2.5 seconds; thus, the spray

distances were 20.85", 10.40", and 6.95" for low, medium, and high dosages respectively.

To check the uniformity of the coverage and accuracy of the equation, some practice tests were done by using steel plates of known areas that were placed at a known height. These plates were weighed before and after applying curing compounds. By using the area of the plate and the weight of the curing compound the coverage could be calculated. A summary of the amount of applied curing compound and the standard deviation for each test is shown in Table 5.6.

Table 5.6 The curing compound coverage and standard deviation

Curing method	Basis	(gal/ft^2)	low	medium	high
C1, Single layer	Poly-Alphamethylstyrene	Coverage	0.0019	0.0040	0.0051
		STD	0.0002	0.0001	0.0000
C2, Single layer	Water-Based, Resin-Based	Coverage	0.0020	0.0037	0.0051
		STD	0.0001	0.0004	0.0002
C3, Single layer	Water-Based, Wax-Based	Coverage	0.0036	0.0048	0.0074
		STD	0.0001	0.0001	0.0003
C3, Double layer	Water-Based, Wax-Based	Coverage	0.0027	0.0041	0.0056
		STD	0.0001	0.0001	0.0003
1-day wet + C3 Single	Water-Based, Wax-Based	Coverage	-	0.0038	-
		STD	-	0.0002	-

A double layer of C3 was tested as well. This application was achieved by applying two layers whose sum would equal the required value. Also, the combination of 1 day wet curing and a medium application rate of C3 was tested.

The measurement of the beam deflection over time and its weight change were explained previously. For the length change two ends of the specimen are attached to a flat aluminum plate with the uncoated surface facing the plate to measure the curling

deflection with a caliper that is accurate to 0.0005". The weight of the sample is also measured with time using a scale that is accurate to 0.1 grams.

<u>5.2.2.2 Concrete beams</u>

5.2.2.2.1 Materials

The cement, aggregate, fly ash, and moisture barrier used in this experiment were the same as in described previously for concrete beams. Materials include cement type I according to ASTM C 150 and dolomitic limestone and natural sand aggregates as well as a Class C ASTM C 618 fly ash. To seal the concrete beam samples, a synthetic moisture barrier was used as a form liner. The interface between the beam and the water membrane was sealed with hot glue to ensure a good bond was maintained throughout the test. The cement chemical analysis per ASTM C 114 and the phases' concentrations are shown in the following Table 5.7.

Table 5.7 Chemical analysis of the cement used for concrete beams and the phase concentration

Chemical Test Results			
SiO_2	21.13	Fe_2O_3	2.55
Al_2O_3	4.71	CaO	62.06
MgO	2.37	SO_3	3.18
Phase concentrations			
C_3S	52.14	C_3A	7.69
C_2S	20.22	C_4AF	7.96

5.2.2.2.2 Mixture proportions and methods

The mixture proportion and the mixture procedure were explained in chapter 5.1. However, this concrete was not air entrained. The water to cement ratio used in this experiment was equal to 0.41 for concrete beams. All of the aggregate, both coarse and fine, were charged into the mixer along with approximately two-thirds of the mixing water. The combination was mixed for three minutes. Next any clumped fine aggregate was removed from the walls of the mixer. Then the cement was loaded into the mixer,

followed by the remaining mixing water. The mixer was turned on for an additional three minutes. Once this mixing period was complete, the mixture was left to "rest" for the following two minutes while the buildup of material along the walls of the mixer was removed. Next the mixer was started and the admixtures were added and the mixer was allowed to run for the remainder of the three minutes (ASTM C 192). The slump (ASTM C 143), unit weight (ASTM C 138) and the air content (ASTM C 231) were measured.

5.2.2.2.3 Sample preparation, casting and curing

In this experiment the size of the concrete specimen investigated was 7.5′×6″×8″, with all sides sealed with a synthetic moisture barrier except the top surface for each specimen. These specimens were all stored on their side in an environmental chamber at 73° F temperature and 40% relative humidity. After placing and vibrating the concrete in 3 different layers, the top surface was made flat with a screed. Next a micro-surface was applied with a burlap drag, and then the surface was finally tined using a comb. The comb had transverse grooves 1/16″ wide, 1/4″ deep, and center to center spacing of 1″ between the tines based on ODOT Standard Specification for Highway Construction. For this testing only curing compounds C3 and C1 were investigated. A single layer of C3, single layer of C1, and a double layer of C3 were investigated in this experiment. The layers were applied in two equal coatings so that their sum equaled the total desired coverage. The beams were flipped on their sides and placed on wooden dowels after 24 hours. This was done to minimize the influence of gravity on the results. After placing the beam on its side, it was fixed at the end with a C-clamp, steel plates, and rubber bearing pads.

5.2.2.2.4 Test procedure and measurement

The RH was measured 5 days after casting. DS1923 Hygrochron Temperature/Humidity Logger iButton sensors were used to measure RH at 4 different distances: 0.5″, 1″, 3″, and 5″ from the finished surface.

The curling height of the beam was measured at two different locations: 45″, and 89.5″ from the end of the beam. The deflection gauges were fixed using magnets on the steel support beneath the concrete beam. The accuracy of this gage was 0.0005". Also, the surface strain of the beam was measured after flipping the beam. Curing compound was sprayed on the samples about 2 hours after casting with a similar method as with

the paste beams. In order to obtain the desired coverage, many repetitions were completed and checked with steel plates. This allowed for very precise nozzle height and speed to be found that corresponded to a known amount of coverage. The amount of compound used for these experiments was chosen as 5.0 m^2/L (200 ft^2/gal) based on the ASTM C 309; therefore, the double layer with C3 (C3, D, medium) was performed in two different layers each with 100 ft^2/gal coverage.

5.2.3 Experimental results

<u>5.2.3.1 Paste beams</u>

Figure 5.26 and Figure 5.27 show weight losses and deflection over time, respectively, for different application rates of curing compound C2. Label "C2, S, low" means a single layer of C2 in medium rate and so on. These values are shown as they are typical results for one of these tests.
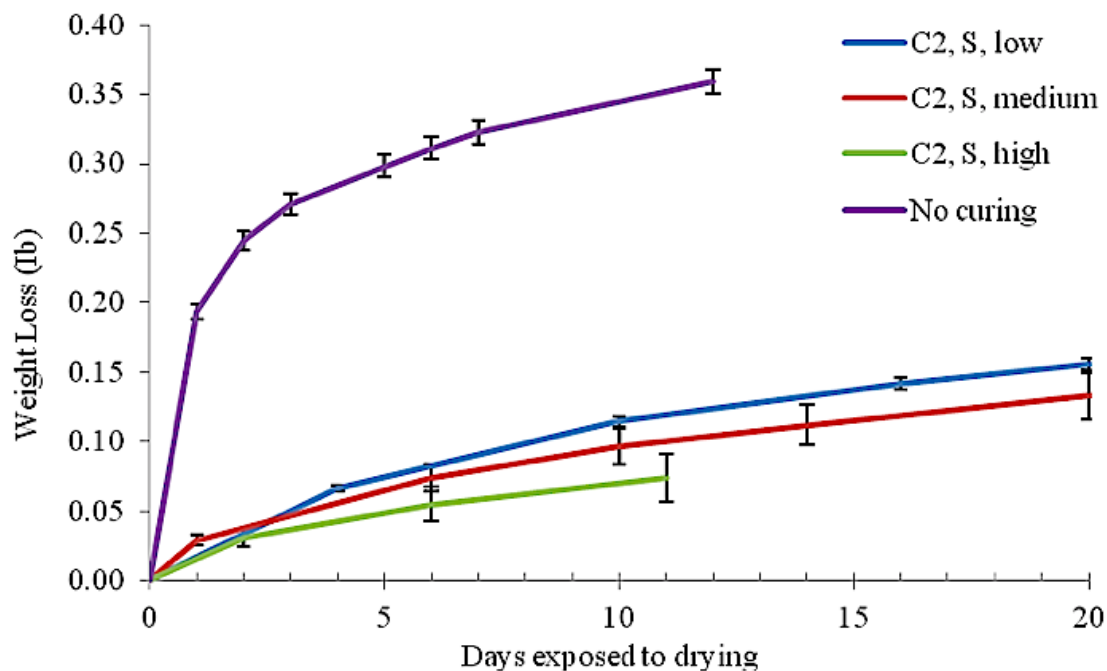
Figure 5.26 Moisture loss for a paste beam vs. time for C2 in single layer compared to no-curing method
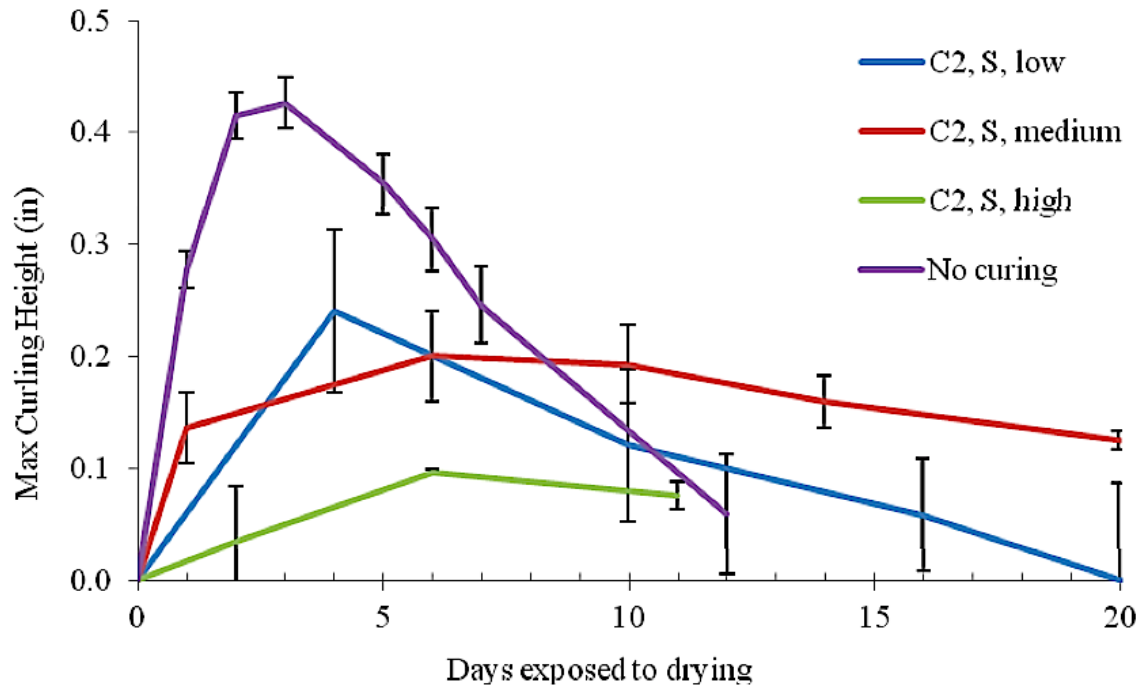
Figure 5.27 The maximum curling height vs. age for C2 in single layer compared to no-curing method

Figure 5.28 summarizes the deflection results for all curing compounds and shows the maximum deflection that the specimen experienced versus the application rate of different curing compounds. Also included in the graph is a line showing the deflection for a specimen with no curing compound, one day of wet curing, and a specimen that was cured for 1-day and covered with a single layer of curing compound C3. Also, the graph includes the maximum curling height for 1 day of wet curing to be compared and discussed later.
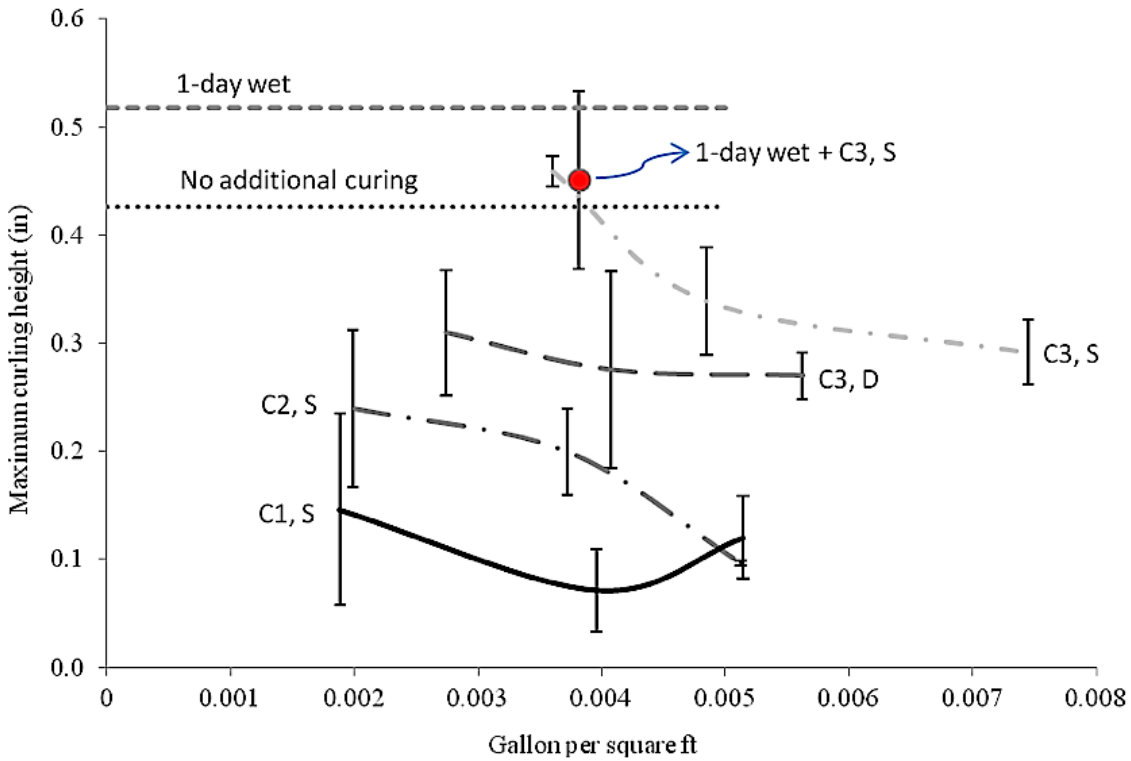
Figure 5.28 Comparison between highest deflections vs. different coverage of curing compounds on paste beams

Figure 5.29 shows the weight loss versus the coverage after 11 days for the different applications of curing compounds. The graph is shown at 11 days because this provided a good amount of time for drying and this measurement existed for all of the data.
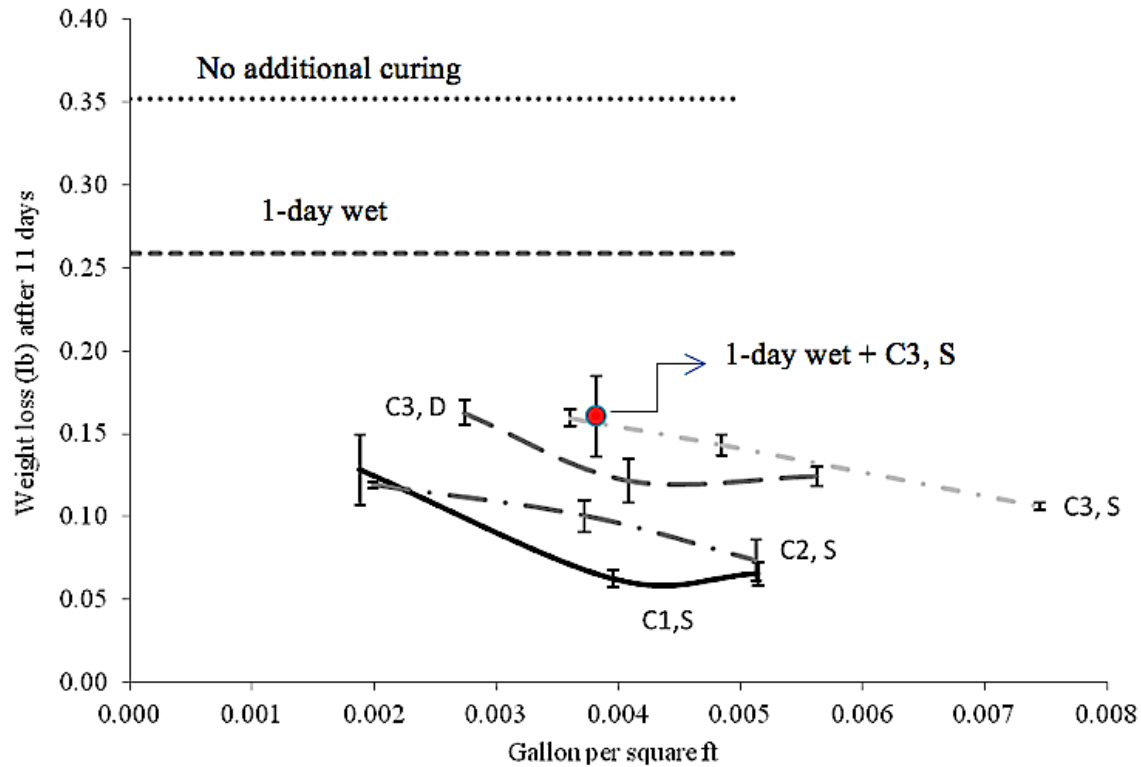
Figure 5.29 Comparison between weight losses vs. different coverage of curing compounds on paste beams after 11 days

Figure 5.30 and Figure 5.31 show the maximum curling deflection and the weight loss after 11 days versus additional curing time for the wet cured specimens in comparison with specimens cured with curing compounds. A number of curing compound techniques of interest have been included including a single layer of C3 with a medium application. Also, graphs include the combination of 1-day wet curing with a single layer of C3 in medium application rate to be compared later.
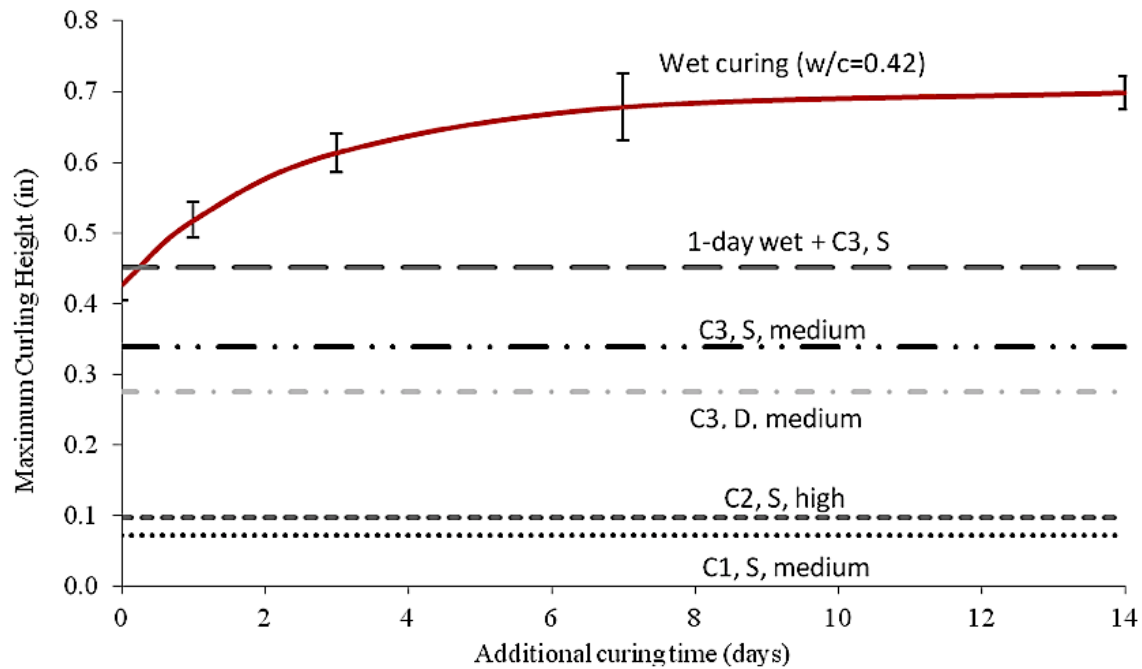
Figure 5.30 The maximum deflections of wet cured paste beams vs. additional curing time compared to curing compound methods
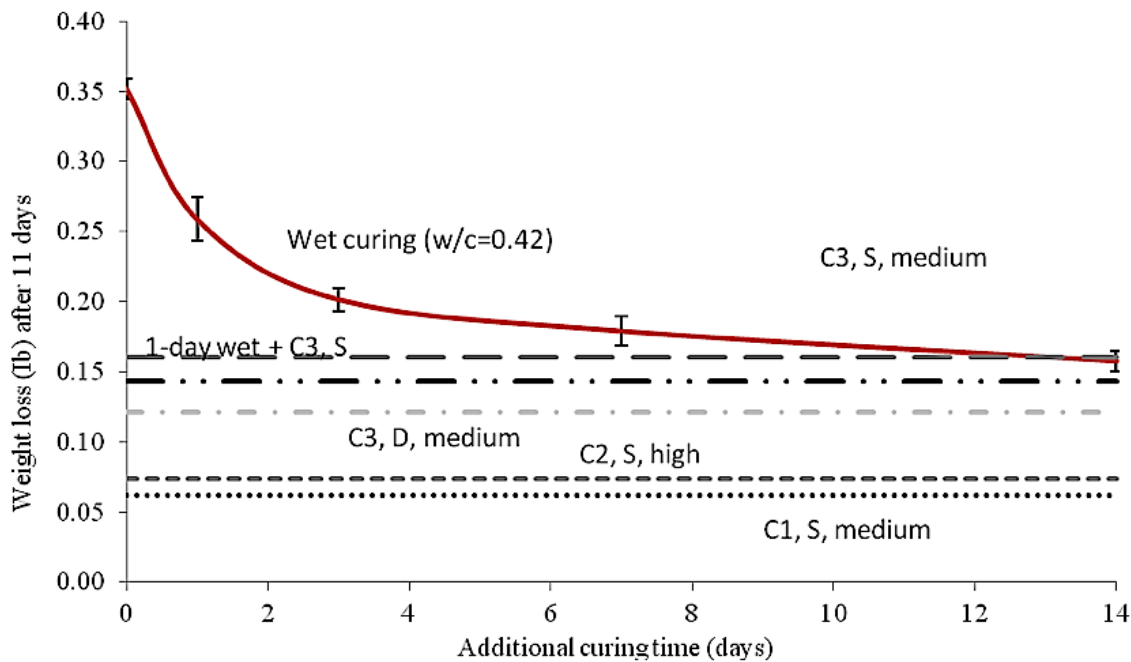
Figure 5.31 The weight losses of wet cured paste beams after 11 days vs. additional curing time compared to curing compound methods

Figure 5.32 shows the surface strain of the concrete beams with different curing compounds compared to those with no curing.
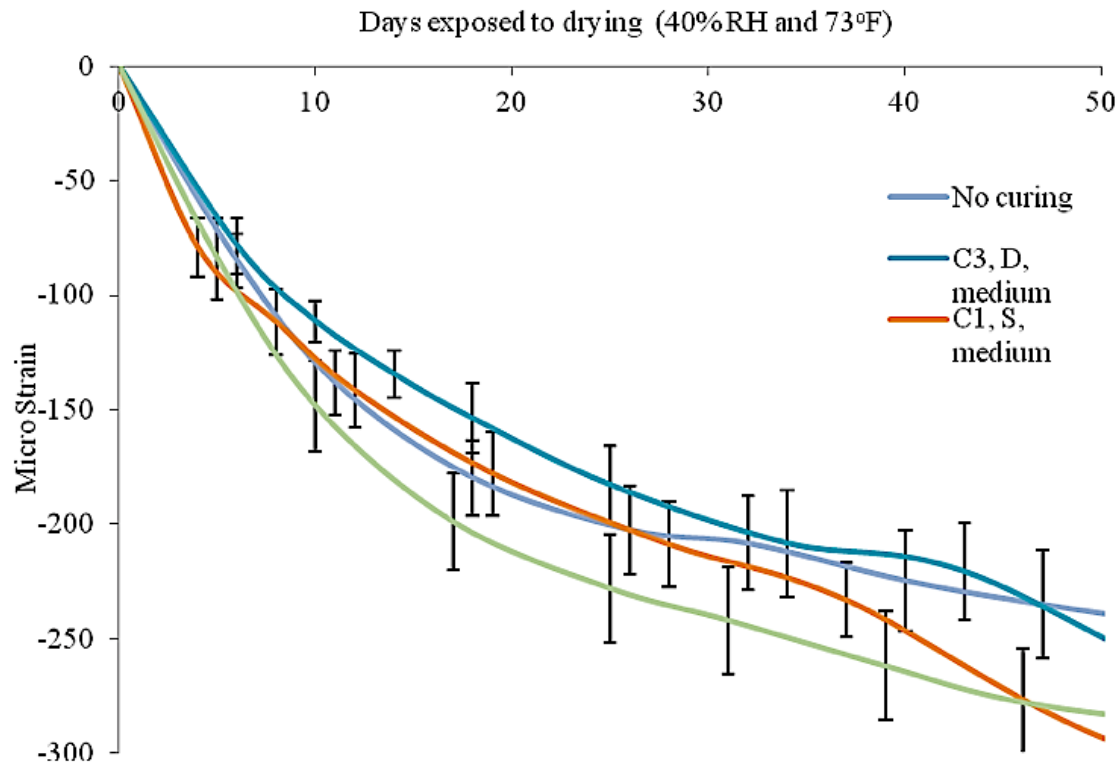
Figure 5.32 Surface strain of the concrete beams with curing compounds vs. time

Figure 5.33 and Figure 5.34 show the typical graphs for the relative humidity of the beam during the exposure and RH profiles at different depths of the beam with a double layer of C3.
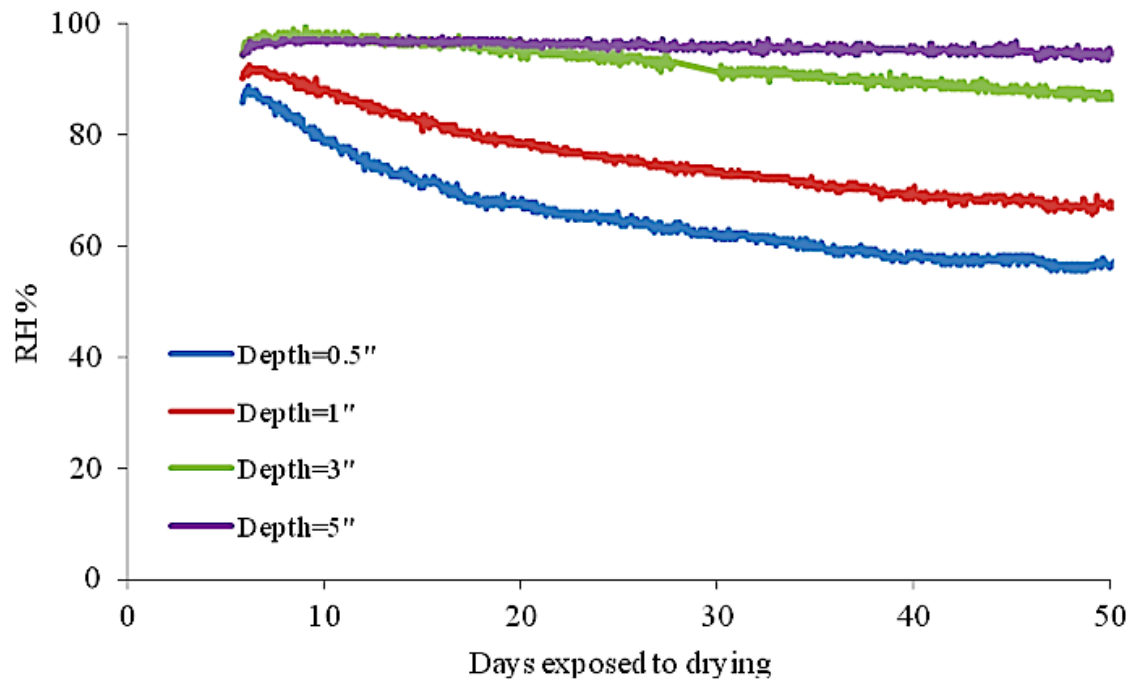
Figure 5.33 Relative humidity at different depths of concrete beam C3-D during the age
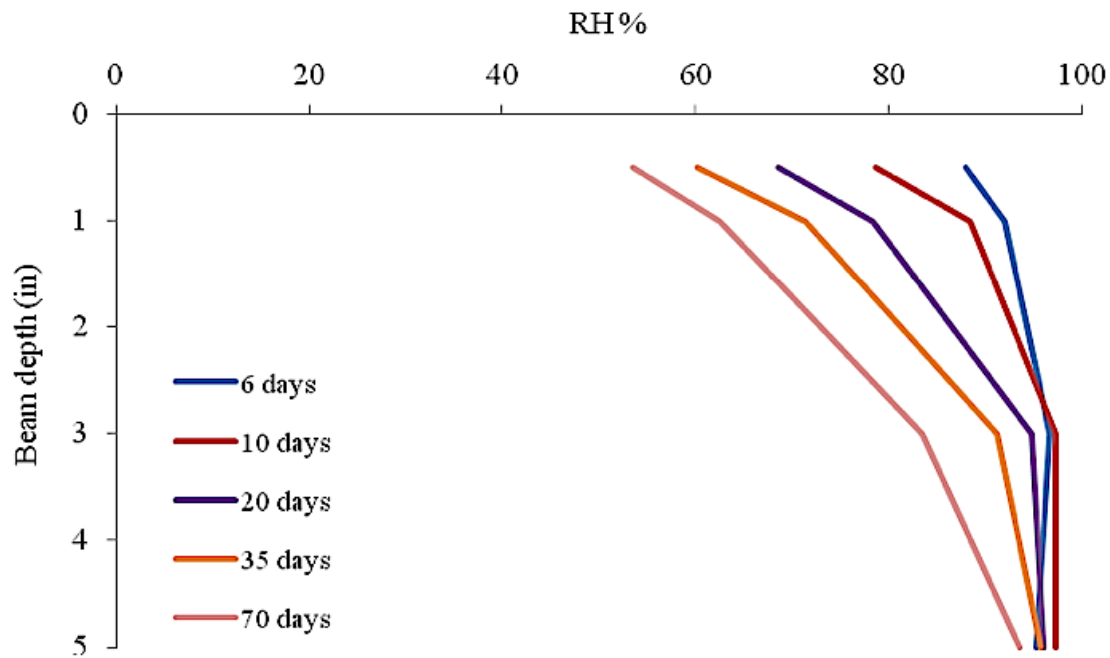
Figure 5.34 RH profiles for 6, 10, 20, 35 and 70 days after exposure for concrete beam C3-D

Figure 5.35 shows the area under the relative humidity profiles for the abovementioned beams over the age after exposure; however RH measurement was started 5 days after casting due to the concerns about early age performance of the RH gages.
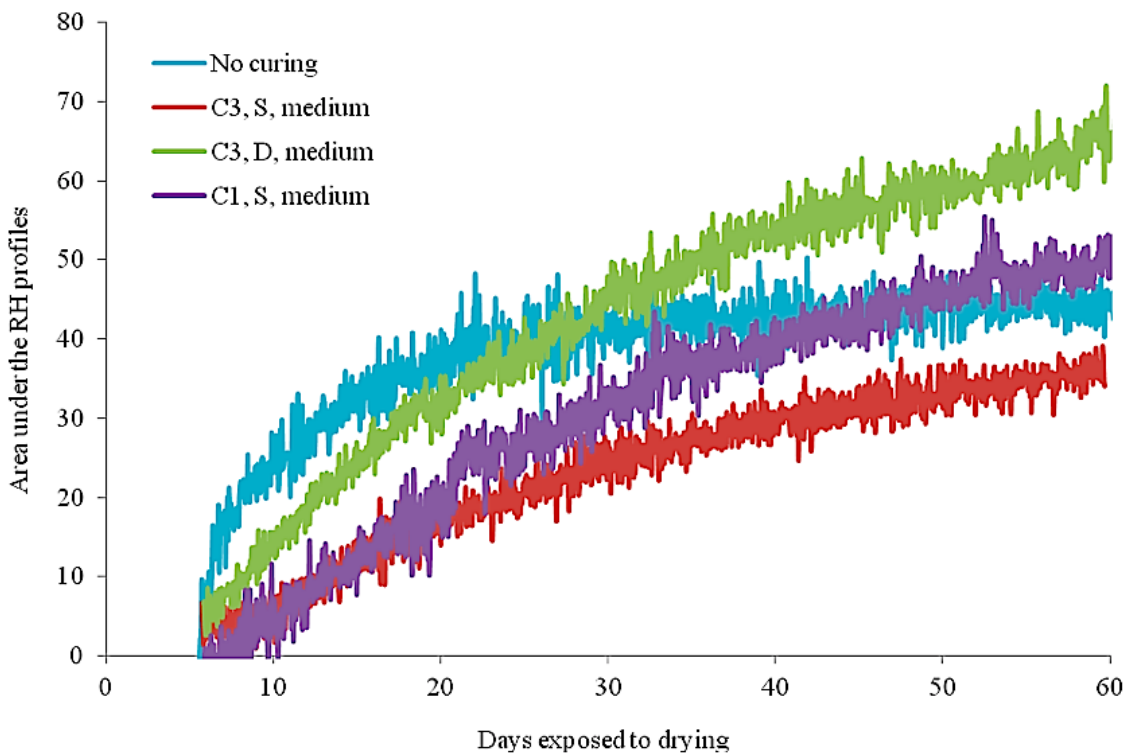
Figure 5.35 Integrated area under the RH profiles vs. time for concrete beams

5.2.4 Discussion

5.2.4.1 Paste beams

Figure 5.26 shows that the curing compound C2 has reduced the water loss when compared to the specimen with no curing. As the application increased the curling decreased. Figure 5.27 shows curling height is less with a higher coverage of curing compound compared to no curing. The curing compound retains the moisture content for a longer age by making a thin membrane, but it does not terminate the loss of moisture completely.

In Figure 5.28 it can be seen that, typically, as the amount of curing compound applied increased, the maximum curling height of the specimen decreases. The C3 curing compound in a single layer reduces curling with higher application rates; however, the

low application rate of C3 in a single layer had a very similar amount of curling as the sample with no curing compound. The deflection from the samples with 1 day of additional wet curing plus a single layer of C3 also had a similar performance as the sample with no curing. There is a slight improvement over the sample with 1 day of wet curing. The double layer of C3 shows a slight reduction in curling from the increase in the curing compound application. Of the samples investigated, it was surprising that there was not much improvement in performance with an increase in the application of the curing compound. The increase in application of C2 also decreased the maximum deflection. Finally, the increase in application rate of C1 also did not show much of a difference. It was observed that the effectiveness of a curing compound has some limiting value in three of the different experiments. It appears that a curing compound has a certain application thickness that is needed to ensure effectiveness. If more curing compound is applied than this limit value, then there is not much benefit in the performance. Furthermore, it appears that a double layer of curing compound reaches threshold limit at a lower volume of curing compound application than a single layer of curing compound. This probably is associated with the increased effectiveness in coverage for a double application of curing compound.

Figure 5.29 shows that all of the specimens after 11 days of drying that used curing compounds had a lower loss of moisture then those that did not. The moisture retention capability of the single layer of curing compound was the highest with C1 and the lowest with C3. The double layer of C3 did show an improvement in performance over the single layer. This data suggests that a curing compound does a much better job of keeping the water inside of the paste specimen than other methods. Also it appears that some curing methods are more effective than others at keeping moisture in a sample.

Figure 5.30 shows that each of the curing compounds has the ability to reduce curling below levels of wet curing in the specimen. It can also be seen that the prolonged wet curing increased the curling of the specimen as discussed in chapter 2.1. Figure 31 shows that after 11 days of drying that all of the curing methods were able to keep the moisture loss less than the specimen that had the 14 days of wet curing or less. This ability to keep moisture in the specimen helps to minimize the curling from the

differential shrinkage. Figure 5.31 also validates that the best curing compounds always have the least water loss and that even more additional wet curing only increases the water content and shrinkage possibility due to the finer pore structure compared to curing compounds.

The combination of 1-day wet curing plus curing compound C3 when compared to 1-day wet curing method shows that rapid drying of the surface of the samples that did not contain curing compound should be avoided. The best curing environment is to keep the concrete continuously wet during the curing period. The curing and protection should not be discontinued suddenly (ACI 224R-2001).

5.2.4.2 Concrete beams

Figure 5.32 shows the double layer of C3 has the least surface strain, while the single layer of the same curing compound in the same coverage has the most surface strain. C1 in a single layer has smaller strain than C3 in a single application in the same coverage. The no-curing method curls up very slowly after about 25 days while other beams continue curling.

Some different trends were obtained in the concrete beam data than those in the paste beams. For example, sample C3, S was found to perform worse than the no curing. This was unexpected. However, the error bars for the two samples do overlap one another, and so there is no statistical difference between the results.

Although it is difficult to tell, it may be that the specimen with the single layer of C3 was not applied uniformly over the tined surface of concrete beam. Although C1 had the best performance on the paste beams, this was not the case on the concrete beams. One observation that the double layer of C3 performs better than the single layer of C1 was unexpected. This could be attributed to the ability to provide a much more uniform coverage of the double layer of C1.

Figure 5.33 and Figure 5.34 show the typical graphs of relative humidity over the depths. The RH in deeper depths decreases more slightly, and RH profiles show the speed of the RH reduction is higher for the top of the beam than its bottom.

Figure 5.35 shows that a no-cured sample has a faster drying rate than other beams at the early age, while samples with curing compounds have a slower drying rate. After

about 25 days the slope of the drying rate of the no curing technique becomes zero, while this slope is increasing for other samples covered with curing compounds.

In the previous chapter about the paste beams it was explained that the no-curing technique has a faster water loss rate; this is true about the concrete beams, as well. The porous surface of a non-cured beam loses the construction water faster until after about a month when the curling rate seems to decrease. Other beams covered with curing compound continue curling up as long as this moisture loss rate increases, Figure 5.35.

5.2.5 Conclusions

Different curing compounds with different coverages were compared. The poly-alphamethylstyrene-resin-based curing compound (C1) had the best performance with a comparable coverage rate in the paste beam tests. The water and wax based curing compound (C3) curing compound performed the worst and the water and resin based curing compound (C2) was between these two. As the coverage of the curing compound increased so did the ability to limit moisture loss and therefore curling. A double layer of a curing compound was shown to provide improved performance over a single layer of curing compound.

Curing compounds appear to limit moisture loss to a greater degree than wet curing of up to at least 14 days or no curing methods. This reduction in moisture loss seems to correspond to a reduced amount of differential shrinkage and therefore curling in the specimens investigated.

In the concrete beams it was found that the double layer of the water and wax based curing compound performed better than the poly-alphamethylstyrene-resin-based curing compound. This is likely because it was applied in a double layer and therefore achieved a better coverage. This is especially important for applications with textured surfaces and with conditions that are not as favorable in the laboratory. Similar suggestions have been made by Shariat and Pant (1984). The uniformity of the application of the curing compounds is an important variable that needs to be controlled.

In summary it is suggested that a double layer of the resin based curing compound should be used for curing concrete pavements. This choice was made as it is a balance between cost of the produce and performance.

5.3 IMPACT ON CURING METHODS TO REDUCE CURLING IN CONCRETE FROM TEMPERATURE DIFFERENTIALS WITH SMALL SPECIMENS

5.3.1 Introduction

Curling in concrete is affected by both temperature and moisture. Temperature gradients within concrete at setting can lead to a built in curl within a concrete pavement. This built in curl can lead to long term performance issues from cracking. Several curing methods have been investigated to minimize the difference in the temperature gradient in the fresh concrete at setting.

The testing presented is from a scaled version of a larger slab that was allowed to hydrate outside. Larger scale tests were also completed but will be presented in the project summary report.

5.3.2 Methodology

5.3.2.1 Experiment preparation

The preparation of the experiment consists of various tasks:

1. Preparation of formwork
2. Preparation of Burlene liners
3. Preparation of wooden thermocouple support dowels
4. Installation of Burlene liners and thermocouple dowels into formwork
5. Preparation of thermocouple wires
6. Installation of thermocouples into preassembled formwork
7. Concrete is placed

The following is a brief explanation of the procedure previously described.

The forms used are purchased steel forms. The form is divided into the two equal sections with the use of a plywood separator. The samples were 9.5"x6"x6". Two additional plywood squares are placed at either end of the forms to complete the form. The two plywood squares at the ends of the forms are sawn in half and include a ½"

hole directly in the center as a means to convey the thermocouple wires for each sample. Figure 5.36 shows one of the steel forms with the plywood separators in place.
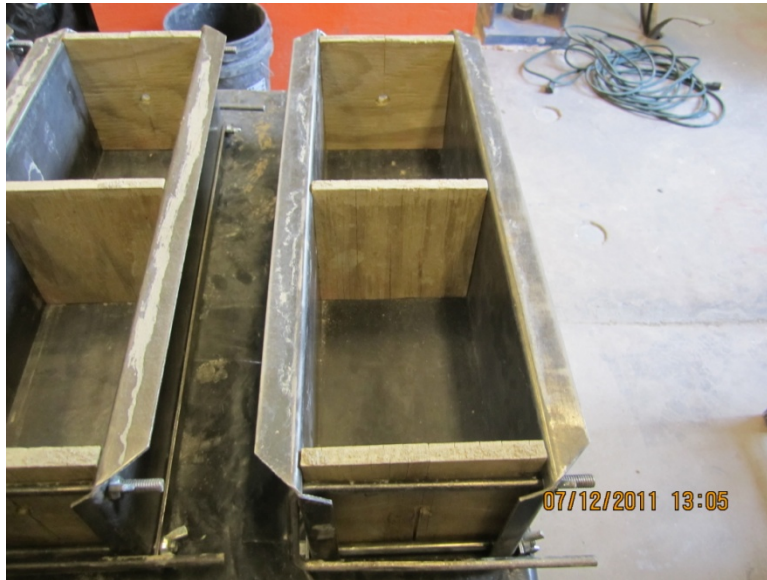
Figure 5.36 Assembled formwork with plywood separators in place

Burlene is a commercially available product which consists of a two ply fabric made of hair like fibers on one side and a moisture barrier on the other. The Burlene liners are prepared for each sample which act as a thermal and moisture barrier for all but the top surface of the sample. The liners are pre-cut in a cross like pattern and then folded to their final shape. The edges of the liners are taped together with tape to complete the liner. Figure 5.37 shows a Burlene liner that has been cut and taped into its final shape.
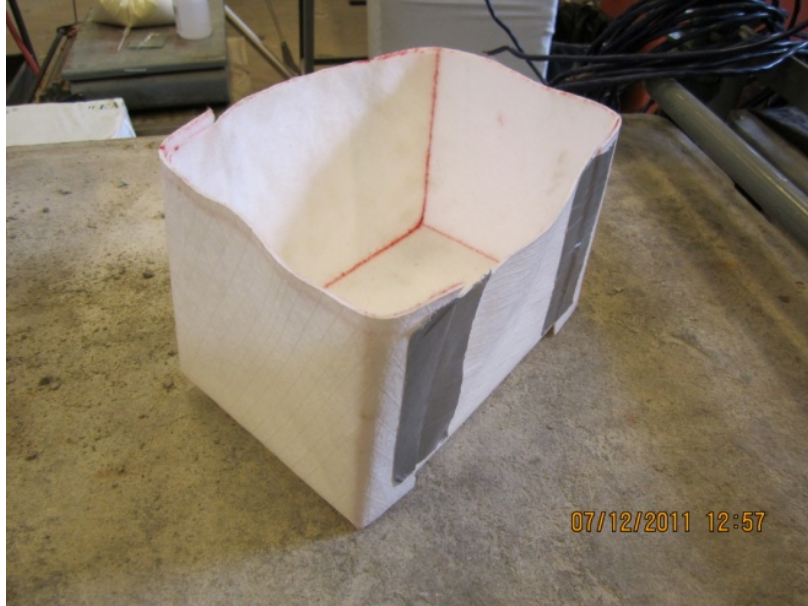
Figure 5.37 Assembled Burlene liner

The wooden thermocouple dowel supports are made of a piece of laminated plywood with three holes made by a 0.5" dia. drill bit at depths of 1/2", 3" and 5-1/2" from the top of the sample. Figure 5.38 shows a wood dowel that is ready for use. There are also dimensions given on Figure 5.38 which show where the holes are made relative to the outside dimensions of the dowel.

Figure 5.38 Laminated plywood dowel with dimensions

The dowels are assembled within the liners inside the forms. The dowels are attached at the center of the sample by hot glue. Three temperature measurements were taken per sample.

Figure 5.39 shows the image of a completed assembly with labels.
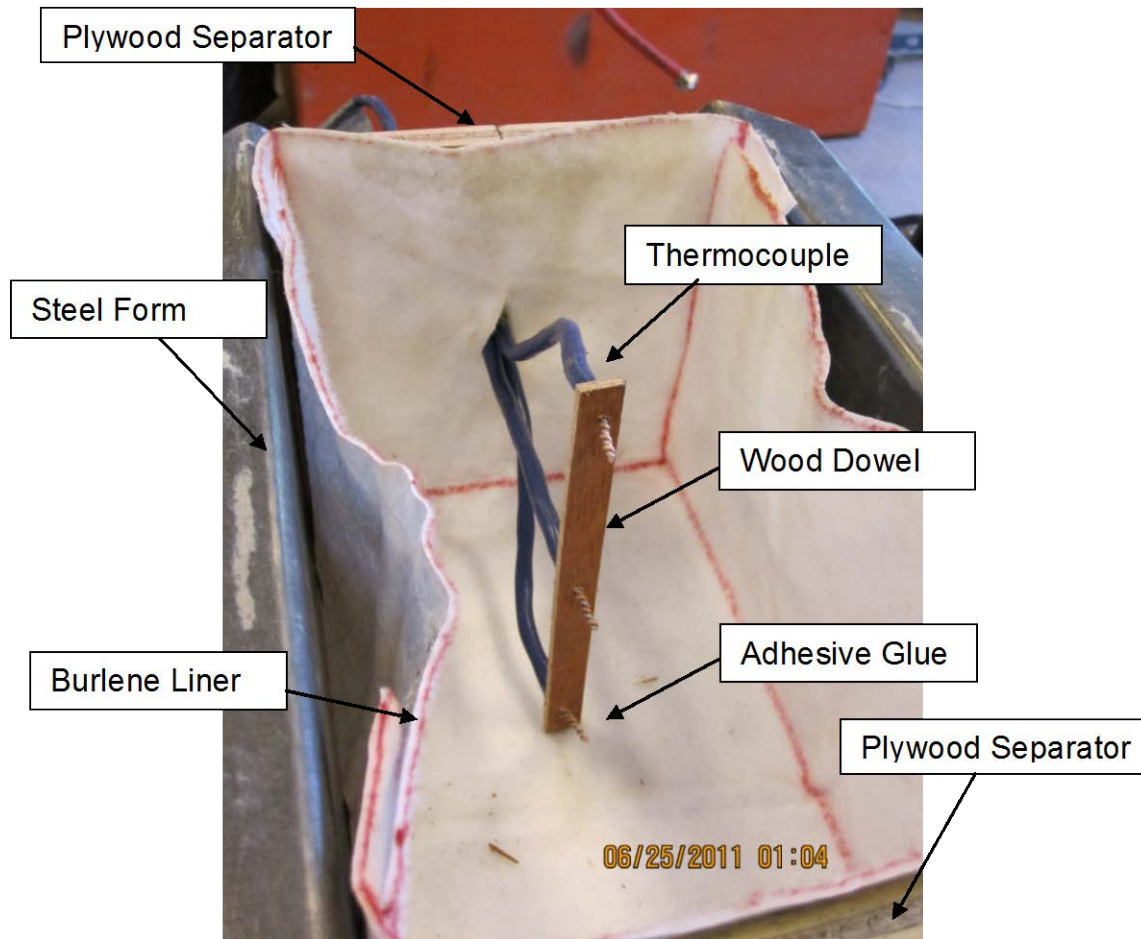
Figure 5.39 Assembled thermocouple, dowel, liner & form

Concrete mixtures were prepared as outlined in section 5.2.2.2 in this document. The samples were placed with three lifts. After each lift, the sample was vibrated. Once the three lifts are place, the samples are smoothed off to the surface of the form.

The individual samples and data recording equipment were then moved outside to a hard packed dirt surface clear of vegetation where: the forms were removed, samples spaced evenly, and the curing methods were applied.

5.3.3 Discussion

5.3.3.1 Overview

A temperature gradient at different time periods was developed and compared for each sample. Ideally, a curing method should produce a near uniform gradient throughout the depth of the sample. This will minimize the temperature differential at setting and minimize the built in curl in the specimen.

During each trial, two samples of each curling method were investigated. Results from the samples were found to be very similar.

All following gradient figures show temperature gradients up until six hours. If no data is shown for the zero time segment of a figure, it is a result of the short amount of time required to configure the second data logger after the first is completed and recording data.

5.3.3.2 Curing methods tested

In the following test, the focus was on the ability for a covering to insulate the concrete. Six investigations were made consisting of varying combinations of curing methods. If methods were determined to be minimally effective at insulating the samples, then further testing of those methods was not pursued.

The most informative data from the six investigations is presented in the following. More findings will be presented in the Phase 1 summary report.

The methods investigated and reported here are:

1. No Cure (control method)
2. Misting
3. Single Layer of Curing Compound
4. Two Layers of Wet Burlap
5. Two layers of Wet Burlap covered by One Layer of Blue Tarp
6. Two layers of Wet Burlap covered by One Layer of Clear Plastic
7. Two layers of Dry Burlap
8. Six Layers of Dry Burlap
9. One Layer of Burlene

On the following figures, there are dashed designation lines which represent temperatures at various depths of the sample. The two designators named Air and Ground represent the ambient air and ground temperatures immediately above and beneath the sample.

.3.3.3 No curing method

This method is considered the benchmark between all of the other tests. Conventionally this is thought to be the worst curing situation. The samples where no curing techniques were used showed that initially the samples surface remained cooler than the ground temperature. At three hours, the greatest difference in the temperature at the surface versus the rest of the sample can be seen. Afterward the sample begins to cool in a relatively uniform manner as the surrounding temperatures lessened. Figure 5.40 shows the temperature gradients for the no cure method.
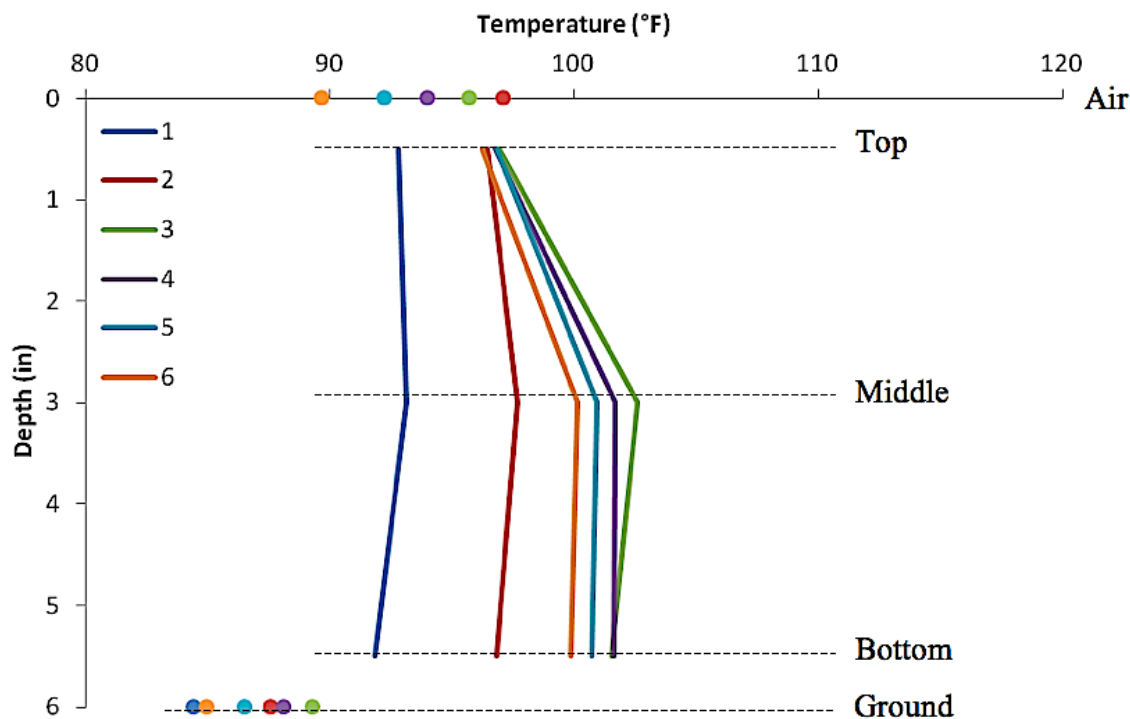
Figure 5.40 No-cure temperature gradients

5.3.3.4 Misting

The misting procedure used for curing involved applying a fine water spray to the sample surface once per hour for six hours after placement. There is not a noticeable

difference at the surface of the sample that can be attributed to the misting process. There is little difference between the no curing and the misting sample. This is likely because the misting is not a large enough volume to make an impact on the mass of concrete. Figure 5.41 shows the temperature gradients for the misting method.
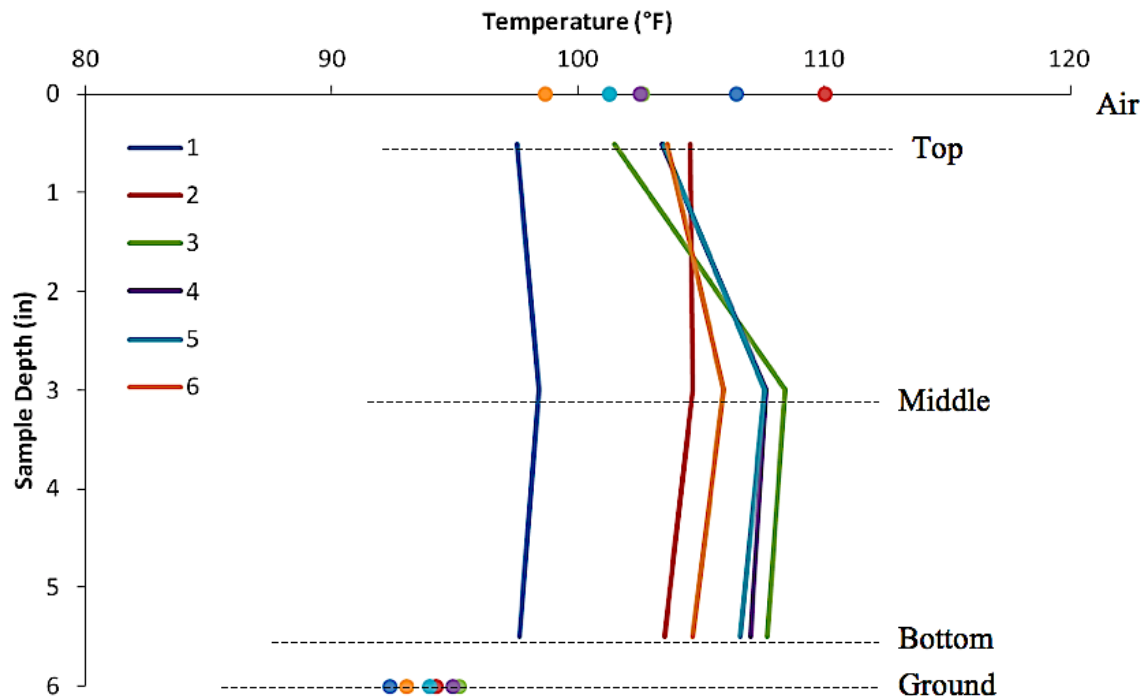
Figure 5.41 Misting at hourly intervals for 6 hours after placement temperature gradients

5.3.3.5 Curing compound

There was little difference between the no cure, misting, and curing compound sample. The surface of the sample was slightly warmer in the sample with the curing compound. This is probably due to the reduced amount of evaporation from the sample. Figure 5.42 shows the temperature gradients for the curing compound method.
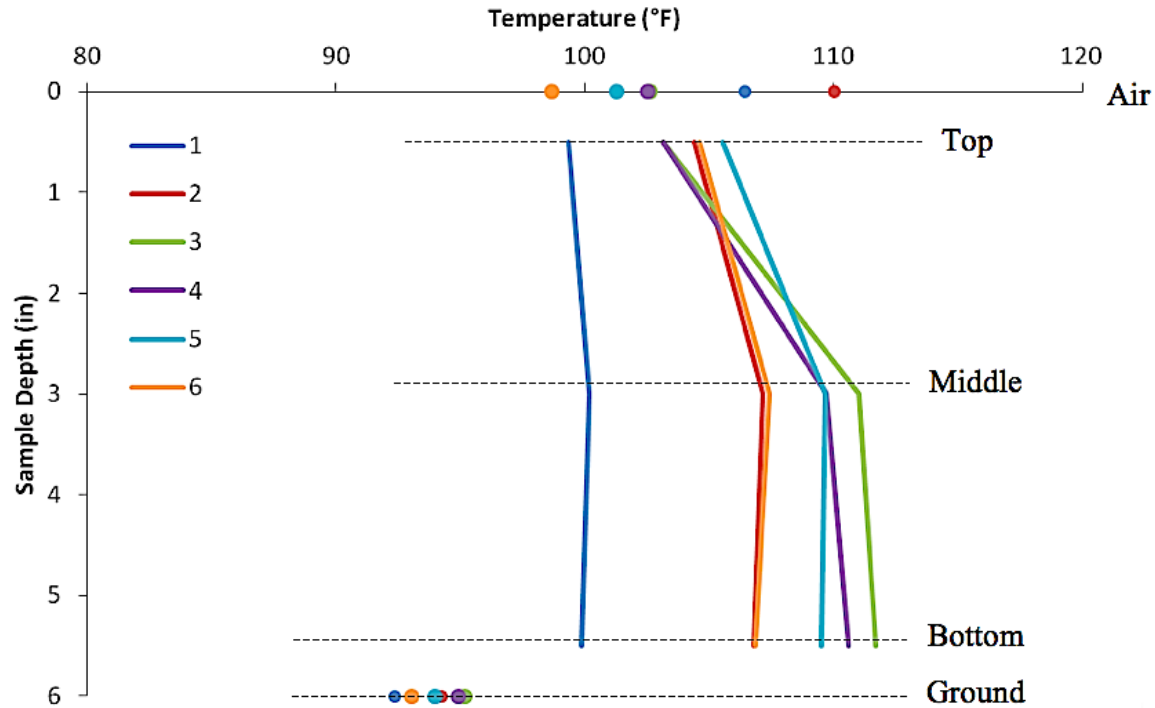
Figure 5.42 Single layer curing compound temperature gradients

5.3.3.6 Two layers of wet burlap

Wet burlap showed a much more uniform temperature gradient than all of the other previous curing methods investigated. The burlap likely acts as a covering that minimizes surface evaporation and also insulates the sample. Figure 5.43 shows the temperature gradients for the two layers of wet burlap method.
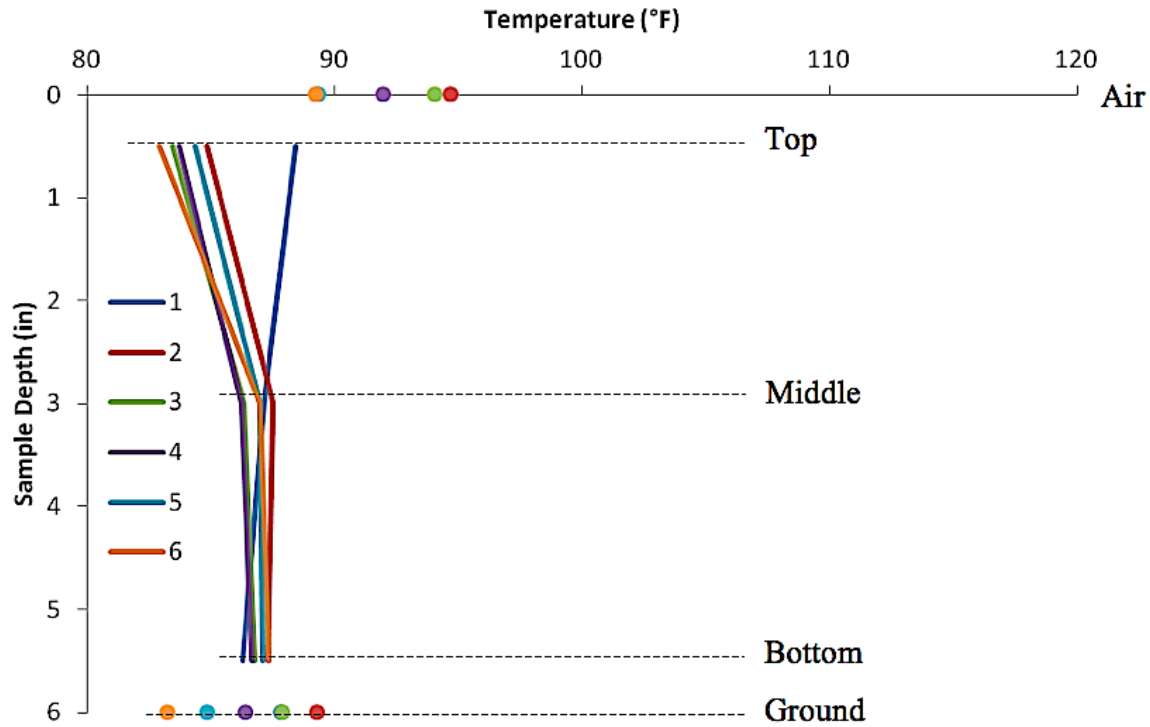
Figure 5.43 Two layers wet burlap temperature gradients

5.3.3.7 Two layers of wet burlap covered by one layer of blue tarp

The sample where wet burlap was covered with blue tarp kept the surface of the sample much hotter than the rest of the samples. During the last three hours the middle of the sample became the hottest portion of the sample. Also, as the surface heats then cools, the bottom of the sample continuously heats. The tarp used is a woven material which does not let the air near the sample. Figure 5.44 shows the temperature gradients for the two layers of wet burlap covered with a single layer of blue tarp.
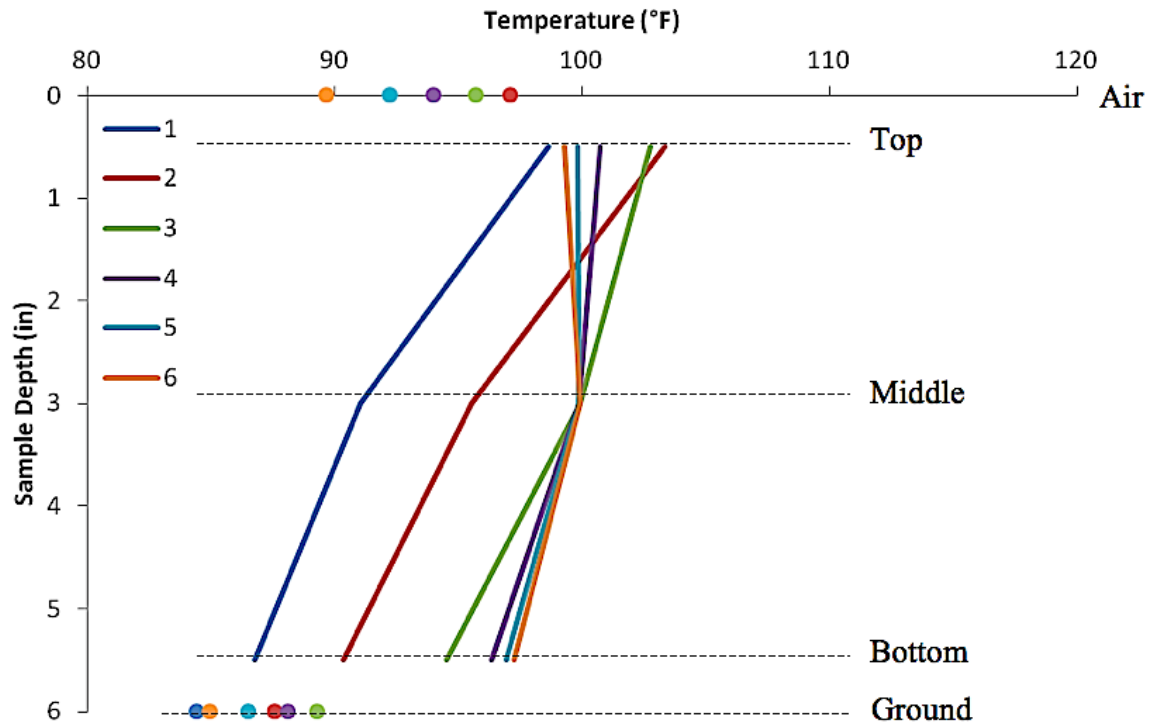
Figure 5.44 Two layers wet burlap & one layer blue tarp temperature gradients

5.3.3.8 Two layers of wet burlap covered by one layer of clear plastic

The use of wet burlap with a clear plastic covering showed different temperature gradients at different times. The top material became very hot during the testing. The wet burlap seemed to insulate the concrete. Figure 5.45 shows the temperature gradients for the two layers of wet burlap covered with a single layer of clear plastic.
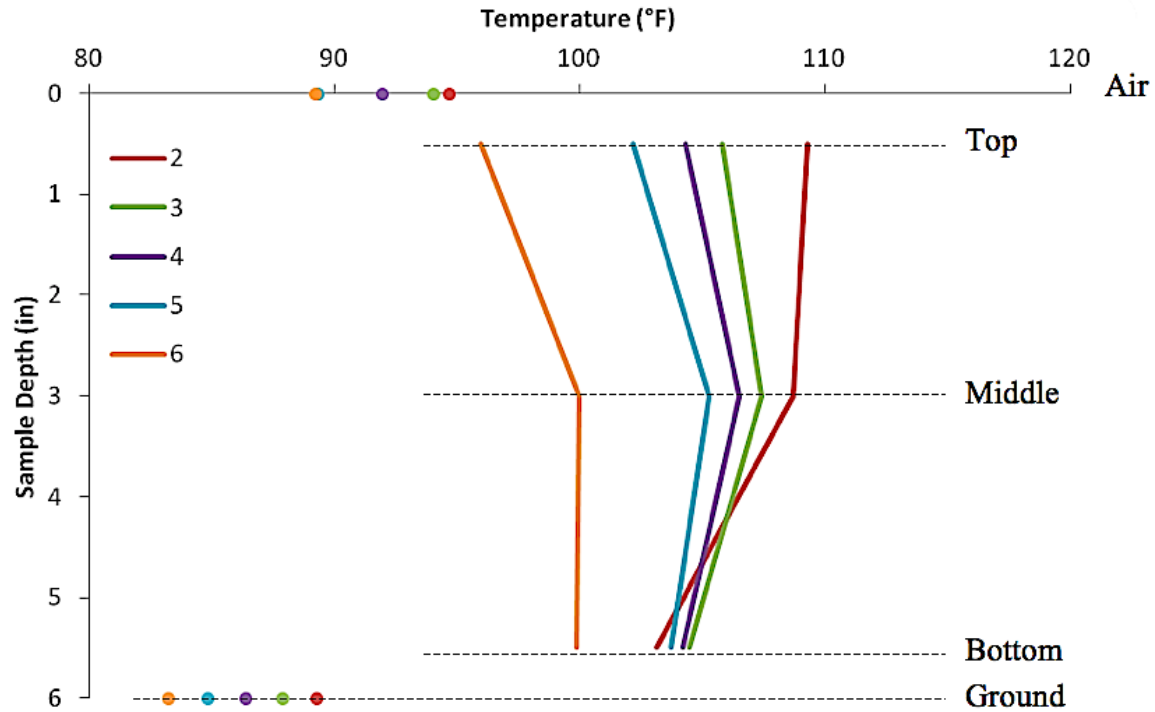
Figure 5.45: Two layers wet burlap & one layer clear plastic temperature gradients

5.3.3.9 Two layers of dry burlap

Dry burlap showed very uniform gradients during curing. The gradients here are quite constant after second hour of curing and show a uniform temperature variation throughout the sample. Figure 5.46 shows the temperature gradients for the sample with two layers of dry burlap.
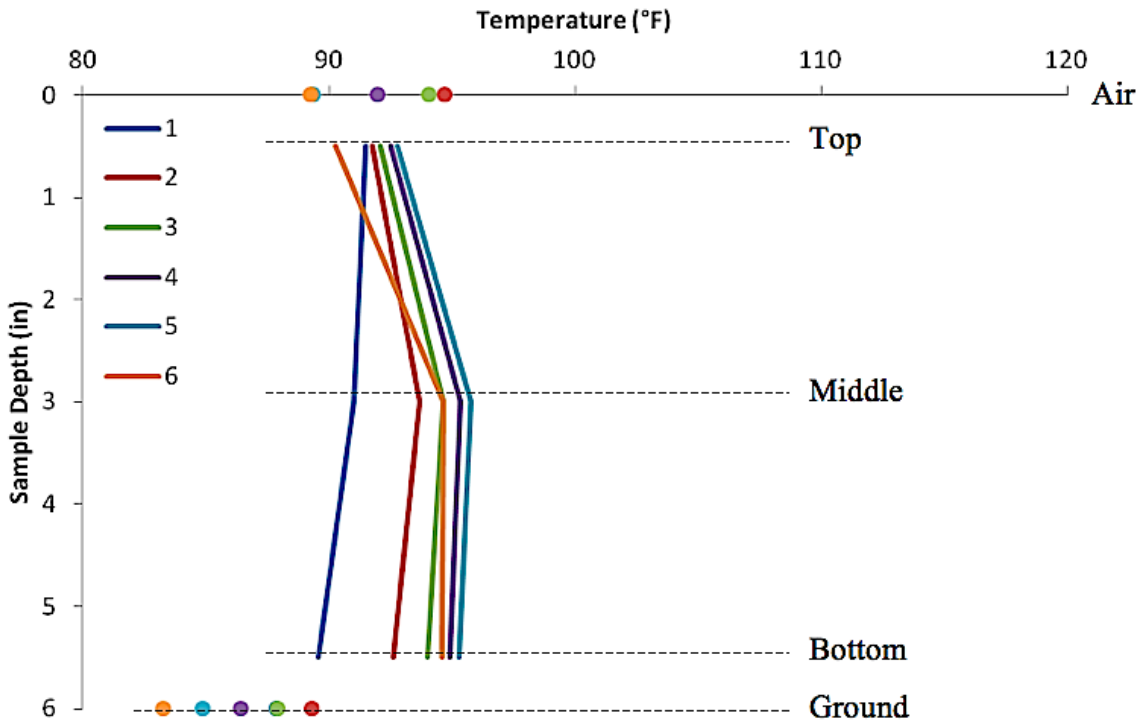
Figure 5.46 Two layers of dry burlap temperature gradients

5.3.3.10 Six layers of dry burlap

This method showed very acceptable gradients by the standards of the current methodology. The temperature continues to rise throughout the measured time interval, however unlike other methods; the samples keep a uniform temperature gradient. While not completely vertical, the gradients are very constant showing that the curing method allows the sample to maintain constant temperature changes in relation to its depth. It is believed that this uniformity is due to air layers between the layers of breathable fabric. These air layers act much like other technologies (ex. layered glass windows in homes) where they insulate the two sides by allowing more gradual changes in temperature. Figure 5.47 shows the temperature gradients for the six layers of dry burlap method.
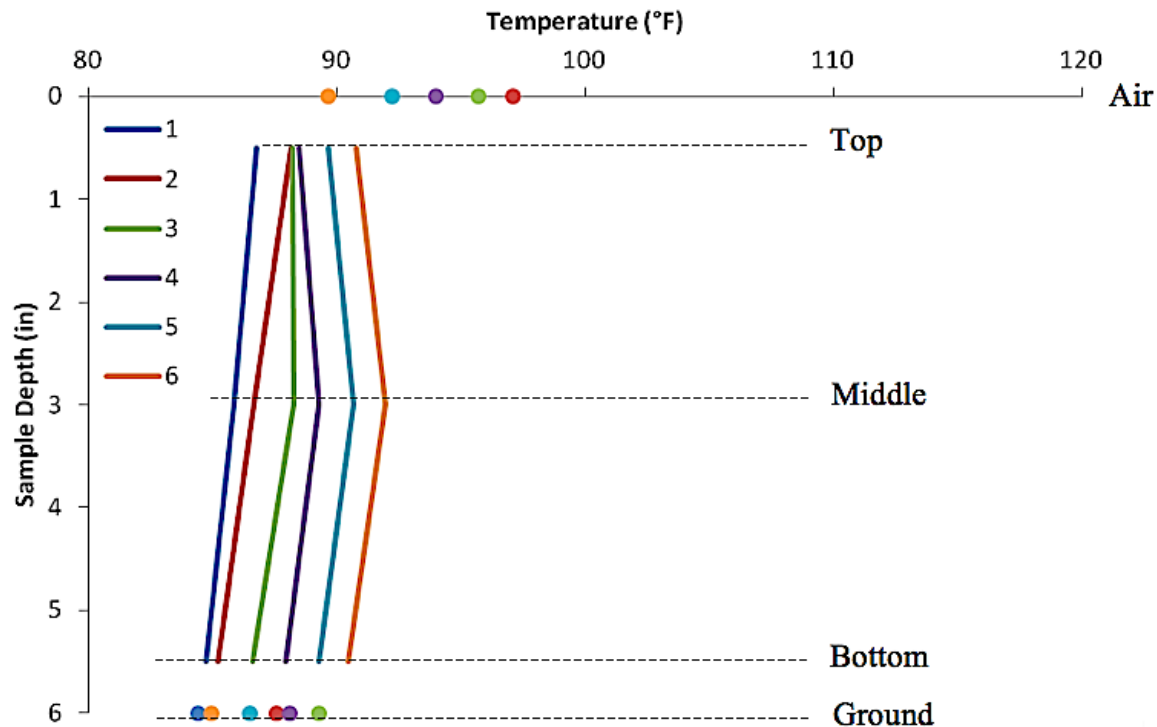
Figure 5.47 Six layers of dry burlap temperature gradients

5.3.3.11 One layer of burlene

The last method tested is a single layer of Burlene. Note that all samples are lined on five of their six sides with Burlene already. This method essentially seals the entire sample with continuous material. This method shows similar trends to other tested methods where the sample heats and then begins to cool after the third hour of curing. This technique provided a uniform curing gradient. Figure 5.48 shows the temperature gradients for a single layer of Burlene.
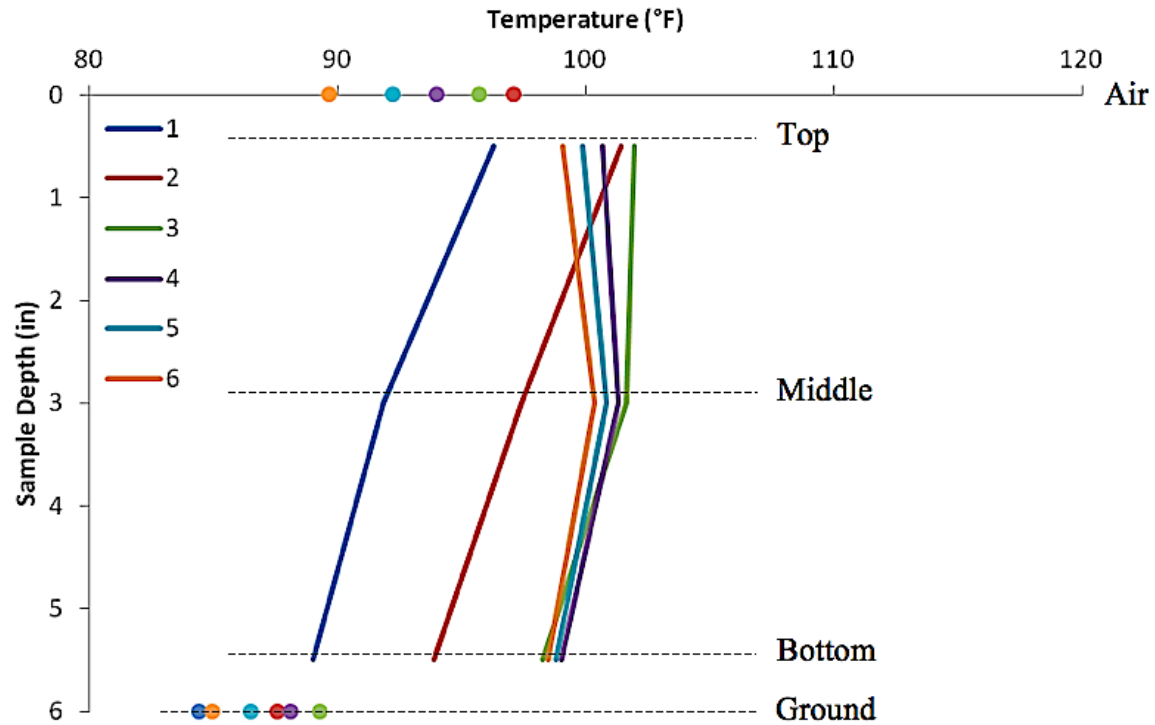
Figure 5.48 One layer of Burlene temperature gradients

5.3.4 Result comparison

Table 5.8 shows the temperature differences of the top and bottom of the samples at two hour intervals beginning at placemen.

Table 5.8 Differences in temperature between the top and bottom of investigated samples at 2, 4 and 6 hours after placement

Curing Method	Investigation Date	Temperature Differences (°F)		
		2(hr)	4(hr)	6(hr)
No Cure	6/10/2011	0.38	4.89	3.64
Misting	7/26/2011	1.07	-3.56	-1.04
Curing Compound	7/26/2011	-2.38	-7.45	-2.23
Two Layers Wet Burlap	6/10/2011	-2.45	-2.91	-4.44
Two Layers Wet Burlap & One Layer Blue Tarp	6/10/2011	-12.98	-4.38	-2.05
Two Layers Wet Burlap & One Layer Clear Plastic	6/10/2011	6.14	0.13	-3.91
Two Layers Dry Burlap	6/10/2011	0.84	2.37	4.34
Six Layers Dry Burlap	6/10/2011	2.9	0.56	0.34
One Layer Burleen	6/10/2011	7.51	1.68	0.63

Upon comparing the temperature gradients to each other groups of curing methods showed similar traits.

The six-layer dry burlap method kept the temperature gradients very uniform.

The two layer dry burlap and the two layer wet burlap have very similar gradients; however the wet burlap kept the overall sample temperature much cooler than the dry burlap method.

The no-cure, single layer curing compound, and misting all showed similar trends in the test. Neither the single-layer curing compound nor the misting methods show a significant difference from the no cure method.

The two layers of wet burlap with one layer of blue tarp and the one layer of Burlene methods showed similar gradients. These methods seem to increase early sample temperatures much more than the previously mentioned methods.

The two layers of wet burlap with one layer of clear plastic showed very non uniform temperature gradients as well as large differences between the gradients over time. This method also showed an increase in early sample temperatures.

5.3.5 Guidance

After evaluating the results, the data supports the notion that temperature related curling is controlled more by the curing methods insulation ability rather than whether or not the method utilizes water. However the use of wet burlap also promotes hydration in the concrete by supplying additional water. There is no noticeable difference of the single layer curing compound, hourly misting, and no curing method.

There were concerns from the research team that these samples were not large enough to isolate the thermocouples in the center of the slab. Because of this larger samples were investigated. After comparing the results the research team feels more comfortable with the data from the larger samples.

5.4 METHODS TO REDUCE CURLING IN CONCRETE FROM TEMPERATURE DIFFERENTIALS WITH LARGE SPECIMENS

5.4.1 Introduction

Larger samples were used to investigate the impact of curing on the temperature gradients in the concrete. This work was done to compliment the small specimens.

5.4.2 Methodology

5.4.2.1 Experiment Preparation

Collapsible wood forms were used that are 36"x36"x8". The earth beneath the forms was turned, compacted by hand, and leveled. Once the form was assembled and leveled off, sand was used to fill the bottom so that an 8" sample depth was achieved. A wooden thermocouple stake was used to support the thermocouples in the fresh concrete. This was made by taking a surveying dowel with three 0.25" diameter holes at depths of 0.5", 4.0" and 7.5" from the top of the sample. Figure 5.49 shows a wood dowel that is ready for use.
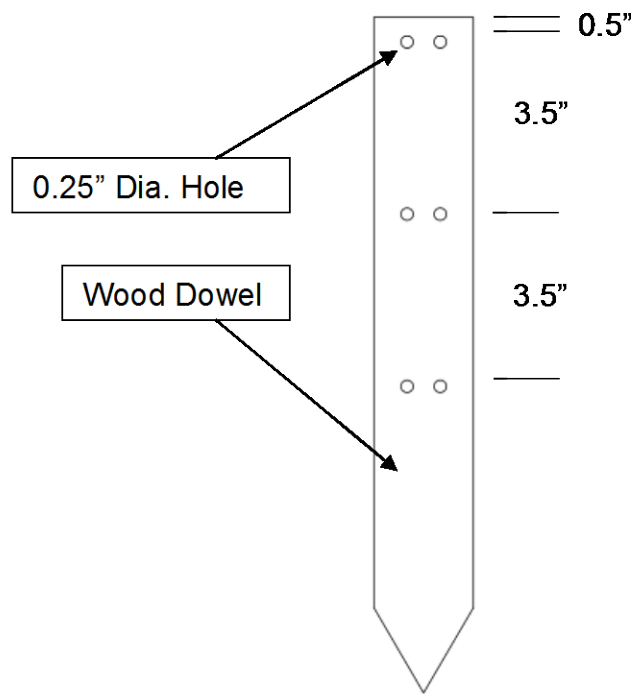
Figure 5.49 Wood dowel with dimensions

The dowels are hammered into the ground at the center of the form. The tops of the dowels were leveled with tops of the wood forms. Six temperature measurements were taken per sample for redundancy. Figure 5.50 shows the image of a completed assembly with labels.
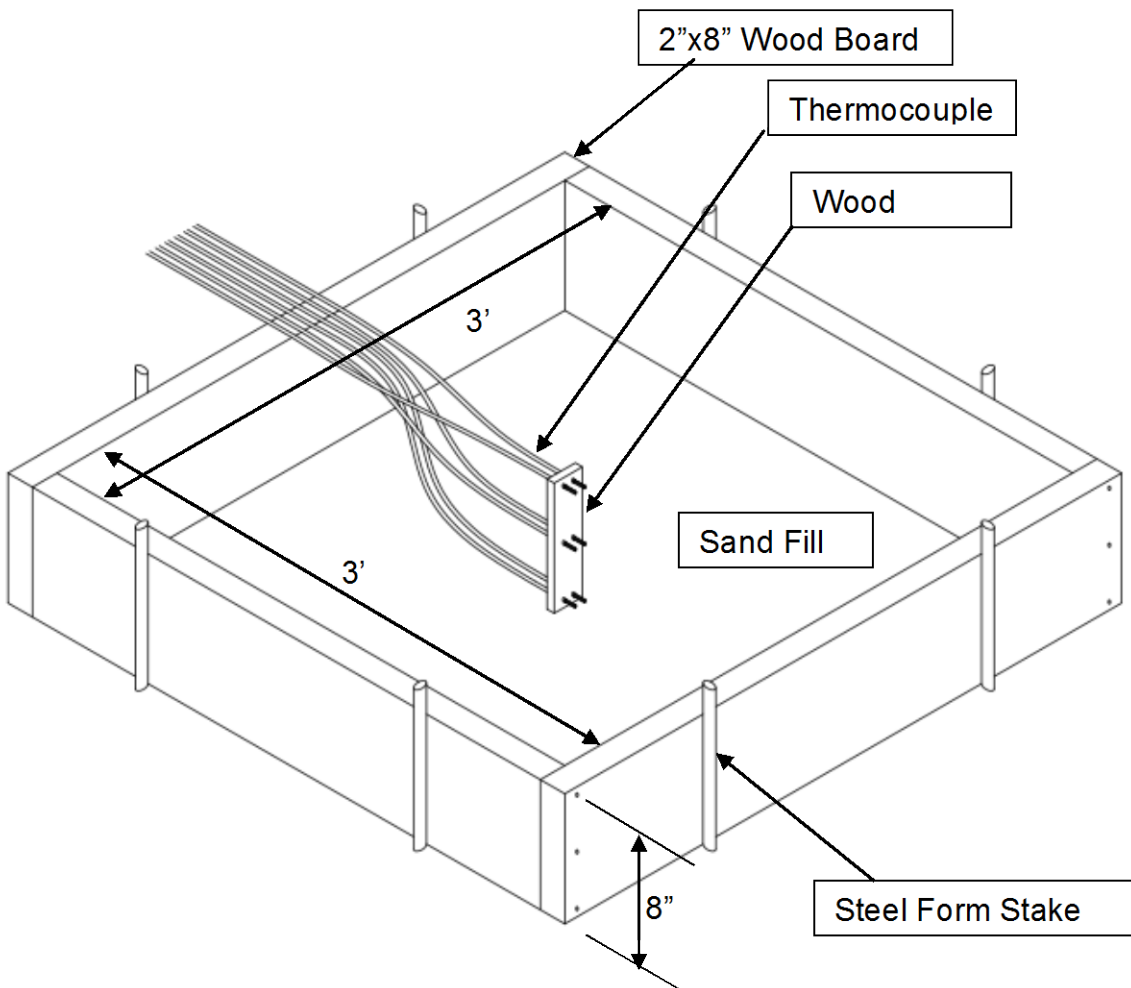
Figure 5.50 Assembled thermocouple, dowel, liner & form

Concrete mixtures were designed as outlined in section 5.2.2.2 in this document. The mixture was ordered from a local batch plant and the concrete was delivered to the site. The samples were placed with two lifts. After each lift, the sample was vibrated. Once the three lifts are in place, the samples were finished to the surface of the form. After the samples were finished, the curing methods were applied.

5.4.3 Discussion

5.4.3.1 Overview

A temperature differential at different time periods was measured for each sample. Ideally, a curing method should produce a near uniform temperature differential throughout the depth of the sample. This will minimize the temperature differential at setting and minimize the built in curl in the specimen.

The time intervals presented in the following figures are approximated to account for the time required for the concrete to arrive from the batch plant and the samples to be made and curing methods applied.

5.4.3.2 Curing methods tested

Three investigations were made consisting of varying combinations of curing methods. These methods were chosen to coincide with some of the smaller samples from section 5.3.

The methods investigated and reported here are:

1. No cure (control method)
2. Misting
3. One layer of curing compound
4. One layer of wet burlap
5. One layer of wet burlap covered by one layer of clear plastic

These investigations took place on three separate days each having noticeably differing outside temperatures. These days had different mean temperatures that allowed different conditions to be compared.

On the following figures, there are dashed lines which represent temperatures at various depths of the sample. The two lines named "air" and "ground" represent the ambient air and ground temperatures immediately above and beneath the sample. These two ambient temperatures were taken with separate thermocouples placed outside of the samples.

5.4.3.3 No curing

This method is considered the benchmark between all of the other tests. Conventionally this is thought to be the worst curing situation. The samples where no curing techniques were used showed that initially the samples surface remained cooler than the ground temperature. At four hours, the greatest difference in the temperature at the surface versus the rest of the sample can be seen. Afterward the sample begins to cool in a relatively uniform manner as the surrounding temperatures decreased. Figures 5.51, 5.52, and 5.53 show the temperature differentials for the no cure method.
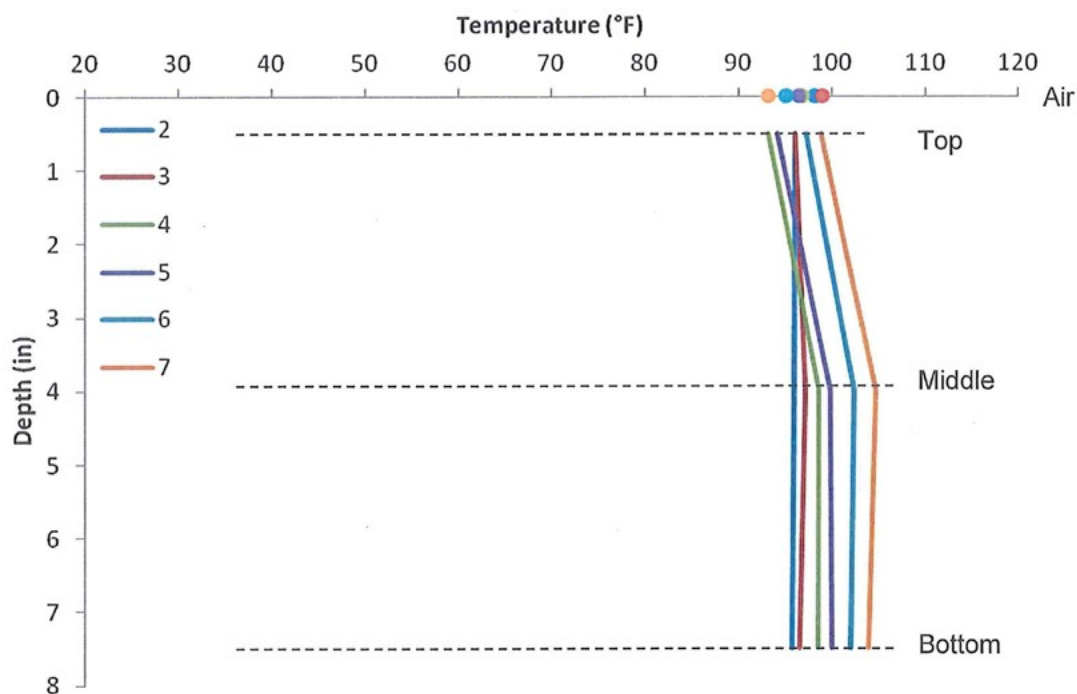
Figure 5. 51 August 29, 2011 no cure temperature differentials 29, 2011 no cure temperature differentials
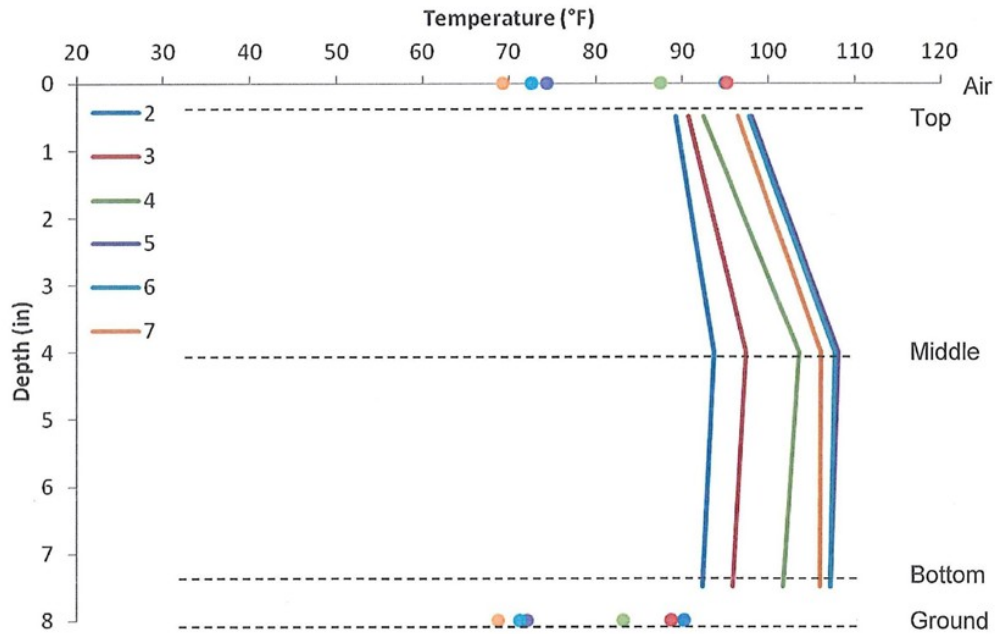
Figure 5. 52 October 4, 2011 no cure temperature differentials
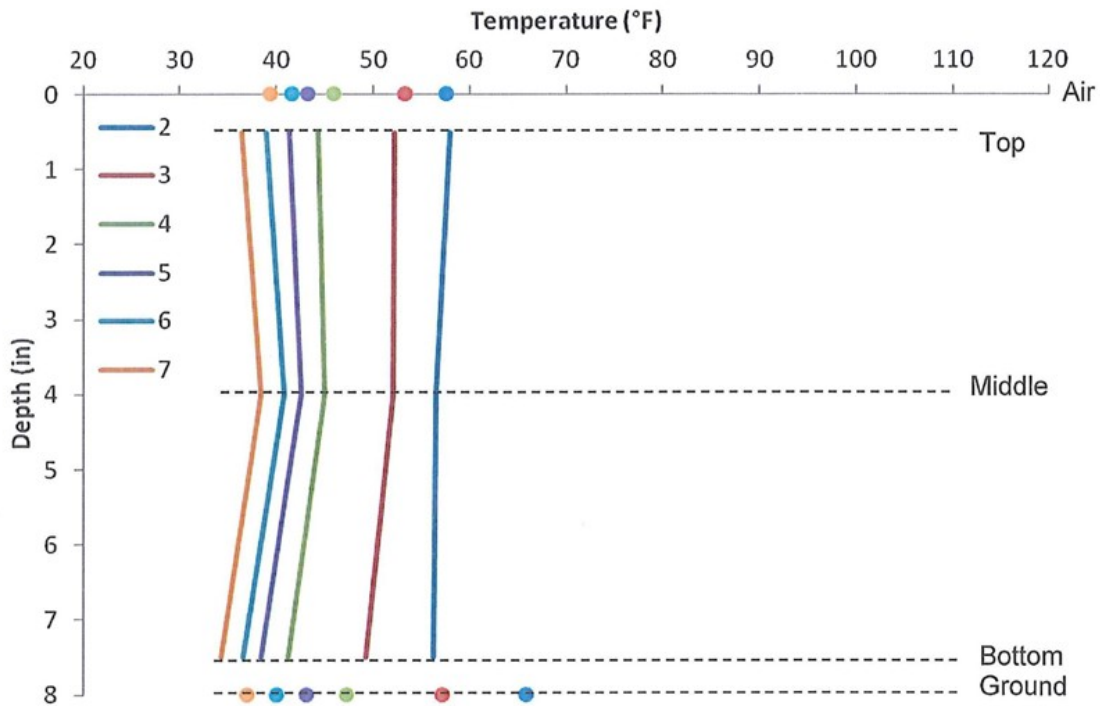
Figure 5. 53 November 30, 2011 no cure temperature differentials

A fine water spray was applied to the sample surface of the sample once per hour for six hours after placement. Figures 5.54 and 5.55 show the temperature differentials for the misting method. There is no noticeable difference between the no curing and the misting sample. This is likely because the misting is not a large enough volume to make an impact on the mass of concrete.
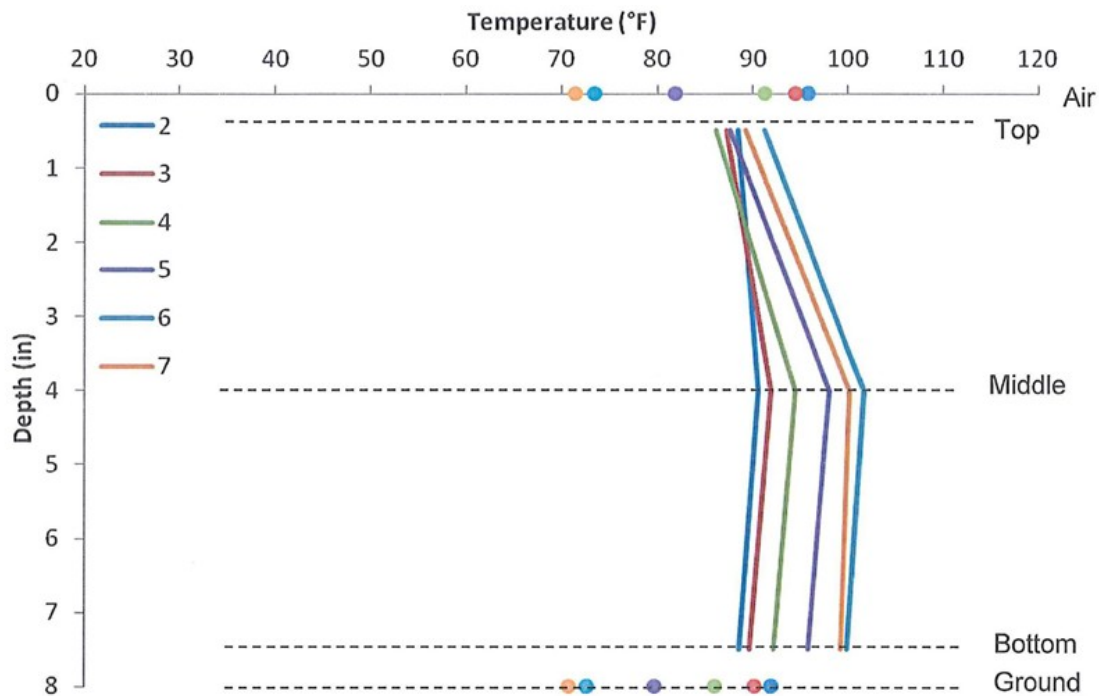
Figure 5. 54 October 4, 2011 slab placed and cured with hourly misting
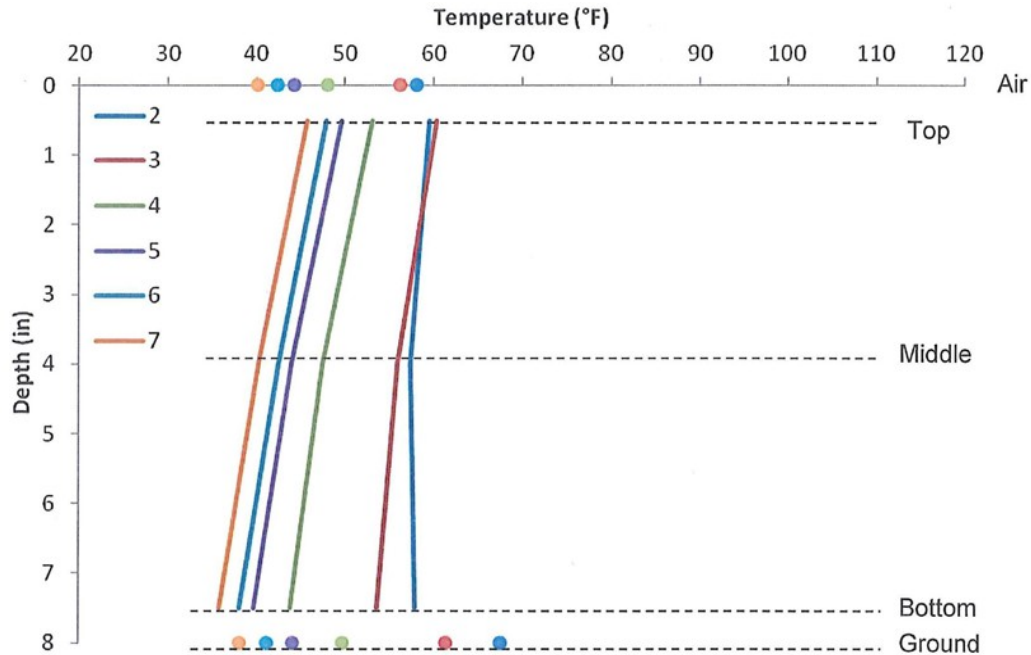
Figure 5. 55 November 30, 2011 slab placed and cured with hourly misting

5.4.3.5 Curing Compound

The surface of the sample was slightly warmer in the sample with the curing compound. This is probably due to the reduced amount of evaporation from the sample. Figures 5.56 and 5.57 show the temperature differentials for the curing compound method.
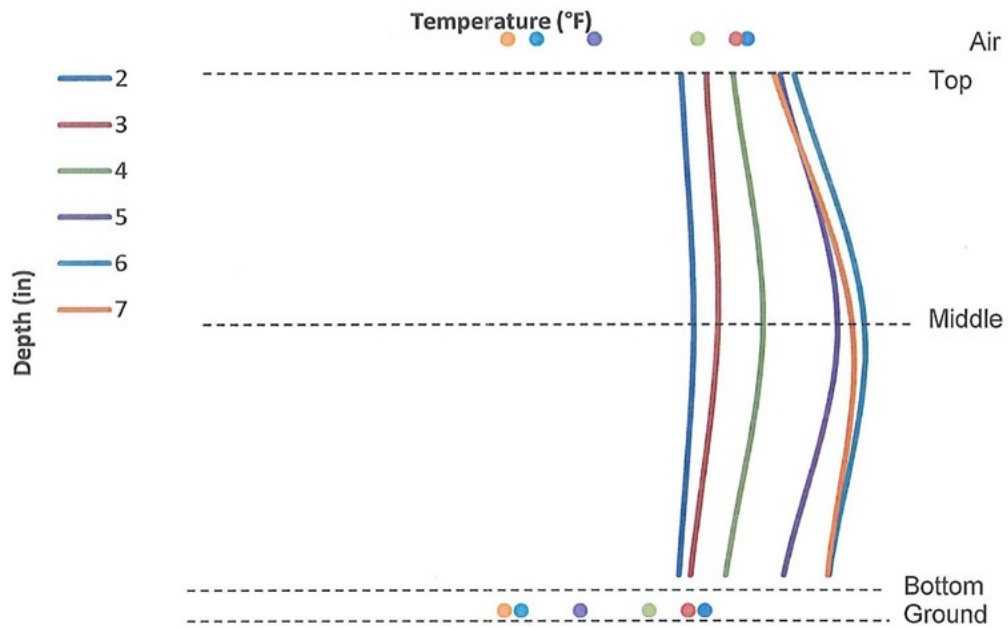
Figure 5. 56 October 4, 2011 single layer curing compound temperature differentials
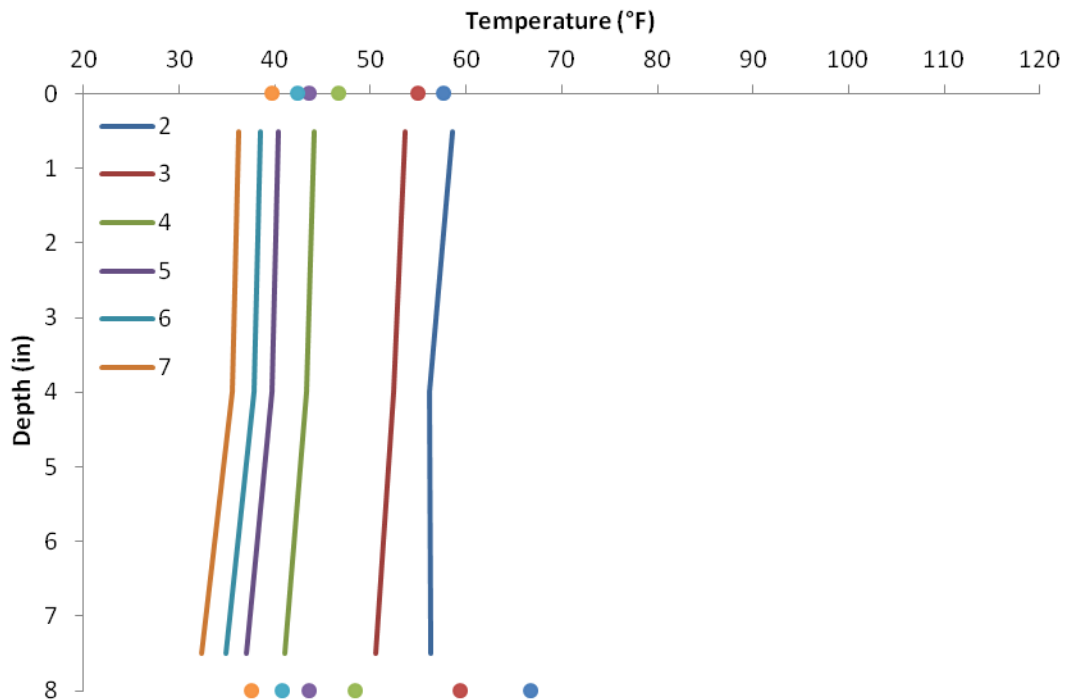
Figure 5. 57 November 30, 2011 single layer curing compound temperature differentials

130

<u>5.4.3.6 Two layers of wet burlap</u>

Wet burlap showed a much more constant temperature differential than all of the other previous curing methods investigated. The burlap likely acts as a covering that minimizes surface evaporation and also insulates the sample. Figure 5.58 show the temperature differentials for two layers of wet burlap.
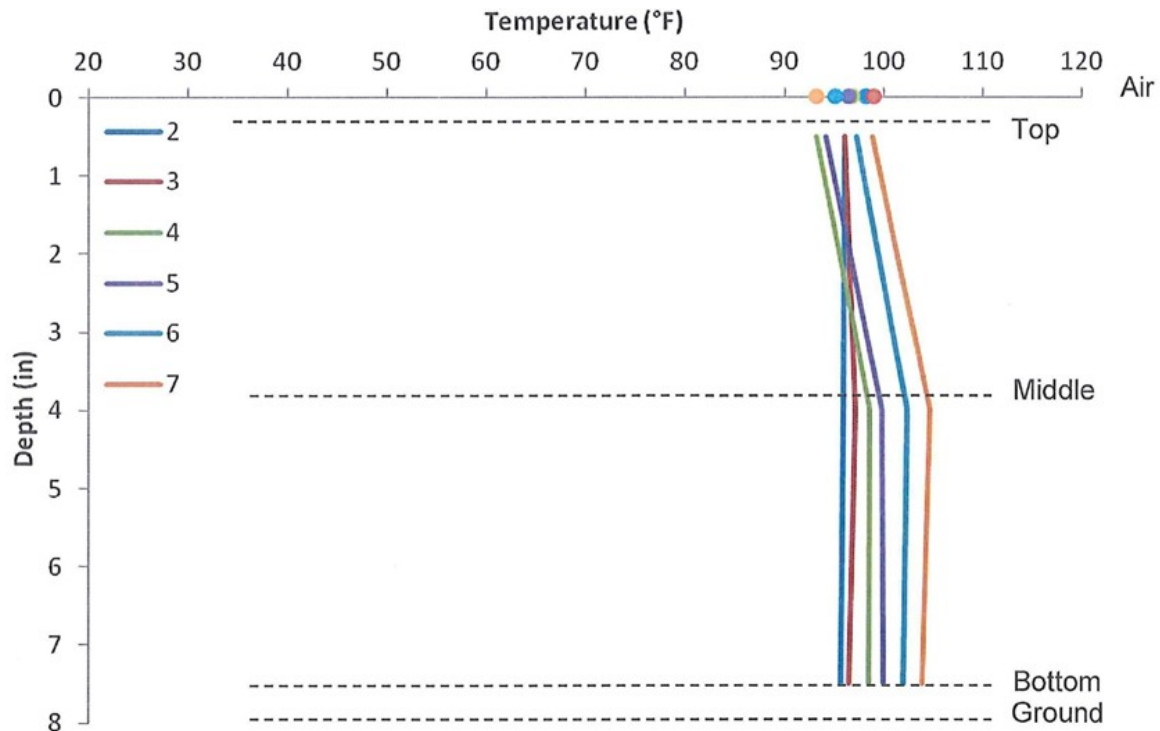
Figure 5.58 August 29, 2011 one layer of wet burlap temperature differentials

<u>5.4.3.7 One Layer of wet burlap covered by one layer of clear plastic</u>

The use of wet burlap with a clear plastic covering showed consistent temperature differentials. The material at the top of the surface was hotter than the other samples. This suggests that the burlap and plastic combination seems to insulate the concrete. Figures 5.59 and 5.60 show the temperature differentials for the two layers of wet burlap covered with a single layer of clear plastic.
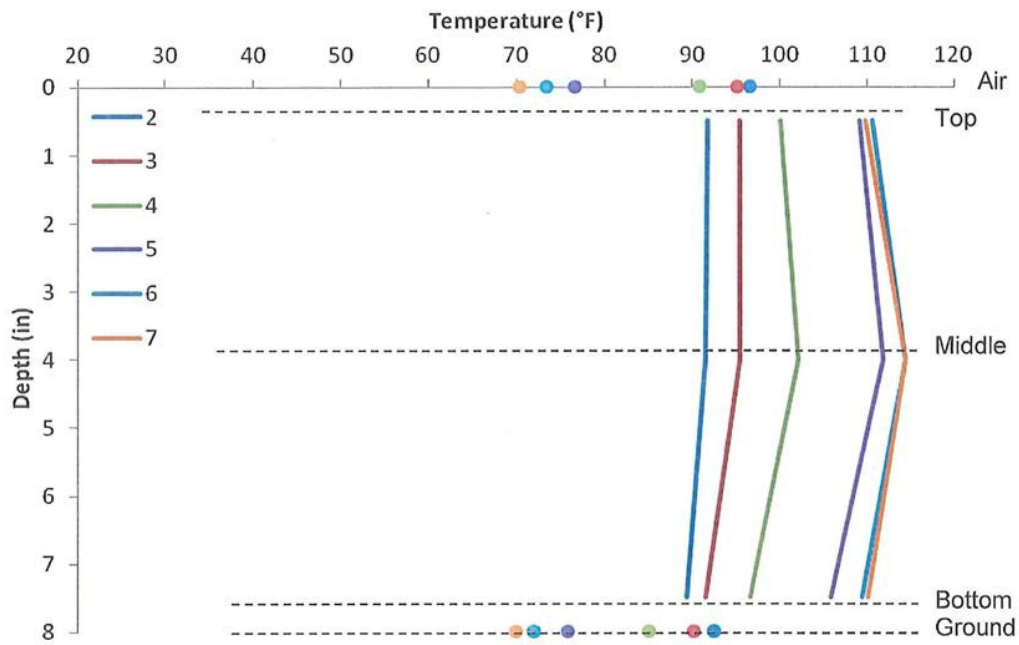
Figure 5.59 October 4, 2011 Temperature differential for one layer of wet burlap and clear plastic
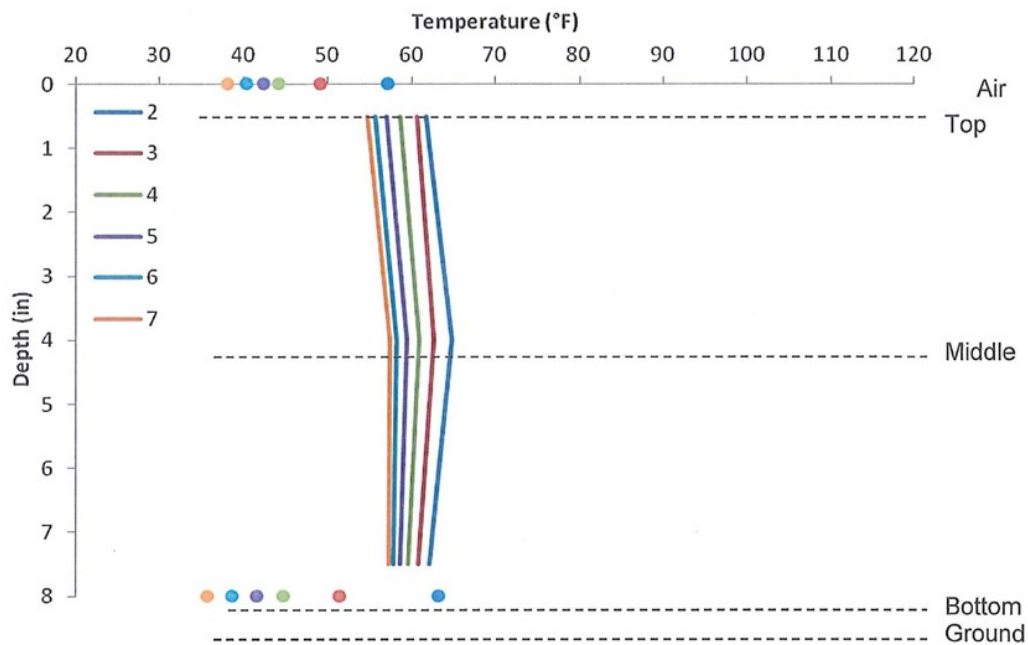
Figure 5. 60 November 30, 2011 temperature differential for one layer of et burlap and clear plastic

5.4.4 Result Comparison

Table 5.9 shows the temperature differences of the top and bottom of the samples at two hour intervals after placement. In the table specimens with a temperature different larger than 4°F were made red and the others were left black.

Table 5.9 Differences in temperature between the top and bottom of investigated samples at 3, 5 and 7 hours

Curing Method	Investigation Date	Temperature Differences (°F)		
		3 (hr)	5 (hr)	7 (hr)
No Cure	8/29/2011	-0.5	-5.9	-5.1
	10/4/2011	5.0	9.1	9.6
	11/30/2011	3.0	2.9	2.2
Misting	10/4/2011	-2.4	-8.3	-10.1
	11/30/2011	6.7	9.9	10.0
Curing Compound	10/4/2011	1.7	-0.4	-5.8
	11/30/2011	3.1	3.3	3.8
One Layer Wet Burlap	8/29/2011	-9	-10	-12.2
One Layer Wet Burlap & One Layer Clear Plastic	10/4/2011	3.9	3.4	-0.3
	11/30/2011	-0.2	-1.6	-2.5

The samples that used a curing compound and one layer of burlap and clear plastic had the lowest temperature differentials of the samples investigated. It is interesting that these two curing methods are the most commonly used. The sample that used a single layer of wet burlap showed the highest temperature differential. This is likely due to the evaporation from the surface of the wet burlap.

The sample that was misted and not cured showed similar trends to the single layer of wet burlap.

5.4.5 Guidance

After evaluating the results, the data suggests that temperature related curling is controlled by the insulation and ability to minimize evaporation. This is similar to what was found with smaller sample testing.

The use of clear plastic directly on fresh concrete is not suggested if temperature related curling is a concern. However if clear plastic is used on burlap then this can reduce evaporation and keep temperatures constant.

The research team has more confidence in these findings. This work will be used a solid foundation for future work to be completed in Phase II.

5.4.6 Other efforts

Larger sample testing will continue into Phase 2 of the project. Other future efforts in the advancement of this test may possibly include, but are not limited to; the testing of different curing methods, use of a climate controlled chamber during curing, modification to sample design, and/or monitoring a greater spectrum of atmospheric conditions during curing for outside testing.

6.0 PROVIDE REGIONAL MATERIAL INPUT PARAMETERS THAT CAN BE USED IN THE MEPDG FOR THE DESIGN OF RIGID PAVEMENTS

The MEPDG user manuals have suggested that more accurate pavement designs can be determined if accurate material input values can be obtained for local materials. Through the sensitivity analysis contained in this report and through discussions with ODOT it has been determined that the following parameters should be further investigated for Oklahoma paving concrete mixtures:

1. Strength Testing
2. Coefficient of thermal expansion (CTE)
3. Concrete Shrinkage

6.1 STRENGTH TESTING

The strength of a mixture depends on the cementing materials in the mixture, the water to cement ratio, and the bond between the aggregates and the paste. To evaluate these parameters 4" x 8" compression cylinders (AASHTO T 22 "Standard Method of Test for Compressive Strength of Cylindrical Concrete Specimens") and flexural beams (AASHTO T 97 "Standard Method of Test for Flexural Strength of Concrete (Using Simple Beam with Third-Point Loading)") will be prepared for a number of the mixtures prepared for the CTE and shrinkage testing and tested for strength at 7, 14, 28, and 90 days of hydration. This testing will not only provide ODOT with a range of results for the common mixtures used in the state but will also provide a correlation between the two measurements. Based on the results it was found that the relationship between the compressive and flexural strength of the specimens closely followed Equation 7.1.

Equation 6.1

$$\sigma\, flexural = 9.5\sqrt{f\,'c}$$

The relation is shown in Figure 6.1 and is a similar value as to what is suggested in the MEPDG design manual.

Table 6.1 Mixture designs

Mixture #	Mixture Description	Slump (in)	Unit wt. (lb)	Air Content (%)
1	5.5 sacks Lafarge	0.75	147.4	5.5
2	5.5 sacks Lafarge 20% red rock	1	146	6.1
3	5.5 sacks Lafarge 20% Muskogee	1.5	151.4	6.7
4	5.5 sacks Holcim 20% red rock	1	154.2	5.3
5	5.5 sacks Buzzi 20% red rock	1.25	152.6	6.25
6	5.5 sacks Lafarge 20% GRDA	1.25	152.5	6
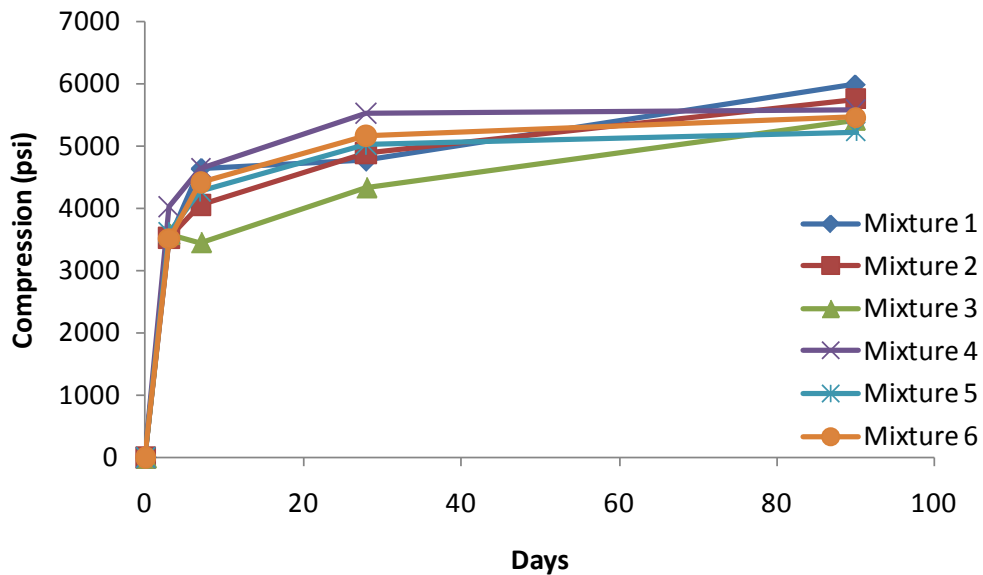
Figure 6.1 Compressive strength versus time for the different mixtures.
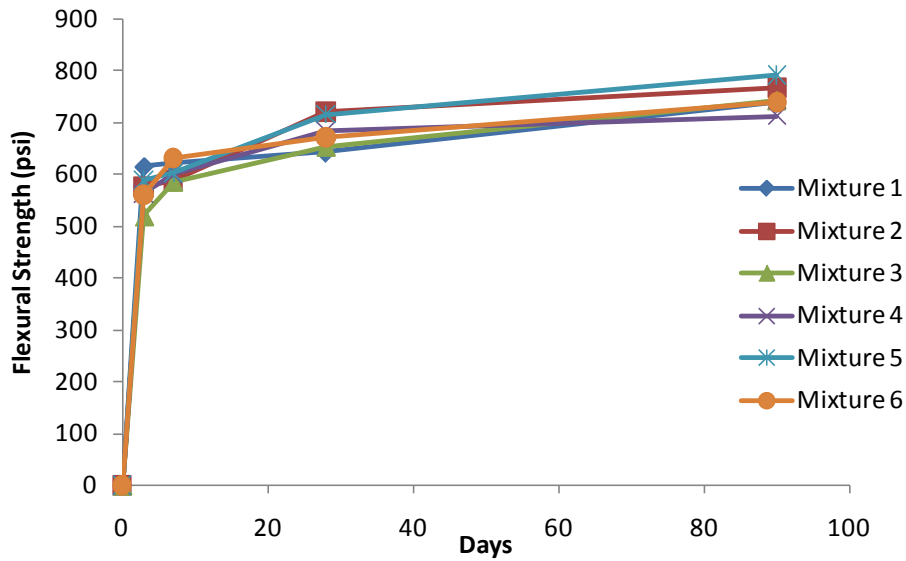
Figure 6.2 Flexural strength versus time for the different mixtures.

$9.5 (f'c)^{0.5}$
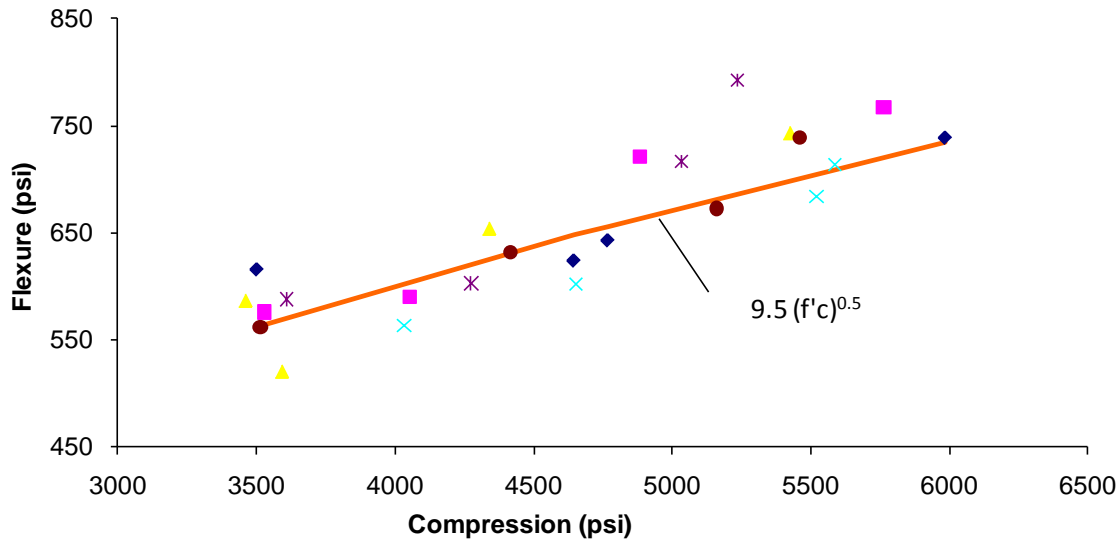
Figure 6.3 A comparison between flexural and compressive strength for the mixtures.

6.2 COEFFICIENT OF THERMAL EXPANSION

6.2.1 Introduction

The coefficient of thermal expansion (CTE) is the amount of strain a material experiences for a given change in temperature. The CTE is an important parameter

when investigating the performance of a concrete pavement as it contributes to the stresses a concrete pavement experiences from environmental temperature changes. These stresses can be a result of warping and curling, a combination of thermal strains combined with traffic loading, and frictional stresses between the pavement and the sub base. (Huang, 2004)

The CTE of a mature concrete depends on the individual CTE of the paste, fine aggregate, coarse aggregate and the volume each one makes up of the mixture. However, the CTE of a mixture is most influenced by the type of coarse aggregate used, as this material typically makes up around 50% of the volume of the mixture. ODOT has significant interest in finding the CTE values for common concrete pavement mixture designs for the state of Oklahoma. These are important inputs for the Mechanistic Empirical Pavement Design Guide (MEPDG).

A special testing apparatus is described in AASHTO T 336-09 "Standard test method for the coefficient of thermal expansion of hydraulic cement concrete" to investigate the CTE of a concrete specimen. There have been challenges with repeatability of commercial devices at the beginning of this project. Because of that the research team decided to build a custom device. Since that time commercial units have improved but are still being investigated.

6.2.1.1 Background

Several test methods exist for determining the CTE of concrete. Most widely used is AASHTO TP 60-00 (TP 60). The TP 60 was recently modified and re-designated as AASHTO T 336-09 (T 336) when it was discovered that there was an error regarding the calibration of the testing equipment. Currently, all state departments of transportation (DOT) use T 336 with the exception of Texas (Tanesi, et al. 2010).

6.2.1.2 T 336

The measurement of CTE with T 336 is achieved by measuring the length change of a saturated concrete specimen as it is subjected to different temperatures. The temperatures required by the method are obtained by using a water bath with a pump to cycle water in the chamber. Deformation of the frame is accounted for by measuring a

steel specimen of known CTE in the apparatus. A correction factor is then determined to account for the frame deformation (American Association of State Highway and Transportation Officials 2009).

6.2.1.3 Prior issues encountered with T 336

Researchers at Auburn University encountered issues with determining the CTE of the same concrete specimens at the same temperatures with different linear variable differential transformers (LVDT) even though the LVDTs were of the same make and model. The Auburn researchers hypothesized that these different CTE values were caused by heat transfer through the components of the testing frame and LVDT. (Sakyi-Bekoe 2008)

Several proposed modifications were made to minimize these effects. These modifications include:

1. A machined ceramic collar (high temperature glass-mica stock) to isolate the LVDT from the cross bar.
2. A machined ceramic spacer (high temperature glass-mica stock) to isolate the tip of the LVDT from the water.
3. A machined Invar cylinder to isolate the ceramic spacer from concrete specimen and water.

These three components are listed in Figure 6.4.
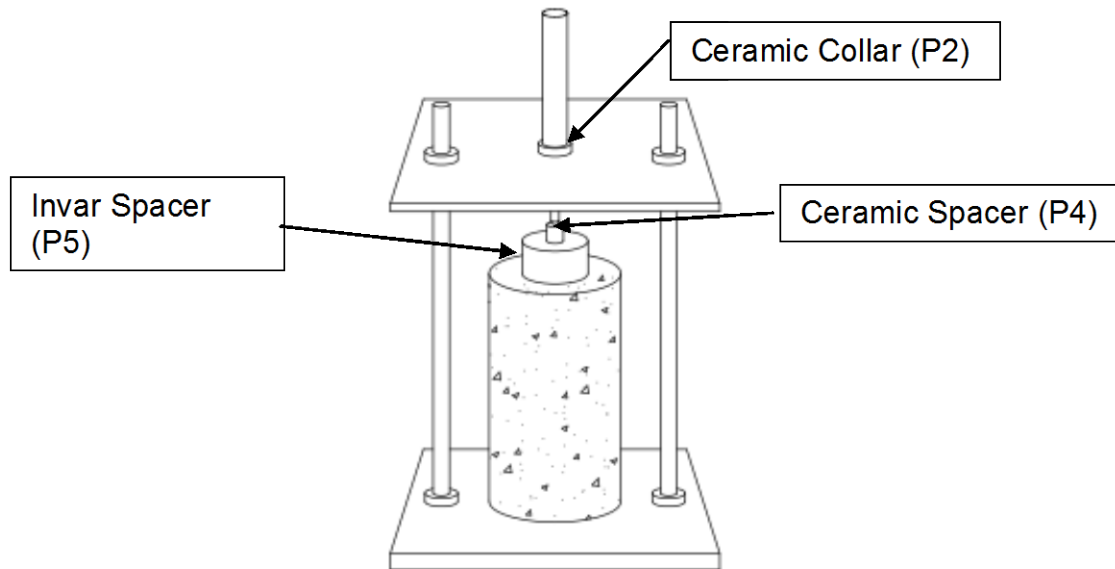
Figure 6.4 Assembled CTE frame and sample with labels

The "P" designations found in the labels of Figure 6.4, as well as various other locations in this chapter, represent the component numbering assigned to each individual part of the testing apparatus. These designators are meant to help relate the images to one another as well as associate them with the overall apparatus.

6.2.1.4 The current test method

In addition to these changes the researchers at OSU felt it was important to have a test setup that was able to continuously measure the length change of the sample. This is not currently required in the test method.

Currently, in T 336, a sample is cooled to 50°F ± 2°F for a period of time long enough to reach thermal equilibrium in the sample. The measured LVDT length is then recorded and the sample is heated to 122°F ± 2°F until it is at equilibrium and the length is again recorded with the LVDT.

6.2.2 Apparatus

This section details the specific apparatus constructed to evaluate the CTE of concrete cylinders.

6.2.2.1 Rigid support frame

Figure 6.5 shows an exploded assembly diagram of the apparatus used to evaluate CTE.
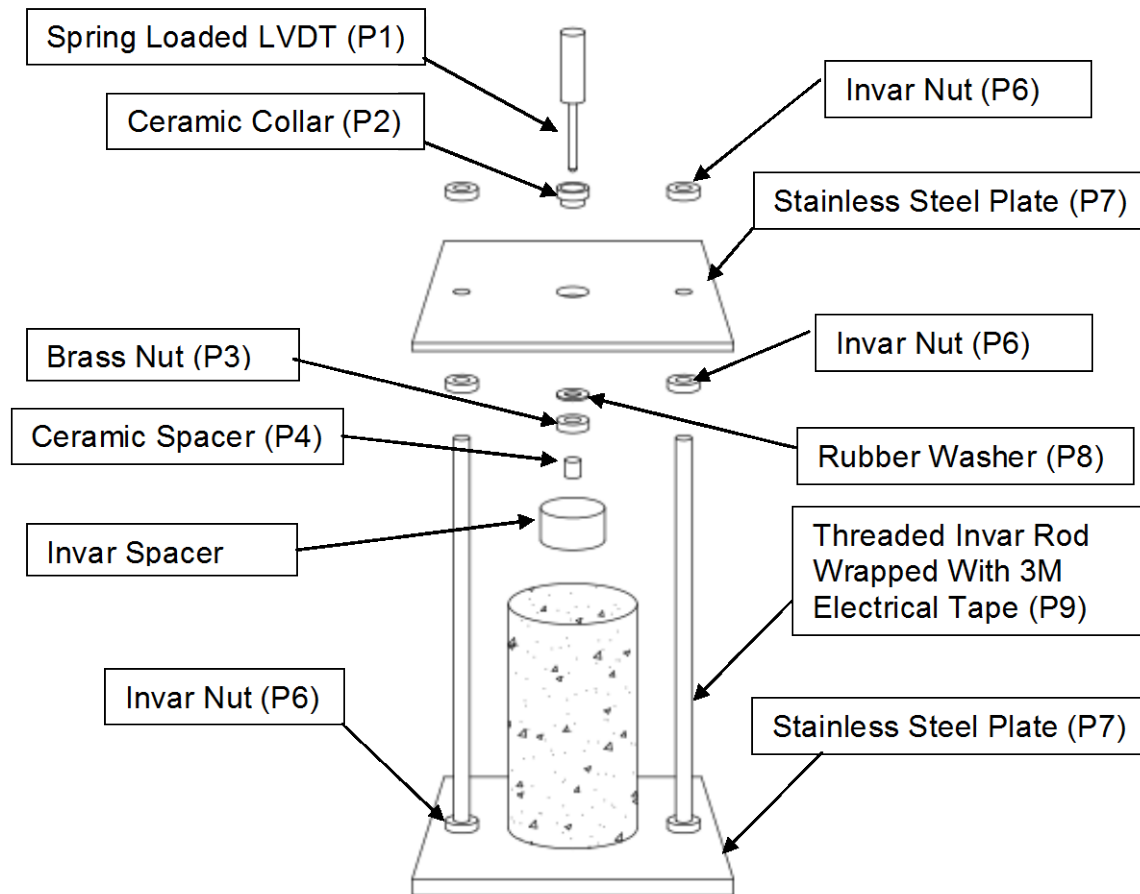
Figure 6.5 Exploded assembly of CTE frame and sample with labels

6.2.2.1.1 Frame

The rigid support frame was constructed in accordance with Appendix X.1 of T 336. The top and bottom plate are stainless steel, while the vertical support rods are machined from Invar. The rods are wrapped with tape for protection against corrosion the full length between the two stainless steel plates. Three semi-spherical support buttons are

equally spaced along a 2" diameter about the bottom plate. Figure 6.6 shows one of the frames prior to placement of an LVDT.
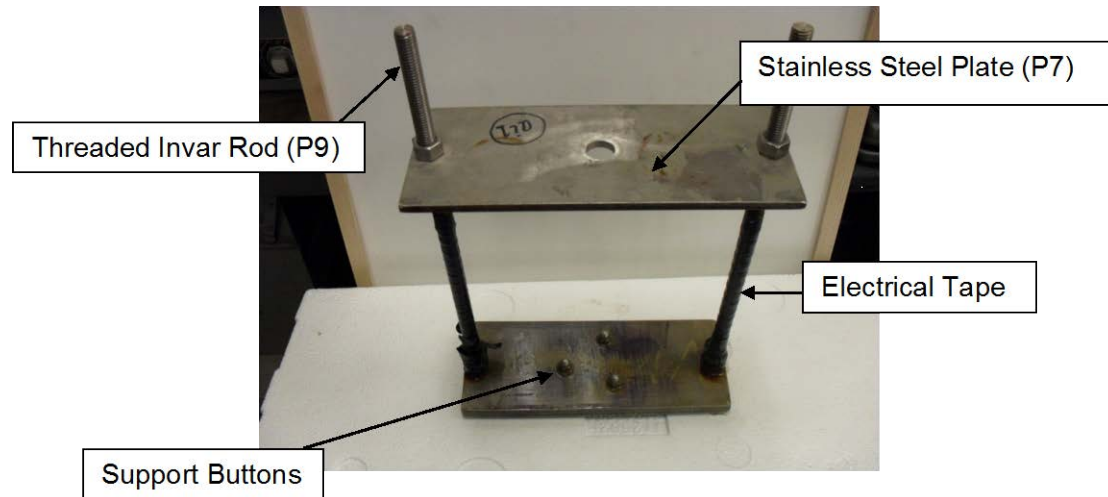
Figure 6.6 Assembled rigid frame with labels

6.2.2.1.2 Ceramic Collar

A ceramic collar was used to insulate the LVDT from the top plate of the frame. The collar was threaded to mate with the LVDT. It seats the LVDT in place on the plate with a metal nut and rubber washer and is threaded to match the LVDT. Figure 6.7 shows on of the ceramic collars constructed by OSU.

Figure 6.7 Ceramic collar (P2) suggested by Auburn University

6.2.2.1.3 Ceramic spacer

A ceramic spacer was machined and positioned concentrically on top of the Invar spacer supporting the piston head of the LVDT. This ceramic spacer is thought to insulate the LVDT from the radiant heat from the water.

6.2.2.1.4 Invar Spacer

An Invar spacer was machined and positioned concentrically with the concrete cylinder. The Invar is used to separate the LVDT from the surface of the sample and serves as a visible measure of water level within the holding tank. Both the ceramic spacer (P4) and the invar spacer (P5) are marked along their radius to aid in alignment. These can be seen in Figure 6.8.
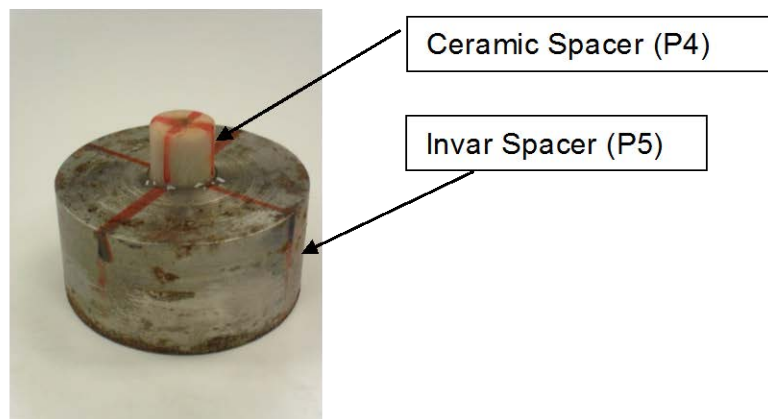
Figure 6.8 Ceramic spacer (P4) aligned on top of invar spacer (P5)

6.2.2.2 Water bath

This section details the components used for the water bath.

6.2.2.2.1 Circulator

A VWR Signature Heated/Refrigerated water circulator was used for maintaining the desired water temperature within the holding tank. It has a readout accuracy and

temperature stability of ±0.25°C and ±0.1°C respectively. The circulator has internal storage large enough to contain a single frame & LVDT assembly. The external holding tank was used by OSU so that two samples could be evaluated at once. The circulator can be seen in Figure 6.9.
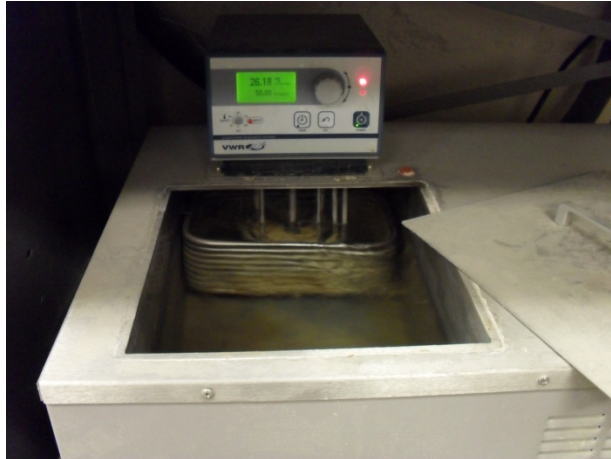
Figure 6.9 VWR water circulator

6.2.2.2.2 Vibration damper

A concrete block was cast in-line with the water out line from the circulator before the holding tank. This mass of concrete reduces vibrations in the water from the circulator before they reach the holding tank. The concrete block was cast around the outlet line between the circulator and the holding tank. Figure 6.10 shows the vibration damper.

Figure 6.10 Concrete vibration damper

6.2.2.2.3 Holding tank

The holding tank is made from a 10 gallon cooler. The lid has been replaced with a removal wood cover which has a viewing window and openings for the LVDT wiring. The sides of the cooler were tapped to accommodate an inlet and outlet hose for water circulation.

The lid of the holding tank consists of a removable wood frame with a clear plastic viewing window. A rectangular hole was cut in the viewing window to allow the LVDT and wiring to pass through while still providing some insulation to the holding tank. Figure 6.11 shows the lid of the holding tank. Figure 6.12 shows the complete CTE assembly and is labeled.

Figure 6.11 Holding tank lid
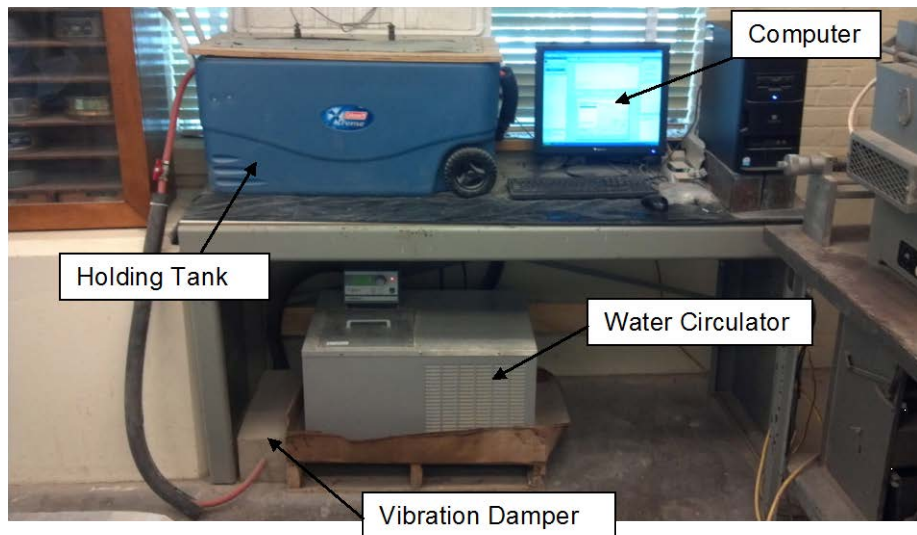
Figure 6.12 Complete CTE apparatus with labels

6.2.2.3 Linear variable differential transformer

The GCD-121-125 Schaevitz gage head LVDT. These are DC LVDTs and are of the spring loaded category. This LVDT is widely used by the FHWA, Auburn University, and the University of Texas. Figure 6.13 shows an image of the gage head LVDT.

146

Figure 6.13 Schaevitz LVDT

6.2.2.3.2 Signal carrier

A National Instruments NI USB 9162 C series USB signal carrier was used to connect the LVDT's to the computer software. This was chosen as it allowed a continuous measurement to be taken for both of the LVDTs. The signal carrier allows communication from the LVDT to the computer software. Figure 6.14 shows the USB carrier used in this experiment.

Figure 6.14 National Instruments USB signal carrier

6.2.2.3.3 LabVIEW software

The software package used to gather and record the voltage data from the LVDTs was LabVIEW 2009. The software allowed output of the voltages into Microsoft Excel spreadsheets for further analysis. Excel spreadsheets were developed at OSU to

analyze the signal data from LabVIEW. These spreadsheets make CTE calculations in accordance with T 336.

6.2.3 Methodology

6.2.3.1 LVDT Calibration

A rigid frame was used to calibrate the LVDTs individually. The LVDT was first placed in the rigid frame and its gauge head was extended to its full length. The voltage at this length was recorded. Figure 6.15 shows the calibration of an LVDT.
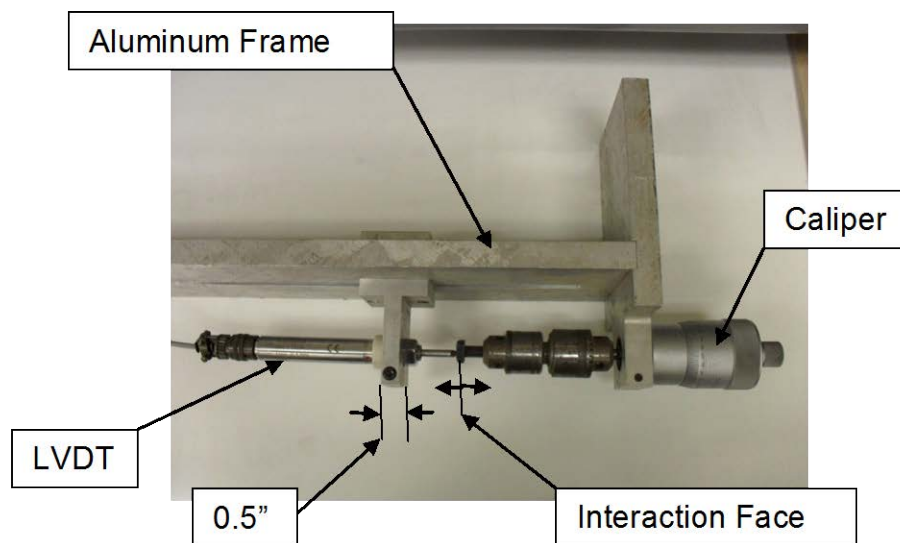
Figure 6.15 LVDT calibration assembly with LVDT in place

Increasing displacements of 0.025" are imposed on LVDT with a very precise mechanical caliper and their relative voltages recorded. These displacements are made until the gauge head is complete compressed. The data is plotted in a voltage versus displacement graph, and the calibration equations are derived based on the slopes of these lines. Literature suggests that calibration should be done every six months. (Tanesi, et al. 2010)

Figure 6.16 shows the results of a successful LVDT calibration. The solid line represents actual data recorded while dashed line is the best fit line from which the calibration equation is derived.
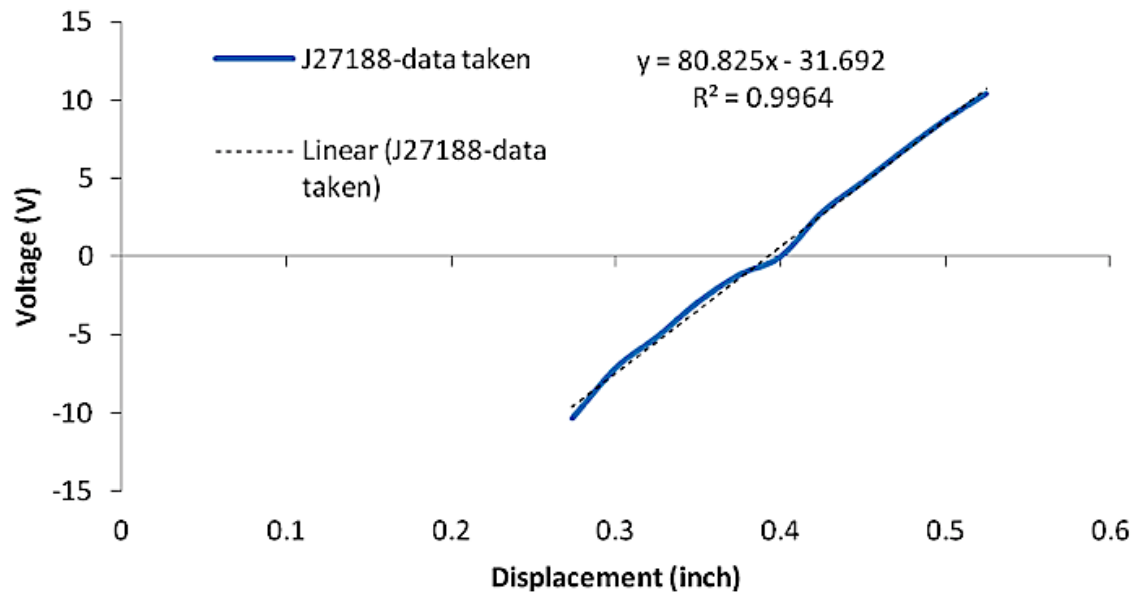
Figure 6.16 Calibration results from LVDT J27188

6.2.3.2 Frame calibration

The correction factor for each rigid frame was found in accordance with T 336. A third party laboratory was used to evaluate the CTE of a 410 stainless steel calibration specimen. The same specimen was then evaluated by OSU to determine the correction factor for each frame.

The third party laboratory reported the average CTE as $5.8\pm0.1\times10^{-6}/°F$. The specimen was 4" in diameter, 7" in length, and was evaluated in a custom quartz dilatometer in air according to a modified ASTM E228-06. The reported average CTE was calculated as a secant slope of the polynomial regression evaluated at the temperature extremes of 50 and 122°F.

6.2.3.3 Sample preparation

This section details the steps which take place to prepare the individual samples for testing.

6.2.3.3.1 Sample size

A premeasured jig was used to cut to concrete specimens to a length of 7.0±0.1" with a wet saw. Samples used are 4" diameter concrete cylinders. Table 6.2 shows a

standard mix design used during the CTE sample preparation. All sample mixes were performed on the same volume percentage.

Table 6.2 Typical CTE mix design used for all samples

	Weight (lb)	Volume (%)
cement	451.2	8.5
fly ash	112.8	2.5
water	231.2	13.7
rock	1850	42.3
sand	1244	28
air	-	5
sum	3889.2	100

6.2.3.3.2 Sample submersion period

All samples are submerged in a saturated lime water bath for a period no less than 48 hours and until the incremental weight change when measured in 24 hour intervals is less than 0.5% as per T 336.

6.2.3.3.3 Sample marking and average length

Samples are marked across their diameter at 45° intervals on the top and bottom faces of the cylinder. A digital caliper is used to take measurements at these intervals around the entire cylinder. These eight measurements are averaged to attain the samples overall average length. Figure 6.17 shows a sample being measured for average length.

Figure 6.17 CTE cylinder during measurement with alignment markings

6.2.3.4 Apparatus preparation

This section details the steps which take place to prepare the water bath and rigid frame prior to sample placement.

6.2.3.4.1 Water bath temperature

The water bath temperature is at room temperature at the time when the samples are placed in the reservoir. After sample placement, data recording is begun and the initial ramp temperature is set to 50°F. Samples are evaluated for an interval of 24 hours at which time data is collected and a new ramp at 122°F is begun. The same recording interval is maintained. Two more intervals follow for each sample resulting in two 50°F and two 122°F intervals per sample.

T 336 currently requires that the samples are heated and then cooled until thermal equilibrium is reached. This equilibrium is described as the condition when consistent readings of the LVDT are recorded to the nearest 0.00001 inch at 10 minute intervals over a half hour period. OSU takes length measurements every 150 seconds over a 24 hour period. This period and interval combination was chosen to better insure that strain equilibrium within the sample was reached every time.

Figure 7.19 shows the relation to the deflection readings from a LVDT to the temperature intervals. Notice that it takes multiple hours for the sample to reach

equilibrium. This trend is the reason why OSU evaluates each temperature interval for 24 hours to ensure equilibrium.

Since the interference does require filtering of the data, it was important to OSU researchers to record more than enough data to provide accurate CTE results with every trial after the filtering took place.

6.2.3.5 Sample placement

Samples are placed concentrically with the center of the LVDT and the three support buttons on the bottom plate of the rigid frame. On top of the sample are the Invar and ceramic spacers. Alignment markers placed along the diameters of both spacers and the sample allow for proper alignment. Figure 6.18 shows the alignment of the components and a sample.
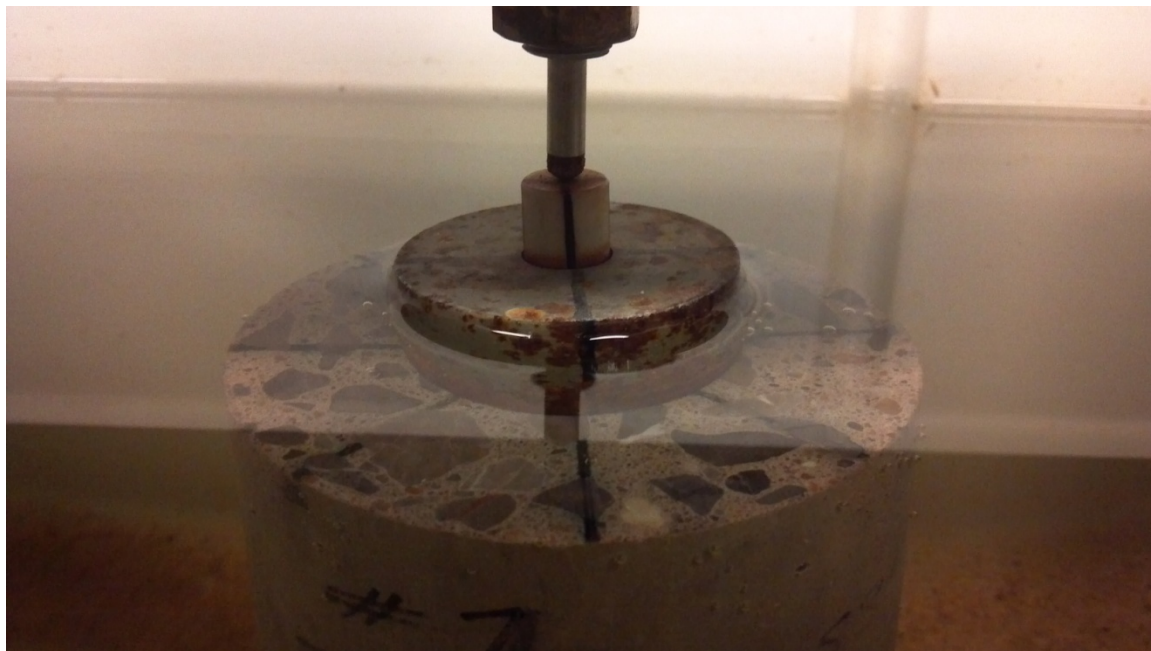
Figure 6.18 Aligned LVDT, Ceramic Spacer, Invar Spacer And Sample In The Holding Tank

6.2.3.6 Software Execution

The LabVIEW software begins recording LVDT voltages at 150 second intervals once the samples have been properly placed and the water bath program had been initiated. After the 24 hour recording period is reached, voltage data is exported to Microsoft

Excel. This is the procedure for a single ramp and is repeated three times for all of the samples investigated.

6.2.3.7 Data Analysis

Once data has been collected from LabVIEW, the voltages are converted into deflections with the conversion formulas previously derived for each LVDT. These deflections are then entered in to Microsoft Excel for analysis as per T 336.

Any noise interference is filtered out of the data by using the filter function imbedded in Excel. This unknown interference is seen on every set of data and has been seen previously by other researchers that have used the same equipment for the same test (Won 2006).

To filter the data, the deflection readings prior to equilibrium should be removed as well as the majority of the visible interference. This provides a rough data set which is a good representation of the actual deflection readings and is followed by a second filtering procedure to further refine the data. Figures 6.19 and 6.20 show deflection data before and after the first filtering process respectively.
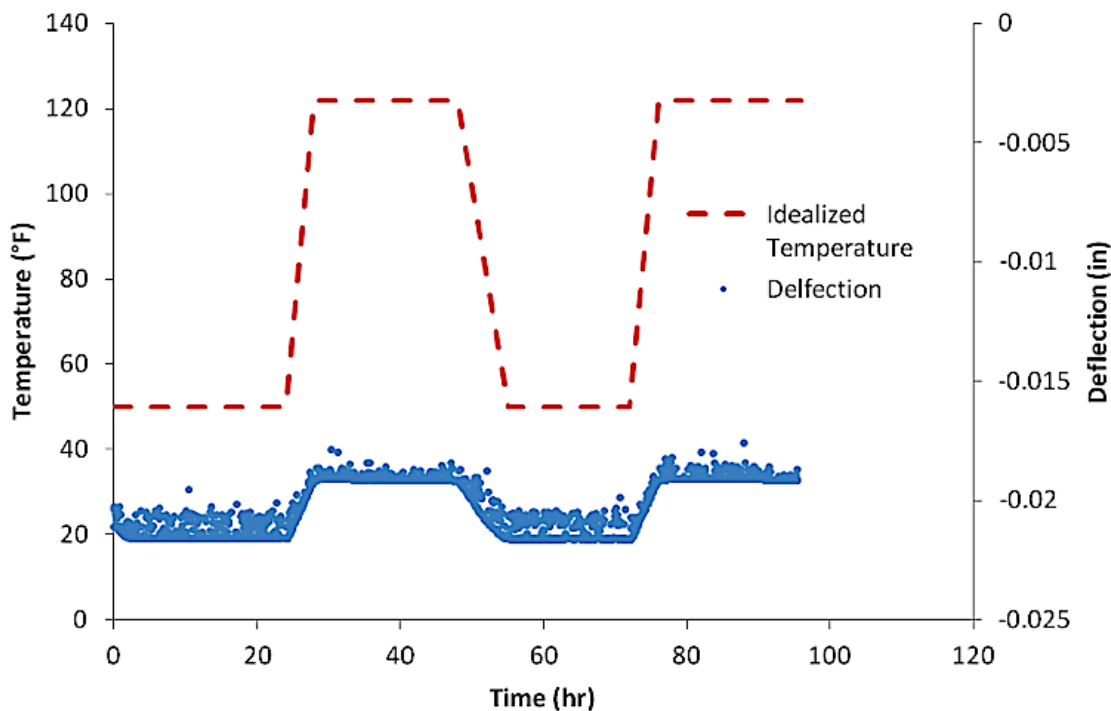
Figure 6.19 Deflection data prior to the first filtering process
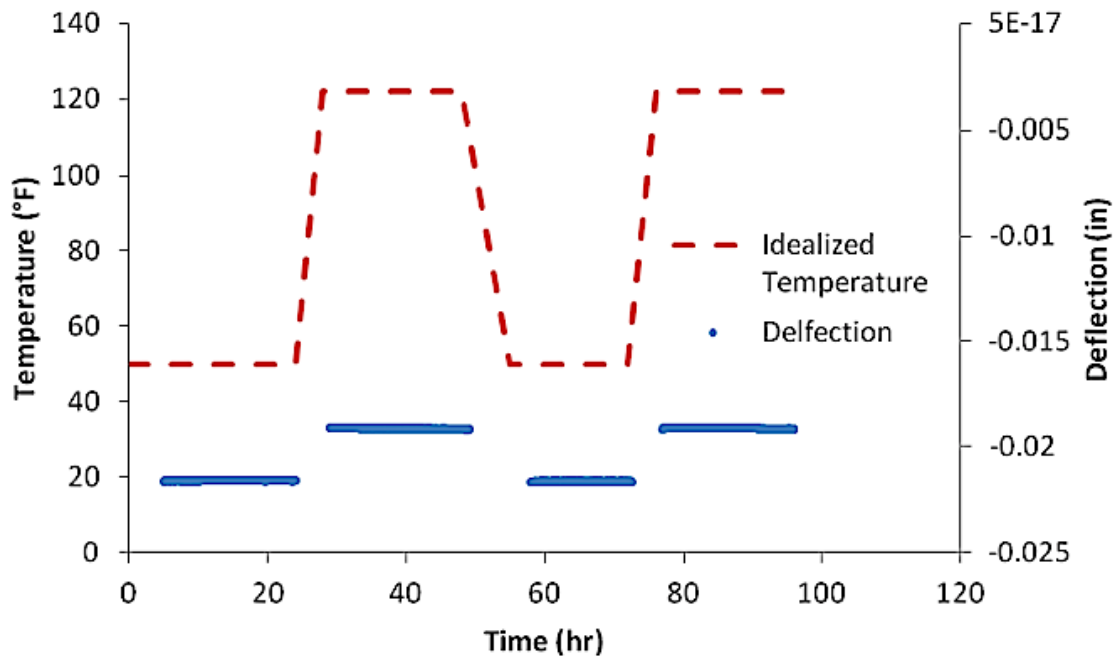
Figure 6.20 Deflection data after the first filtering process

After the data has been filtered the first time, a second filtering process is imposed on the data. This filter consists of taking the difference between each data point. Only data points showing a difference of 0.00002 inches are kept for further use. This is done to ensure that the deflections used for CTE evaluation are as similar as possible further eliminating the possibility of interference being present in CTE evaluation. After the second filtering process, the deflections are averaged to attain representative sample lengths at each temperature extreme. Each sample undergoes 4 temperature extremes which make up 3 temperature ramps as previously described. The average lengths determined at each temperature extreme are then used to calculate the length change the sample undergoes during each ramp.

The need for filtering may not have been experienced in previous CTE testing methods since intervals of 150 seconds were not used for continuous monitoring. With the mentioned filtering procedures, OSU has high confidence in its results and the accuracy of the results can be seen in the low coefficients of variance for each trial.

The three ramps are used to calculate three CTE values, as per T 336, for each sample. This is done to ensure that average CTE value is accurate and has a low coefficient of variance.

6.2.4 Results

Table 6.3 is comprised of all samples evaluated and their average CTE values. The table also includes other relevant information about the aggregates used in each sample. Notice the extremely low coefficients of variance.

Table 6.3 CTE testing results and sample information for all samples tested

Sample	Mineralogy	Abs. (%)	SG (SSD)	Dry Rodded Unit Weight (lb/ft^3)	Avg. CTE (10^{-6}/°F)	Frame	CTE (10^{-6}/°F)	Diff. between frames (10^{-6}/°F)	Std. Dev. (10^{-6}/°F)	COV (%)
Coleman	Dolomitic Limestone	0.55	2.77	173.1	5.3	0	5.2	0.2	0.044	0.85
						1	5.4		0.034	0.62
Cooperton	Dolomitic Limestone	0.92	2.81	147	5.2	0	5.2	0.1	0.028	0.54
						1	5.1		0.11	2.17
Davis	Rhyolite	0.64	2.71	165.6	5.5	0	5.2	0.6	0.062	1.19
						1	5.8		0.17	2.85
Drumwright	Limestone	0.52	2.71	168	5.6	0	5.39	0.3	0.017	0.32
						1	5.71		0.16	2.78
Hartshorn	Limestone	1.13	2.62	169.2	4.5	0	4.5	0	0.054	1.2
						1	4.5		0.098	2.18
N. Troy	Limestone	1.45	2.71	171	5.6	0	5.5	0.2	0.019	0.34
						1	5.7		0.12	2.13
OKAY	Limy Sandstone	3.06	2.51	155.1	5.5	0	5.3	0.4	0.25	4.75
						1	5.7		0.082	1.44
Sawyer	Sandstone	2.02	2.52	156.1	6.8	0	6.9	0.3	0.23	3.4

Sample	Mineralogy	Abs. (%)	SG (SSD)	Dry Rodded Unit Weight (lb/ft^3)	Avg. CTE (10^{-6}/°F)	Frame	CTE (10^{-6}/°F)	Diff. between frames (10^{-6}/°F)	Std. Dev. (10^{-6}/°F)	COV (%)
						1	6.6		0.12	1.84
Richard Spurr (5.5 Sack)	Limestone	0.89	2.67	168.1	5	0	4.7	0.5	0.021	0.44
						1	5.2		0.054	1.04
Ricahrd Spurr	Limestone	0.89	2.67	168.1	5.1	0	4.9	0.4	0.017	0.35
						1	5.3		0.051	0.96
Richard Spurr (6.5 Sack)	Limestone	0.89	2.67	168.1	5.1	0	4.9	0.3	0.034	0.7
						1	5.2		0.035	0.67

Also, note that there is not a noticeable CTE difference between the three Richard Spur samples. These three samples vary in paste content and their results suggest that the CTE value is not dependent on paste content, but is dependent on the aggregate type in the sample.

6.2.5 Discussion

When comparing the average CTE values in Figure 6.21 it can be seen that the majority of the samples are between 5 and $5.5x10^{-6}/°F$. Removing the two outliers (Hartshorn and Sawyer), the average CTE value is $5.4x10^{-6}/°F$. This value is representative of all aggregates except Sawyer, sandstone, which has a higher Average CTE of $6.8x10^{-6}/°F$. Hartshorn is a limestone which showed a low average CTE of $4.5x10^{-6}/°F$. Figure 6.21 shows all CTE values plotted against each other and the average representative CTE. The samples are ordered in relation to this graph on Table 6.3.
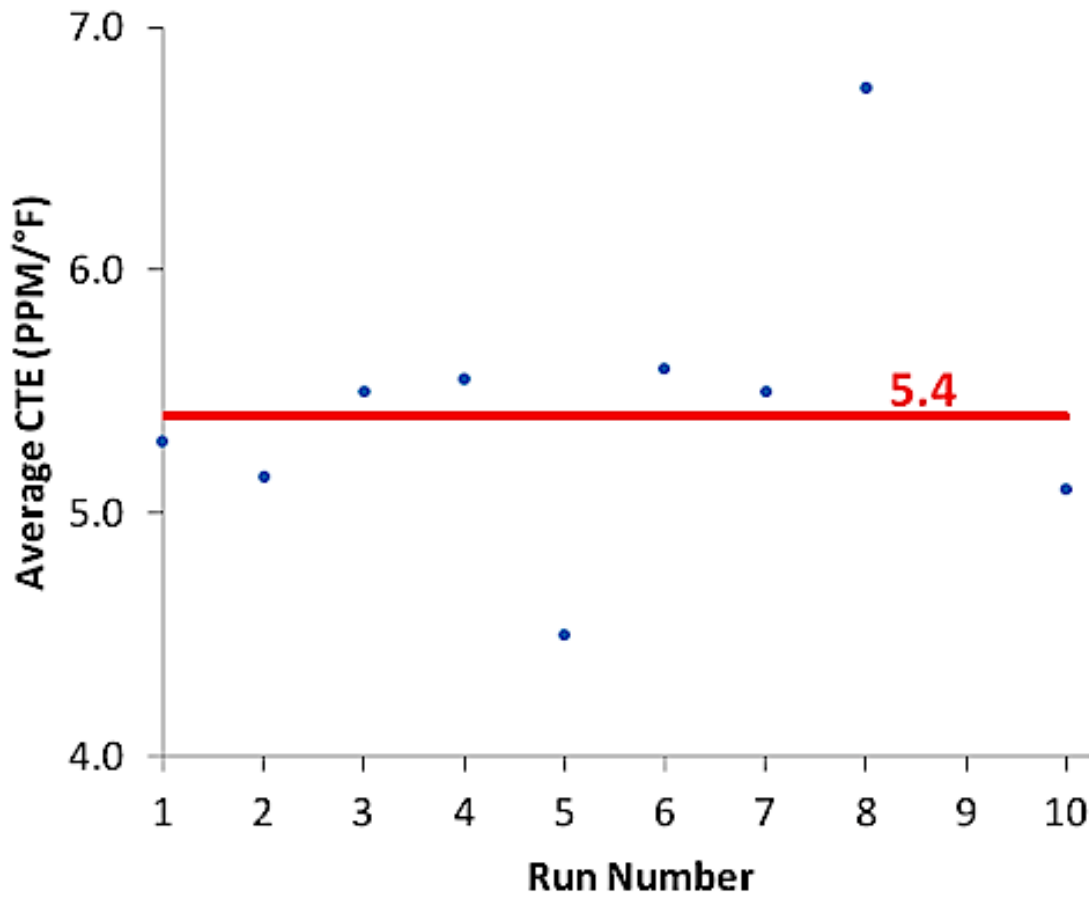
Figure 6.21 Individual average CTE comparison of all samples with overall average CTE value

<u>6.2.5.1 Geometry Change</u>

Random changes in LVDT readings were seen in some samples during the testing.

These changes can be seen in the Figure 6.22 below as non-typical areas.
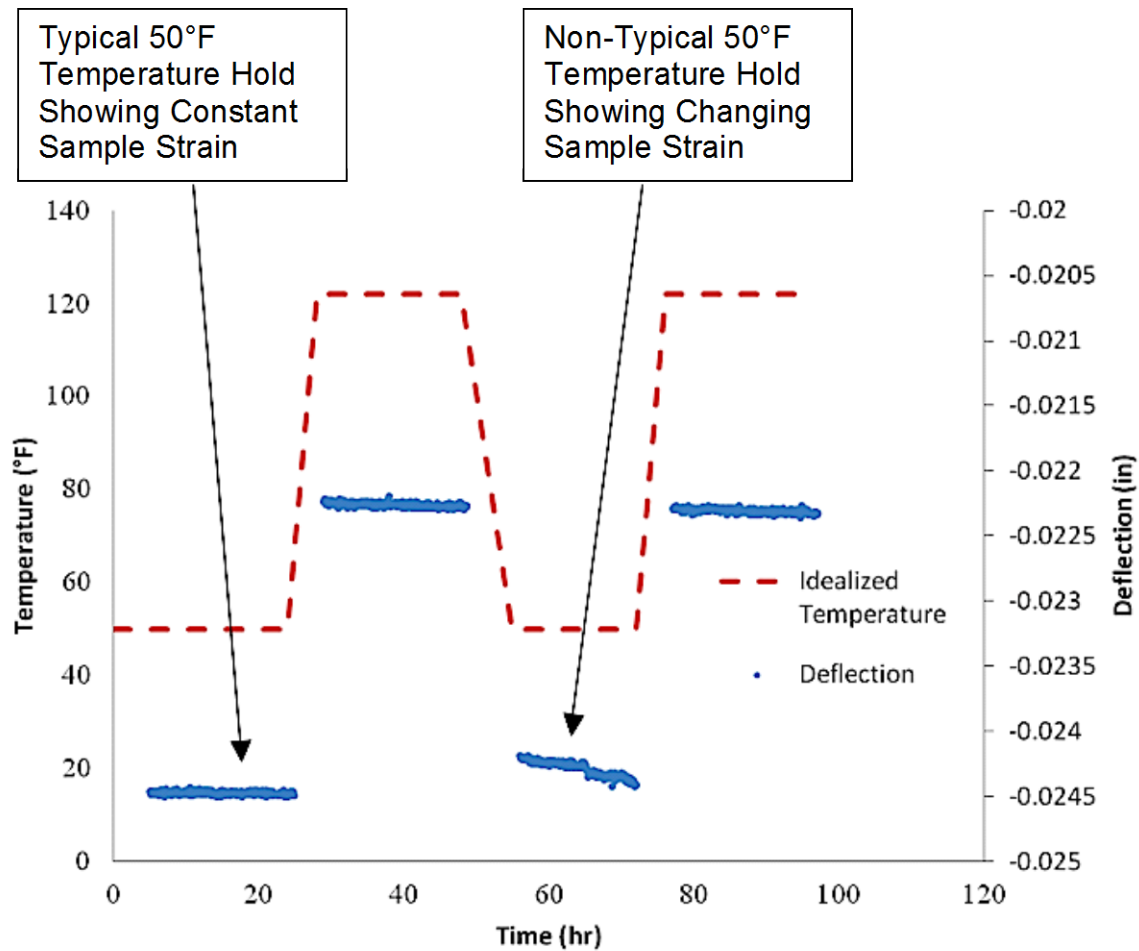
Figure 6.22 Filtered non-constant geometry

The witnessed change comes in the form of a non-uniform strain pattern where one should be present. It is believed that this is due to the LVDT device. When non-typical deflection data were encountered, the sample was re-tested until typical data was collected for the entire dataset. This was done to ensure that the data was not tainted in any way by suspected LVDT errors. These non-typical changes happened at random so it was important to check the unfiltered datasets before CTE evaluation for non-typical data for every sample. ***This observation would not have been made if the LVDT was not continuously measured.***

These errors were encountered on 8 of the 11 investigated samples and so were frequent.

6.2.6 Recommendations

The modified version of the CTE test method developed at Auburn with modifications by OSU showed consistent and repeatable results. This is proven by the low coefficient of variation values.

It appears that the modifications to the apparatus made to isolate the LVDT from varying temperatures was helpful and should be incorporated into future versions of this test.

Measurement intervals at 150 second periods over multiple 24 hour intervals at varying temperatures should be strongly considered in future testing. This ensures that errors in testing are not made and that true sample equilibrium is reached for accurate CTE evaluation.

Filtering of the deflection data prior to CTE evaluation is greatly needed to ensure accurate evaluation of the sample. The interference seen during the continuous monitoring of the samples can greatly influence the calculated CTE of any given sample if it is not removed.

The use of multiple frames is also suggested. Testing samples in different frames and comparing CTE values between the two also help minimize errors.

Random changes in length recorded by the LVDT have been noticed during this testing. The source of these changes is unknown and would not have been observed if continuous measurement was not used. These errors occurred frequently and caused samples to have to be retested.

6.2.6.1 Recommended CTE Values For MEPDG Implementation For Oklahoma

One useful finding from the work is that the majority of the CTE values were similar in value. As shown in Table 6.3 of the nine different aggregates investigated, seven of them were between $4 \times 10^{-6}/°F$ and $5.45 \times 10^{-6}/°F$. This means that ODOT could use $5.4 \times 10^{-6}/°F$ as an input value for the MEPDG for future analysis and provide a reasonable value for all of the aggregates except for Hartshorn and Sawyer. Care

needs to be taken to ensure that the version of the software is formatted to receive data from the recently updated version of the T 336 test. If the version is not the latest, then a correction factor should be used to change the data to the old testing scale.

6.3 DRYING SHRINKAGE OF CONCRETE MIXTURES
6.3.1 Introduction

A task in this project was to provide the necessary shrinkage input parameters for the MEPDG. The input parameters include: ultimate shrinkage, reversible shrinkage and time to develop 50% of the maximum shrinkage. Laboratory tests that use AASHTO T160 "Standard Method of Test for Length Change of Hardened Hydraulic Cement Mortar and Concrete" with modifications suggested by the MEPDG design manual were used (ARA, 2004). These modifications include using a drying environment of 40% relative humidity instead of 50%. As part of this work the ultimate maximum shrinkage and time to develop 50% of the maximum shrinkage was measured. For reversible shrinkage the assumptions within the MEPDG are recommended.

The paste (cementitious and water) in a concrete mixture is responsible for the volume change when dried. Because of the importance of the paste in the mixture several different paste mixtures were investigated to determine the impact on the ultimate shrinkage. The mixtures were very representative of common concrete mixtures in the state of Oklahoma. They had a 0.41 w/cm, 6 sacks of cementitious material, 20% fly ash replacement, and a 60/40 ratio of coarse to fine aggregate. The same coarse and fine aggregate was used for all of the following mixtures. Mixtures were prepared with different cements and fly ashes and work was also done without fly ash and different paste contents (5.5, 6, and 6.5 sacks of total cementitious).

6.3.2 Results

Table 6.4, 6.5, and 6.6 and Figures 6.23 thru 6.28 show the results from the drying shrinkage testing. Table 6.4 and Figures 6.23 and 6.24 show the results for mixtures that contain different cements. Table 6.5 and Figures 6.25 and 6.26 show how mixtures with and without fly ash perform, and Table 6.6 and Figures 6.27 and 6.28 show how the results of mixtures with different paste contents. Three samples were investigated for each of the reported values. The average and one standard deviation are shown on each of the figures. Because not all of the specimens were cast and measured at the same time, shrinkage and weight loss values in Table 6.4, 6.5, and 6.6 have been interpolated from the data to 290 days of drying for comparison.

Table 6.4 Drying Shrinkage For Mixtures With Different Cements

cement	fly ash	w/cm	sacks	ash %	shrinkage (microstrain)	weight loss (%)	Days for 50% of max shrinkage	slump	air
LaFarge	Red Rock	0.41	6	20	608	2.86%	25	1.5"	7%
Holcim	Red Rock	0.41	6	20	563	2.61%	28	1"	6.80%
Buzzi	Red Rock	0.41	6	20	601	2.86%	31	1.75"	9%
			average		591	2.78%	28		

Table 6.5 Drying shrinkage for mixtures with and without fly ash

cement	fly ash	w/cm	sacks	ash %	shrinkage (microstrain)	weight loss (%)	Days for 50% of max shrinkage	slump	air
LaFarge		0.41	6	0	597	2.63%	40	1.5"	6.0%
LaFarge	Red Rock	0.41	6	20	608	2.86%	28	1.5"	7.0%
LaFarge	Oklaunion	0.41	6	20	656	2.80%	25	1.5"	7.0%
LaFarge	Muskogee	0.41	6	20	636	2.88%	25	1.75"	7.8%
LaFarge	GRDA	0.41	6	20	620	2.82%	20	1.5"	7.0%
			fly ash average		630	2.84%	25		

Table 6.6 Drying shrinkage for mixtures with different paste contents

cement	fly ash	w/cm	sacks	ash %	shrinkage (microstrain)	weight loss (%)	Days for 50% of max shrinkage	slump	air
LaFarge	Red Rock	0.41	5.5	20	530	2.40%	25	0.5"	5.0%
LaFarge	Red Rock	0.41	6	20	608	2.86%	25	1.5"	7.0%
LaFarge	Red Rock	0.41	6.5	19	650	3.18%	18	2.5"	9.0%
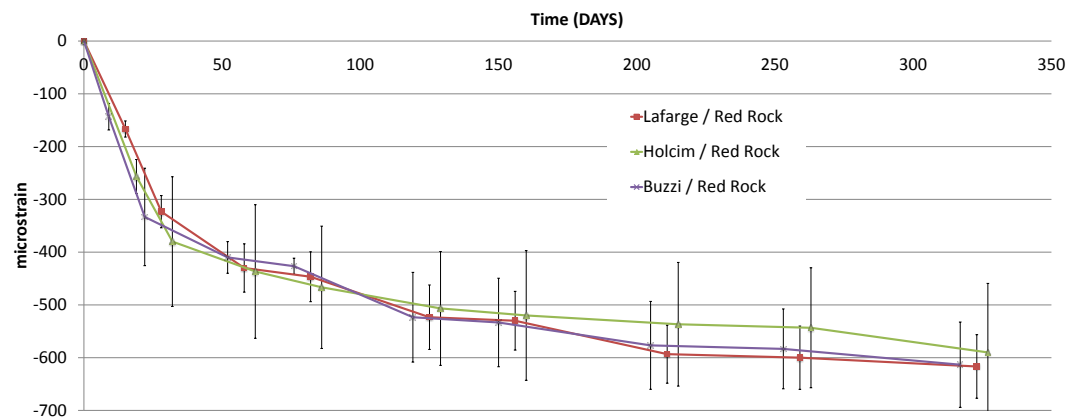
Figure 6.23 Measured strain from drying shrinkage for different cements vs. time
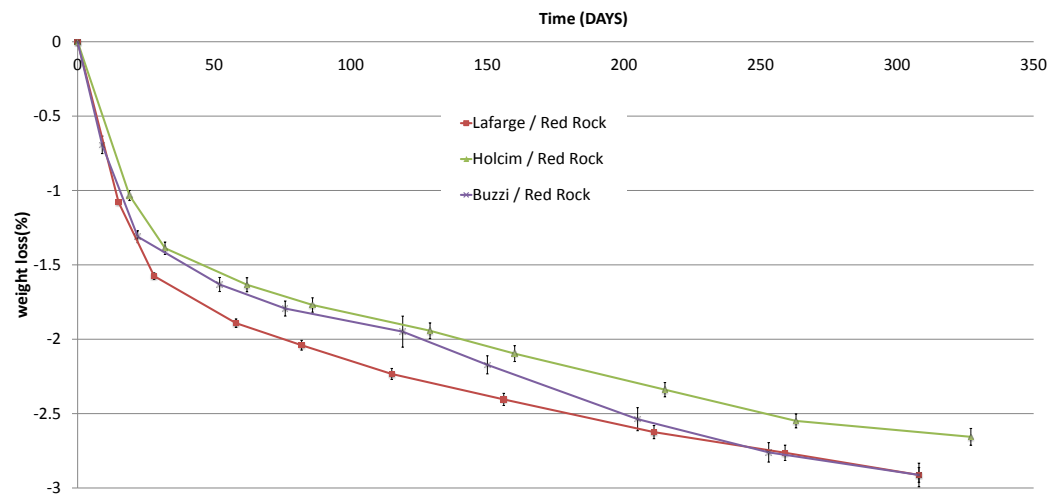
Figure 6. 24 Measured weight loss from drying shrinkage for different cements vs. time
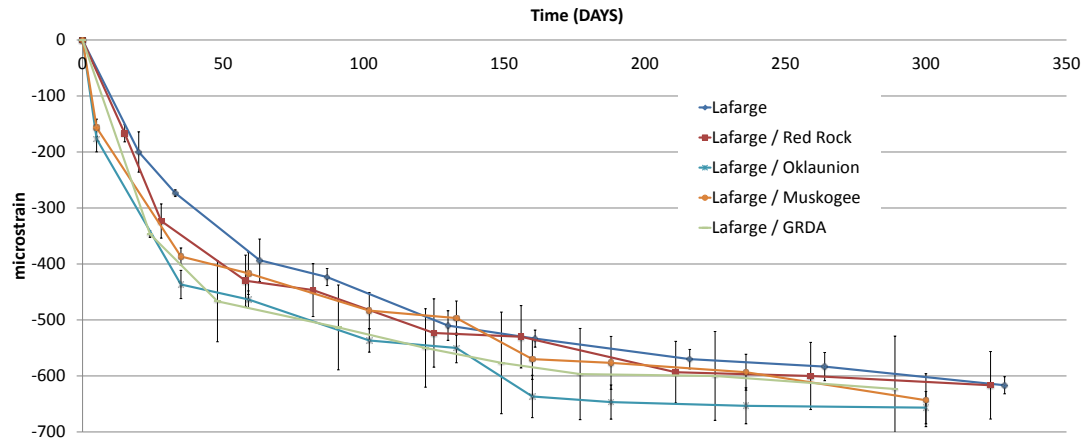
Figure 6. 25 Measured strain from drying shrinkage for different types of fly ash vs. time
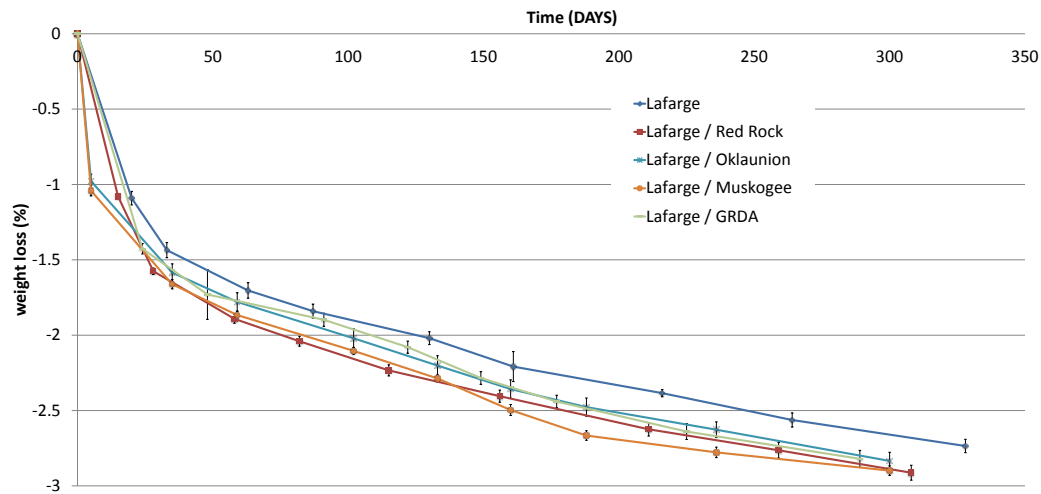
Figure 6. 26 Weight loss from drying shrinkage for different types of fly ash vs. time
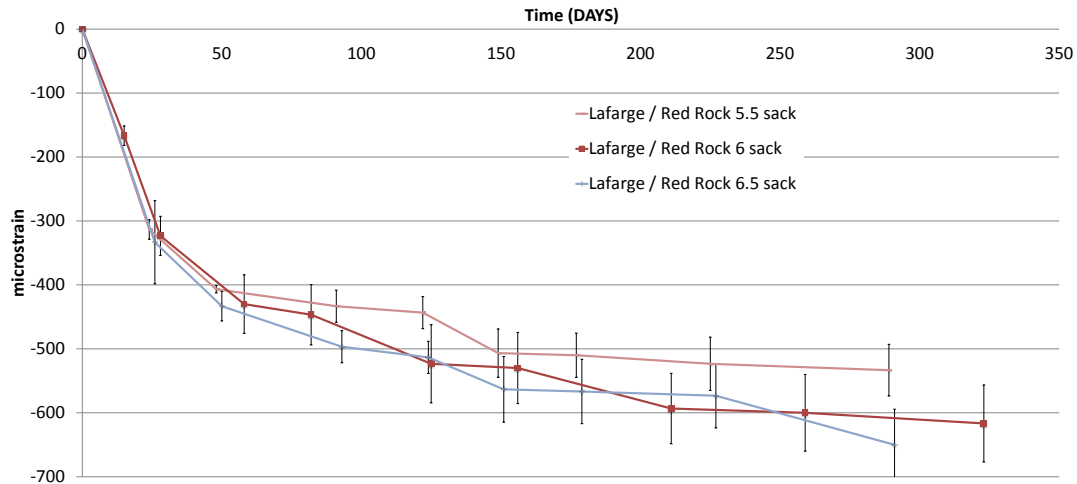
Figure 6. 27 Measured strain from drying shrinkage for different paste contents vs. time
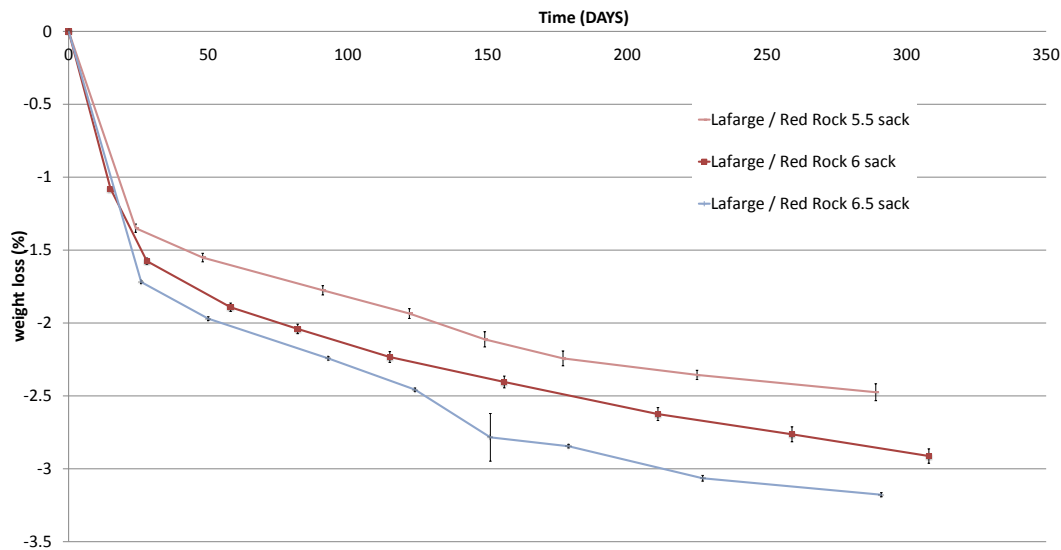
Figure 6. 28 Weight loss from drying shrinkage for different paste contents vs. time

6.3.3 Discussion

As can be seen in Table 6.4 there was no significant difference in the observed shrinkage for the three major cements used in Oklahoma for the same mixture. This means that shrinkage of the concrete would not be expected to change based on changes in the cement type.

168

As shown in Table 6.5 there is a measurable difference between the mixtures with different fly ashes and without fly ash. Red Rock fly ash was found to have the lowest shrinkage and Oklaunion was found to be the highest. There was a 50 micron difference in the ultimate shrinkage strain between the highest and lowest fly ash investigated. However, there was very little difference in the time required to reach 50% of the ultimate shrinkage. Also, there was an average difference between the fly ash mixtures and the non fly ash mixtures of 33 microstrain. ***While differences do exist between concrete mixtures with fly ash it is recommended that an average ultimate shrinkage value of 630 microstrain with 25 days of drying required to reach 50% of the maximum shrinkage.*** This is the average ultimate drying shrinkage strain for the mixtures with fly ash. It is very common for fly ash to be used in the state of Oklahoma. This value is a compromise between the measured values and should provide a conservative estimate for the MEPDG inputs.

For the mixtures with reduced paste content a significantly reduced amount of shrinkage was observed. Of the parameters investigated this had the biggest impact on the ultimate shrinkage performance, as a decrease of paste by 0.5 sack of cementitious showed a decrease in shrinkage of 78 microstrain. For an increase in cementitious material of 0.4 sacks there was an increase in shrinkage of 42 microstrain. It is recommended that ODOT encourage a decrease in paste content in the concrete pavement mixtures as this would promote the long term durability of concrete pavements. The easiest way to obtain this reduction in paste is through the use of optimized graded concrete.

THIS PAGE IS INTENTIONALLY BLANK

7.0 CONCLUSION

This report has provided a summary of the work completed to date on ODOT project 2208 "Development and Implementation of a Mechanistic and Empirical Pavement Design Guide (MEPDG) for Rigid Pavements" and OkTC project OTCREOS10.1-24, "Investigation of the Inputs for the MEPDG for Rigid Pavements". All research has been combined to allow the reader to synthesize the findings.

More work is to be done on these topics in Phase II of this project. Additional work will be done on Task D with an emphasis on field evaluations of pavements. Funding was provided during Phase I for a field instrumentation of a concrete pavement to verify some of the laboratory findings. This effort was delayed until Phase II of the project because of the late arrival of necessary instrumentation and communication with the contractor. This work will be completed as part of Phase II of this project and will provide many important insights.

A summary of findings is provided below:

7.1 SENSITIVITY ANALYSIS OF THE MEPDG

A sensitivity analysis was completed that quantitatively compare the impact of different variables on the design thickness reported in the MEPDG for CRCP and JPCP. The results from the analysis were found to largely match the expected values; however there were several troubling results. These cases were not able to be explained and are likely a bug in the software. Care should be taken by users of the software to use engineering judgment and past experiences to verify results. No combination of variables was investigated beyond what is presented in this paper and so care should be taken in extrapolating the results in other ways then what is presented.

7.2 RECOMMENDATIONS FOR BASE MATERIALS

The reports reviewed suggest that roadways with subgrade drainage systems tend to perform closely with their undrained counterparts in terms of structural integrity. However, with subgrade drainage systems, proper construction procedures, and periodic maintenance of drainage outlets must be completed to ensure the effectiveness

of these systems. Areas with high annual precipitation or soils with low permeability appear to be good candidates for these drainage features.

7.3 UPDATE OF CLIMATIC DATA

Climatic data files have been updated and created for use in designing rigid and flexible pavements in the state of Oklahoma. Average yearly depth to groundwater values have also been compiled for a wide range of geographical locations. This is expected to result in better pavement designs which should translate into an overall reduced life-cycle cost.

7.4 IMPACT OF CURING TECHNIQUES ON THE CURLING OF CONCRETE PAVEMENTS

7.4.1 Comparing wet curing, sealed and no curing

Wet curing on the exposed surface of a beam decreased the rate of weight loss from drying but increased the ultimate curling deflection. This suggests that extended wet curing would be expected to cause an increase in the amount of curling that occurs in a slab on grade. Similar observations have been observed for drying shrinkage in concrete beams but never applied to increases in curling.

Due to the wet curing process, the surface of the beam has a finer pore-structure (Hedenblad 1997) and consequently a higher negative pressure or capillary tension upon drying (Mackenzie 1950; Adamson and Gast 1997; Bentz et al.1998). This increase in capillary tension has been suggested to be the primary mechanism for drying shrinkage (Lane, Scott, and Weyers 1997).

In all of the tests presented a one dimensional drying front was used through use of impermeable boundaries. Nicholson (1981) showed that serious shrinkage curling due to an increase in moisture gradient can occur when concrete slabs are cast on an impervious base. Because curling and drying shrinkage are both a function of potentially free water in the concrete at the time of concrete set, curing methods that retain water in the concrete will delay shrinkage and curling of enclosed slabs-on-ground.

7.4.2 Performance of Curing Compounds

Different curing compounds with different coverage were compared. The poly-alphamethylstyrene-resin-based curing compound (C1) had the best performance with a comparable coverage rate. The water based curing compound (C3) performed the worst and the resin based curing compound (C2) was between these two. As the coverage of the curing compound increased so did the ability to limit moisture loss and therefore curling. A double layer of a curing compound was shown to provide improved performance over a single layer of curing compound.

Curing compounds appear to limit moisture loss to a greater degree than wet curing at least up to 14 days of wet curing or a no curing method. This reduction in moisture loss seems to correspond to a reduced amount of differential shrinkage and therefore curling.

In the concrete beams it was found that the double layer of the wax based curing compound performed better than the poly-alphamethylstyrene-resin-based curing compound. This is likely because it was applied in a double layer and therefore achieved a better coverage. This is especially important for applications with textured surfaces and with conditions that are not as favorable in the laboratory. Similar suggestions have been made by Shariat and Pant (1984). The uniformity of the application of the curing compounds is an important variable that needs to be controlled. Based on the findings in this work the researchers recommend that a double layer of the resin based curing compounds be used for curing concrete pavements. This material provides a nice balance between cost and performance for the materials used in this study.

7.4.3 Curling from Temperature Differentials

The data suggests that temperature related curling is primarily controlled by the insulation and ability to minimize evaporation of the curing method. The use of clear plastic directly on fresh concrete is not suggested if temperature related curling is a concern. However if clear plastic is used on burlap then this can reduce evaporation and keep temperatures constant. The use of white curing compounds also showed satisfactory performance. More work will be done in Phase II of this project.

7.5 INPUTS FOR THE MEPDG FOR OKLAHOMA MATERIALS

7.5.1 Strength

Typical Oklahoma concrete mixtures were investigated and their strengths were determined. Useful input curves were produced for compressive and flexural strength of different mixtures that could be used for the MEPDG. A useful equation was found that relates the flexural and compressive strength data.

7.5.2 Coefficient of Thermal Expansion

The modified version of the CTE test method developed at Auburn with modifications by OSU showed consistent and repeatable results. This is proven by the low coefficient of variation values. It appears that the modifications to the apparatus made to isolate the LVDT from varying temperatures was helpful and is recommended to be incorporated into future versions of this test.

One useful finding from the work is that the majority of the CTE values were similar in value. As shown in Table 6.3 of the nine different aggregates investigated, seven of them were between $4 \times 10^{-6}/°F$ and $5.45 \times 10^{-6}/°F$. This means that ODOT could use $5.4 \times 10^{-6}/°F$ as an input value for the MEPDG for future analysis and provide a reasonable value for all of the aggregates except for Hartshorn and Sawyer. Care needs to be taken to ensure that the version of the software is formatted to receive data from the recently updated version of the T 336 test. *If the version is not the latest, then a correction factor should be used to change the data to the old testing scale.*

7.5.3 Shrinkage

There was no significant difference in shrinkage for the three major cements used in Oklahoma. This means that shrinkage of the concrete would not be expected to change based on changes in the cement type.

There was a measurable difference between the mixtures with different fly ashes and mixtures without fly ash. Red Rock fly ash was found to have the lowest shrinkage and Oklaunion was found to be the highest. There was a 50 micron difference in the ultimate shrinkage strain between the highest and lowest fly ash investigated. However,

there was very little difference in the time required to reach 50% of the ultimate shrinkage. This is a major input for the MEPDG. Also, there was an average difference between the fly ash mixtures and the non fly ash mixtures of 33 microstrain. *While differences do exist between concrete mixtures with fly ash it is recommended that an average ultimate shrinkage value of 630 microstrain with 25 days of drying is required to reach 50% of the maximum shrinkage be used as the input for Oklahoma mixtures that have 6 sacks of cementitious materials with 20% fly ash replacement.* This is the average ultimate drying shrinkage strain for the mixtures with fly ash and is conservative for mixtures that do not use fly ash. This value is a compromise between the measured values and should provide a conservative estimate for the MEPDG inputs.

For the mixtures with reduced paste content a significantly reduced amount of shrinkage was observed. Of the parameters investigated this had the biggest impact on the ultimate shrinkage performance, as a decrease of paste by 0.5 sack of cementitious showed a decrease in shrinkage of 78 microstrain. For an increase in cementitious of 0.4 sacks there was an increase in shrinkage of 42 microstrain. It is recommended that ODOT encourage a decrease in paste content in the concrete pavement mixtures as this would promote the long term durability of concrete pavements. The easiest way to obtain this reduction in paste is through the use of optimized graded concrete.

THIS PAGE IS INTENTIONALLY BLANK

8.0 REFERENCES

ACI Committee 209, 2005, "Report on Factors Affecting Shrinkage and Creep of Hardened Concrete (ACI 209.1R-05)"

ACI Committee 224, 2001, "Control of Cracking in Concrete Structures (ACI 224R-01)"

ACI Committee 302, 2006, "Guide for Concrete Slabs that Receive Moisture-Sensitive Flooring Materials (ACI 302.2R-06)"

ACI Committee 302, 2004, "Guide for Concrete Floor and Slab Construction (ACI 302.1R-04)"

ACI Committee 308, 2001, "Guide to Curing Concrete (ACI 308R-01)"

ACI Committee 360, 2006, "Design of Slabs-on-Ground (ACI 360R-06)"

Adamson, A. W., and A. P. Gast, 1997, "Physical Chemistry of Surfaces," 6th ed. Wiley InterScience, New York.

American Association of State Highway and Transportation Officials. "AASHTO T336-09 Standard Method of Test for Coefficient of Thermal Expansion of Hydraulic Cement Concrete." Washington D.C., 2009.

AASHTO M 148, "Standard Specification for Liquid Membrane-Forming Compounds for Curing Concrete"

AASHTO M 252, "Standard Specification for Corrugated Polyethylene Drainage Pipe"

AASHTO M 278, "Standard Specification for Class PS46 Poly (Vinyl Chloride) (PVC) Pipe"

AASHTO T 22, "Standard Method of Test for Compressive Strength of Cylindrical Concrete Specimens"

AASHTO T 97, "Standard Method of Test for Flexural Strength of Concrete (Using Simple Beam with Third-Point Loading) (ASTM Designation: C 78-08)"

AASHTO T 160, "Standard Method of Test for Length Change of Hardened Hydraulic Cement Mortar and Concrete (ASTM Designation: C 157/C 157M-06)"

AASHTO T 336, "Standard Method of Test for Coefficient of Thermal Expansion of Hydraulic Cement Concrete"

AASHTO TP 60-00 (2005), "Standard Method of Test for Coefficient of Thermal Expansion of Hydraulic Cement Concrete"

Anderson, T., and Roper, H., 1977, "Influence of an Impervious Membrane Beneath Concrete Slabs on Grade," Symposium, Concrete for Engineering, Institute of Engineers, Brisbane, Australia, Aug., pp. 51-56.

ARRA Inc., 2004, "Guide for Mechanistic-Empirical Design of New and Rehabilitated Pavement Structures", NCHRP Project 1-37A, Mar. 2004.

ASTM International. "C143/143M-10a Standard Test Method for Slump of Hydraulic Cement Concrete." *C09.60*, 1922.

ASTM International. "C231/231M-10 Standard Test method for Air Content of Freshly Mixed Concrete by the Pressure Method." *C09.60*, 1949.

ASTM C114 – 11a, "Standard Test Methods for Chemical Analysis of Hydraulic Cement"

ASTM C138/C138M – 10b, "Standard Test Method for Density (Unit Weight), Yield, and Air Content (Gravimetric) of Concrete"

ASTM C150/C150M – 11, "Standard Specification for Portland Cement"

ASTM C156 – 09a, "Standard Test Method for Water Loss [from a Mortar Specimen] Through Liquid Membrane-Forming Curing Compounds for Concrete"

ASTM C231/C231M – 10, "Standard Test Method for Air Content of Freshly Mixed Concrete by the Pressure Method"

ASTM C305 – 11, "Standard Practice for Mechanical Mixing of Hydraulic Cement Pastes and Mortars of Plastic Consistency"

ASTM C309 – 07, "Standard Specification for Liquid Membrane-Forming Compounds for Curing Concrete"

ASTM C618 – 08a, "Standard Specification for Coal Fly Ash and Raw or Calcined Natural Pozzolan for Use in Concrete"

ASTM C1315 – 08, "Standard Specification for Liquid Membrane-Forming Compounds Having Special Properties for Curing and Sealing Concrete"

ASTM E104 – 02 (Reapproved 2007), "Standard Practice for Maintaining Constant Relative Humidity by Means of Aqueous Solutions"

ASTM E228, "Standard Test Method for Linear Thermal Expansion of Solid Materials With a Push-Rod Dilatometer"

Bentz, D. P., E. J. Garboczi, and D. A. Quenard, 1998, "Modeling Drying Shrinkage in Reconstructed Porous Materials: Application to Porous Vycor Glass," Modeling and Simulation in Materilas Science and Engineering, Vol. 6, pp. 211-236.

Bentz, D. P.; Jensen, O. M.; Hansen, K. K.; Oleson, J. F.; Stang, H.; and Haecker, C. J., 2001a, "Influence of Cement Practice Size Distribution on Early Age Autogenous Strains and Stresses in Cement-Based Materials," Journal of the American Ceramic Society, V. 84, No. 1, pp. 129-135.

Bisschop J., 2002, "Drying Shrinkage Microcracking in Cement-Based Materials," PhD thesis, Delf University Press, Netherland, 198 pp.

Bradbury, R.D., 1938, "Reinforced Concrete Pavements", Wire Reinforcing Institute, Washington, D.C.

Browne, R. D., 1967, "Properties of Concrete in Reactor Vessels, Group C, Paper 13," Conference on Prestressed Concrete Pressure Vessels, The Institution of Civil Engineers, London, Mar., pp. 131-151.

Byard, Benjamin. Summary of Modifications to AASHTO T 336 (2009). Auburn: Auburn University, 2010.

Carlson, R. W., "Drying Shrinkage of Concrete as Affected by Many Factors," Proceedings of the American Society for Testing and Materials, V. 38, Part II, ASTM, West Conshohocken, Pa., 1938, pp. 419-440.

Carpenter, S. H., M. I. Darter, and B. J. Dempsey. 1979. "Evaluation of Pavement Systems for Moisture-Accelerated Distress." Transportation Research Record 705.

Carrier, R. E., 1983, "Concrete Curing Tests," Concrete International, V. 5, No. 4, Apr., pp. 23-26.

Cather, R., 1992, "How to Get Better Curing," Concrete, The Journal of the Concrete Society, London, V. 26., No. 5, Sept.-Oct., pp. 22-25.

Cather, R., 1994, "Curing: the True Story?" Magazine of Concrete Research, V. 46. No. 168, Sept., pp. 157-161.

Darwin, D.; Browning, J.; and Lindquist, W. D., 2004, "Control of Cracking in Bridge Decks: Observations from the Field," Cement, Concrete and Aggregates, ASTM International, V. 26, No. 2, Dec., pp. 148-154.

Davis, R. E., and Troxell, G. E., 1954, "Properties of Concrete and Their Influence on Prestress Design," ACI JOURNAL, Proceedings V. 50, No. 23, Jan., pp. 381-391.

Duboe, J.B., "An Evaluation of IDOT's Current Underdrain Systems", Illinois Dept. of Transportation – Physical Research Report No. 120, December 1995.

FHWA, Pavement Subsurface Drainage Design Reference Manual, FHWA/USDOT – FHWA-NHI-08-030, February 2008.

Federal Highway Administration. 1994. *Drainable Pavement Systems – Participant Notebook.* (Demonstration Project 87). Publication No. FHWA-SA-92-008. Office of Technology Applications and Office of Engineering.

Federal Highway Administration. 1994a. *Drainable Pavement Systems*, Participants Notebook. Demonstration Project 87, Report No. FHWA-SA-94-062, Washington, DC.

Hall, K.T., Crovetti, J.A., "Effect of Subsurface Drainage on Performance of Asphalt and Concrete Pavements – Analysis of the SPS-1 and SSPS-2 Field Sections", NCHRP Report 583, 2007

Hansen, T. C., and Mattock, A. H., 1966, "Influence of Size and Shape of Member on the Shrinkage and Creep of Concrete," ACI JOURNAL, Proceedings V. 63, No. 2, Feb., pp. 267-289.

Harvey, J.T., 2006, "Analysis of 2002 Design Guide Distress Prediction Models for Jointed Plain Concrete Pavement", Transportation Research Record, 1947.

Hedenblad, G., 1997, "Drying of Construction Water in Concrete," Swedish Council for Building Research, Stockholm, Sweden, 54 pp.

Holt, E., 2002, "Very Early Age Autogenous Shrinkage: Governed by Chemical Shrinkage or Self-Desiccation," Proceedings of the Third International Research Seminar on the Importance of Self-Dessication in Concrete, B. Persson and G. Fagerlund, eds., Lund, pp. 1-26.

Jackson, F. H., and Kellerman, W. F., 1939, "Tests of Concrete Curing Materials," ACI JOURNAL, Proceedings, V. 36, June, p. 481.

Jensen, O. M., and P. F. Hansen, 2001, "Autogenous Deformation and RH change in Perspective," Cement and Concrete Research, Vol. 31, pp. 1859-1865.

Jensen, O. M., and P. F. Hansen, 2001, "Water-Entrained Cement-Based and Materials: I-Principles and Theoretical Background," Cement and Concrete Research, Vol. 31, pp.647-654.

Jensen, O. M., and Hansen, P. F., 1996, "Autogenous Deformation and Change of Relative Humidity in Silica Fume Modified Cement Paste," ACI Materials Journal, V. 93, No. 6, Nov.-Dec., pp. 539-543.

Justnes, H.; Ardoullie, B.; Hendrix, E.; Sellevold, E. J.; and Gemert, D. V., 1998, "The Chemical Shrinkage of Pozzolanic Reaction Products," Fourth CANMET/ACI/JCI Conference: Advances in Concrete Technology, SP-179, American Concrete Institute, Farmington Hills, MI, pp. 191-205.

Kada, H., M. Lachemi, N. Petrov, O. Bonneau, and P. Aitcin. "Determination of the coefficient of thermal expansion of high performance concrete from initial setting." Materials and Structures, 2002: 35-41.

Kannekanti,V., 2006, "Sensitivity Analysis of 2002 Design Guide Distresses Prediction Models for Jointed Plain Concrete Pavement", Transportation Research Record, 1947.

Keene, P. W., "The Effect of Air-Entrainment of the Shrinkage of Concrete Stored in Laboratory Air," Magazine of Concrete Research, V. 13, No. 38, 1961, pp. 55-60.

Lane, D. S.; Scott, M. L.; Weyers, R. E., 1997, "Relationship between Capillary Pore Pressure and Early Shrinkage Cracking of Concrete," VTRC Report No. 97-R12, Virginia Transportation Research Board.

Lyse, I., "Shrinkage of Concrete," Proceedings of the American Society for Testing and Materials, ASTM, V. 35, 1935, pp. 383-395.

Mackenzie, J. K., 1950, "The Elastic Constants of a Solid Containing Spherical Holes," Proceedings of the Physical Society, Vol. 683, pp. 2-11.

Mahboub, K.C., Liu, D.L., Allen, D.L., "Evaluation and Analysis of Highway Pavement Drainage", Kentucky Transportation Center – Research Report KTC-03-32/SPR-207-00-1F, October, 2003.

Mallela, J., 2005, "Measurement and Significance of Co-efficient of Thermal expansion in Concrete Rigid pavement", Transportation Research Record, 1919.

Mather, B., 1987, "Curing of Concrete," Lewis H. Tuthill International Symposium on Concrete and Concrete Construction, SP-104, G. T. Halvorsen, ed., American Concrete Institute, Farmington Hills, Mich., pp. 145-159.

Mather, B., 1990, "Curing Compounds," Concrete International, V. 12, No. 2, Feb., pp. 40-41.

McDonald, D. B., and Roper, H., 1993, "Prediction of Drying Shrinkage of Concrete from Internal Humidities and Finite Element Techniques, in Creep and Shrinkage of Concrete," Proceedings of the Fifth International RILEM Symposium, Z. P. Bazant and I. Carol, eds., E&FN Spon, London, pp. 259-264.

Meeks, K. W., and Carino, N. J., 1999, "Curing of High Performance Concrete: Report of the State-of-the-Art," NISTR 6295, National Institute of Standards and Technology, Building and Fire Research Laboratory, Gaithersburg, Md., Mar., 191 pp.

Mills, R. H., 1966, "Factors Influencing the Cessation of Hydration in Water Cured Pastes," Symposium on Structure of Portland Cement Paste and Concrete, HRB SR 90, Highway Research Board, Washington, pp. 406-424.

Monfore, G. E., 1963, "A Small Probe-Type Gage for Measuring Relative Humidity," Journal of the PCA Research and Development Laboratories, V. 5, No. 2, pp. 41-47.

Ndon, Udeme J., and K.L. Bergeson. "Thermal Expansion of Concretes: Case Study in Iowa." *Journal of Materials in Civil Engineering*, 1995: 4:246-251.

Nicholson, L. P., 1981, "How to Minimize Cracking and Increase Strength of Slabs on Grade," Concrete Construction, Sept., pp. 739-742.

Perenchio, W. F., 1997, "The Drying Shrinkage Dilemma- Some Observations and Questions About Drying Shrinkage and its Consequence," Concrete Construction, V. 42, No. 4, pp. 379-383.

Pickett, G., 1946, "Shrinkage Stresses in Concrete," ACI JOURNAL, Proceedings V. 42, No. 1, pp. 165-204, and V. 42, No. 2, pp. 361-398.

Pickett, G., 1956, "Effect of Aggregate on Shrinkage of Concrete and Hypothesis Concerning Shrinkage," ACI JOURNAL, Proceedings V. 52, Jan., pp. 581-590.

Pihlajavaara, S. E, 1964, "On the Interrelation of the Moisture Content and the Strength of Mature Concrete and its Reversibility," Report Series III, State Institute for Technical Research, Finland, Building 76.

Pihlajavaara, S. E, 1965, "Estimation of the Drying of Concrete," Proceedings, RILEM Symposium on the Problem of Moisture in Buildings, Helsinki, Finland, Aug.

Powers, T. C., 1948, "A Discussion of Cement Hydration in Relation to the Curing of Concrete," Proceedings, Highway Research Board, V. 27, pp. 178-188.

Radlinska, A., Rajabipour, F., Bucher, B., Henkensiefken, R., Sant, G., and Weiss, J., 2008, "Shrinkage Mitigation Strategies in Cementitious Systems: A Closer Look at Differences in Sealed and Unsealed Behavior", Journal of the Transportation Research Board, Vol. 2070, pp. 59-67.

Sakyi-Bekoe, K. Assessment of the Coefficient of Thermal Expansion of Alabama Concrete. Auburn: Auburn University, 2008.

Schmitt, T. R., and Darwin D., 1999, "Effect of Material Properties on Cracking in Bridge Decks," Journal of Bridge Engineering, ASCE, V. 4, No. 1, Feb., pp. 8-13.

Senbetta, E., 1988, "Concrete Curing Practices in the United States," Concrete International, V. 10, No. 11, Nov., pp. 64-67.

Setter. N., and Roy, D. M., 1978, "Mechanical Features of Chemical Shrinakge of Cement Paste," Cement and Concrete Resaerch, V. 8, No. 5, pp. 623-634.

Shariat, S. M. S., and Pant, P. D., 1984, "Curing and Moisture Loss of Grooved Concrete Surfaces," Transportation Research Record No. 986, pp. 4-8.

Spears, R.E., 1983, "The 80% Solution to Inadequate Curing Problems," Concrete International, V. 5, No. 4, Apr., pp. 15-18.

Springenschmid, R., Plannerer, M, 2001, "Experimental research on the test methods for surface cracking of concrete", Institute for Building Materials, Technical University Munich, Germany, 2001

Standard Specifications for Highway Construction, 1999, Oklahoma Department of Transportation

Steven H. Kosmatka, Beatrix Kerkhoff, and William C. Panarese, 2003, "Design and Control of Concrete Mixtures," Portland Cement Association, 14th Edition.

Suprenant, B. A, and Malisch, W. R., 1999c, "Why Won't the Concrete Dry?" Concrete Construction, July, pp. 29-33.

Suprenant, B. A ., 2002, "Why slabs curl: Part I: A look at the curling mechanism and the effect of moisture and shrinkage gradients on the amount of curling," Concrete International, V. 24, No. 3, April, p. 56-61

Suprenant, B. A ., 2002, "Why slabs curl: Part II: Factors affecting the amount of curling," Concrete International, V. 24, No. 4, April, p. 59-64

Suprenant, Bruce A. "Why Slabs Curl." *Concrete International*, March 2002: 56-64.

Tanesi, Jussara, Gary L. Crawford, Mihai Nocolaescu, Richard Meininger, and Jagan M. Gudimettla. *How will the new AASHTO T336-09 CTE Test Method Impact You?* Washington D.C.: National Research Council, 2010.

Tarr, S. M.; Craig, P. A.; and Kanare, H. M., 2006, "Concrete Slab Repair: Getting Flat is One Thing, Staying Flat is Another," Concrete Repair Bulletin, V. 19, No. 1, Jan.-Feb., pp. 12-15.

Tazawa, E., ed., 1999, Autogenous Shrinkage of Concrete, E&FN Spon, London, 424 pp.

Tazawa, E., and Miyazawa, S., 1995, "Influence of Cement and Admixture on Autogenous Shrinkage of Cement Paste," Cement and Concrete Research, V. 25, No. 2, pp. 281-287.

Tazawa, E.; Miyazawa, S.; and Kasai, T., 1995, "Chemical Shrinkage and Autogenous Shrinkage of Hydrating Cement Paste," Cement and Concrete Research, V. 25, No. 2, pp. 288-292.

Turenne, R. G., 1978, "The Use of Vapor Barriers Under Concrete Slabs on Ground," Building Practice Note No. 8, Division of Building Research, National Research Council of Canada, Aug., p. 3.

U.S. Bureau of Reclamation, 1975, Concrete Manual, 8th Edition, Denver, Colo., 627 pp.

Vandenbossche, J. M. , 2001, "A Review of the Curing Compounds and Application Techniques Used by the Minnesota Department of Transportation for Concrete Pavements", Minnesota Department of Transportation

Westergaard, H.M., 1926a, "Analysis of Stresses in Concrete Pavements Due to Variations of Temperature," Proceedings, Highway Research Board, Vol. 6.

Westergaard, H.M., 1926b, "Stresses in Concrete Pavements Computed by Theoretical Analysis," Public Roads, Vol. 7.

Won, M. "Imporovements of testing procedures for concrete coefficient of thermal expansion." *Journal of the Transportation Research Board*, 2006: 23-28.

Won, M., 2009, "Evaluation of MEPDG with TxDOT Rigid Pavement Database", Center for Transportation Research at the University of Texas at Austin, report #0-5445-3.

Ye, Dan, Anal Mukhopadhyay, and Dan G. Zollinger, 2009, "Laboratory and Field Evaluation of Concrete Paving Curing Effectiveness," FHWA/TX-10/0-5106-3, Texas Department of Transportation.

Ytterberg, R., 1987, "Shrinkage and Curling of Slabs on Grade (Part I)," Concrete International, V. 9, No. 4., Apr., pp. 22-31.

Ytterberg, R., 1987, "Shrinkage and Curling of Slabs on Grade (Part II)," Concrete International, V. 9, No. 5., May, pp. 54-61.

Ytterberg, R., 1987, "Shrinkage and Curling of Slabs on Grade (Part III)," Concrete International, V. 9, No. 6., June, pp. 72-81.

Zaghloul, S., 2006, "Investigation of Environmental and Traffic inputs on Mechanistic-Empirical Pavement Design Guide Prediction", Transportation Research Record, 1967.